



5-2008

## **Resilient Modulus and Strength Index Properties of Stabilized Base for Tennessee Highways**

Wesley M. MacDonald  
*University of Tennessee - Knoxville*

Follow this and additional works at: [https://trace.tennessee.edu/utk\\_gradthes](https://trace.tennessee.edu/utk_gradthes)



Part of the [Civil and Environmental Engineering Commons](#)

---

### **Recommended Citation**

MacDonald, Wesley M., "Resilient Modulus and Strength Index Properties of Stabilized Base for Tennessee Highways. " Master's Thesis, University of Tennessee, 2008.  
[https://trace.tennessee.edu/utk\\_gradthes/402](https://trace.tennessee.edu/utk_gradthes/402)

This Thesis is brought to you for free and open access by the Graduate School at TRACE: Tennessee Research and Creative Exchange. It has been accepted for inclusion in Masters Theses by an authorized administrator of TRACE: Tennessee Research and Creative Exchange. For more information, please contact [trace@utk.edu](mailto:trace@utk.edu).

To the Graduate Council:

I am submitting herewith a thesis written by Wesley M. MacDonald entitled "Resilient Modulus and Strength Index Properties of Stabilized Base for Tennessee Highways." I have examined the final electronic copy of this thesis for form and content and recommend that it be accepted in partial fulfillment of the requirements for the degree of Master of Science, with a major in Civil Engineering.

Eric Drumm, Major Professor

We have read this thesis and recommend its acceptance:

Baoshan Huang, Dayakar Penumadu

Accepted for the Council:

Carolyn R. Hodges

Vice Provost and Dean of the Graduate School

(Original signatures are on file with official student records.)

To the Graduate Council:

I am submitting herewith a thesis written by Wesley Michael MacDonald entitled “Resilient Modulus and Strength Index Properties of Stabilized Base for Tennessee Highways.” I have examined the final electronic copy of this thesis for form and content and recommend that it be accepted in partial fulfillment of the requirements for the degree of Master of Science, with a major in Civil Engineering.

Eric Drumm  
Major Professor

We have read this thesis  
and recommend its acceptance:

Baoshan Huang

Dayakar Penumadu

Accepted for the Council:

Carolyn R. Hodges  
Vice Provost and  
Dean of the Graduate School

(Original signatures are on file with official student records.)

RESILIENT MODULUS AND STRENGTH INDEX PROPERTIES OF  
STABILIZED BASE FOR TENNESSEE HIGHWAYS

A Thesis  
Presented for the  
Master of Science  
Degree  
The University of Tennessee, Knoxville

Wesley Michael MacDonald  
May 2008

## **Acknowledgements**

Thanks and love goes to my family, who has supported me through all my years of schooling: My parents, Bill and Shannon Allen, and Mike and Edna MacDonald, and my siblings Lauren and Luke MacDonald and Gary Chapman. My thanks and gratitude to Dr. Drumm who has advised and counseled me for the last 3 years. Finally, praise to God for the blessings he has given me.

## **Abstract**

Typical material used by the Tennessee Department of Transportation for highway bases was evaluated for application to the new Mechanistic-Empirical Pavement Design Guide. Two types of granular Tennessee highway base material were mixed with different stabilizers and tested in the lab according to AASHTO T-307 99 (2003). Unconfined Compressive Strength and California Bearing Ratio tests were also done in an effort to correlate these results with resilient modulus. Three different combinations of base and stabilizer were tested and modeling coefficients were produced. Base structural layer coefficients were generated and compared to coefficients currently in use by TDOT.

Keywords: Resilient Modulus, MEPDG, stabilized base, UCS, CBR

# Table of Contents

Chapter	Page
1 Introduction.....	1
2 Materials .....	2
2.1 Aggregates .....	2
2.2 Stabilizers/Binders .....	5
2.3 Moisture Density.....	5
2.4 Equipment .....	7
3 Test Procedure .....	8
3.1 Resilient Modulus Specimen Preparation.....	8
3.2 Resilient Modulus Testing .....	8
3.3 Unconfined Compression.....	10
3.4 California Bearing Ratio .....	10
4 Test Results.....	12
4.1 Resilient Modulus .....	12
4.2 Unconfined Compressive Strength .....	14
4.3 California Bearing Ratio .....	15
5 Discussion of Results.....	16
6 Analysis.....	26
6.1 Overall MEPDG models for Resilient Modulus.....	26
6.2 Layer Coefficients.....	28
6.3 Correlations to Resilient Modulus and Layer Coefficients.....	32
7 Summary and Conclusions .....	37
8 REFERENCES .....	38
APPENDICES .....	42
APPENDIX A.....	43
Literature Review.....	43
APPENDIX B .....	49
Laboratory Test Results .....	49
APPENDIX C .....	107
Materials .....	107
Vita .....	122

## List of figures

Figure	Page
Figure 2-1 Aggregates used in testing (a) Limestone (b) Gravel.....	2
Figure 2-2 Grain Size Distribution of Limestone and Gravel Aggregates. ....	4
Figure 2-3- Moisture Density Curves .....	6
Figure 4-1 Typical 1 second stress-strain response from Resilient Modulus Testing.....	13
Figure 4-2 Typical Final 10 Cycles of Resilient Modulus Test.....	14
Figure 5-1 Typical resilient modulus vs. deviator stress for (a) gravel-cement, (b) limestone-cement, and (c) Limestone-fly ash-lime samples.....	17
Figure 5-2 Typical resilient modulus vs. bulk stress for (a) gravel-cement, (b) limestone-cement, and (c) limestone-fly ash-lime samples.....	18
Figure 5-3 - Resilient modulus comparison of 7 and 28 day samples of (a)Limestone cement, (b) Gravel Cement, and (c) Limestone, fly ash, and lime.	22
Figure 5-4 Typical relationship of resilient modulus with (a) bulk stress, (b) octahedral shear stress, and (c) octahedral shear stress/ bulk stress. ....	24
Figure 6-1 Experimental results vs. Overall models for (a.) Limestone and cement, (b.) Gravel Cement, and (c.) Limestone, Fly Ash, and Lime .....	27
Figure 6-2 Pavement Thicknesses Considered for Finite Element Models.....	30
Figure 6-3 Finite Element Mesh of Medium Pavement (ADINA-AUI 8.4, 2007) .....	30
Figure 6-4 Layer Coefficients for (a) Limestone Cement, (b) Gravel Cement, and (c) Limestone Fly ash Lime.....	35



## List of tables

Table	Page
Table 2-1 Atterberg Limits obtained from portion passing #40 sieve (after Kilday, 2008) .....	4
Table 2-2 Optimum Moisture Content and Maximum Dry Unit Weight .....	7
Table 3-1 Schedule of testing from AASHTO T-307(2003) .....	9
Table 4-1 Unconfined Compression and CBR Test Results .....	15
Table 5-1 Overall Summary of Resilient Modulus Samples .....	20
Table 6-1 Overall model equations for each material .....	26
Table 6-2 Initial Layered Material Properties and Stresses at Mid-layer of Base	31
Table 6-3 Modeled Moduli and Layer Coefficients for Pavements .....	32
Table 6-4 Standard TDOT Base Layer Coefficients .....	32
Table 6-5 Predicted Moduli and Layer Coefficients based on CBR .....	33
Table 6-6 Predicted Resilient Moduli Based on UCS (units = psi) .....	33

# 1 Introduction

New and adaptive technologies, as well as new engineering techniques based on engineering mechanics are allowing designs and methods to be more exact and rely less on conservative empirical estimates that, in the past, might have wasted money. Hence the new Mechanistic-Empirical Pavement Design Guide (MEPDG) was created to allow better precision when designing one of the nation's greatest assets, its transportation system of roads (NCHRP 1-37A, 2004). Most roads and highways are either a flexible pavement (hot-mix asphalt) or a rigid pavement (Portland cement concrete). Though this may be the portion of the road you see, there are actually several distinct layers that make up pavement system. Both rigid and flexible pavements have a layer in between the surface and subgrade, or native ground, called the base, or base course. The base materials act to transfer the loads of the surface material to the earth. The base is usually made of an abundant, readily and locally available material that fulfills certain engineering requirements, such as strength, durability, low cost, high permeability, and ease of placement. In the state of Tennessee, the characteristics of base course material vary with geographic region. West of the Tennessee River, brown rounded gravel with clay is typically used. In Middle and East Tennessee, a crushed limestone is used. Generally these bases are laid without any additives, but in some cases they are modified and stabilized. This report investigates the engineering properties of stabilized, or bound, base course, specifically the property most important to pavement design, resilient modulus. Resilient modulus is the ratio of applied cyclic stress to resilient, or recoverable, strain.

Currently the Tennessee Department of Transportation (TDOT) uses an estimated layer coefficient for stabilized base course when designing pavements. The new MEPDG suggests all agencies submit their widely used materials to a series of test to better model their performance and better engineer their pavements. The results of tests on limestone-cement, gravel-cement, and limestone-fly ash-lime stabilized base materials are contained herein.

## 2 Materials

### 2.1 Aggregates

Two aggregate bases were used in this study: Limestone base, obtained from a quarry in Clarksville, Tennessee and Gravel Base obtained from a quarry in McNairy County, Tennessee. These are both typical materials used as road base by the Tennessee Department of Transportation. Both materials can be seen in Figure 2-1. A detailed description of both materials and their geologic origin was described by Kilday (2008) as follows:

“The limestone base material used for this project came from Vulcan Materials quarry located in Clarksville, Tennessee. This quarry is located in the Western portion of the Highland Rim physiographic region. The Highland Rim completely surrounds the Central Basin and is characterized by rolling terrain dissected by sharply incised valleys with numerous streams. Published geologic information indicates the site lies within the St. Louis Limestone and Warsaw Limestone Formation. These formations typically consist of light to medium gray, very fine to medium-grained, thin to thick-bedded, fossiliferous limestone containing numerous chert stringers and nodules. Soil formed by the in-place solution weathering of the parent limestone formation normally consists of reddish brown silty clay of low to moderate plasticity with occasional zones of high plasticity. Often bands of partially and unweathered chert exist within the overburden soil. The soil/bedrock interface is irregular with soil slots extending into the bedrock unit and more resistant pinnacles protruding into the soil zone.

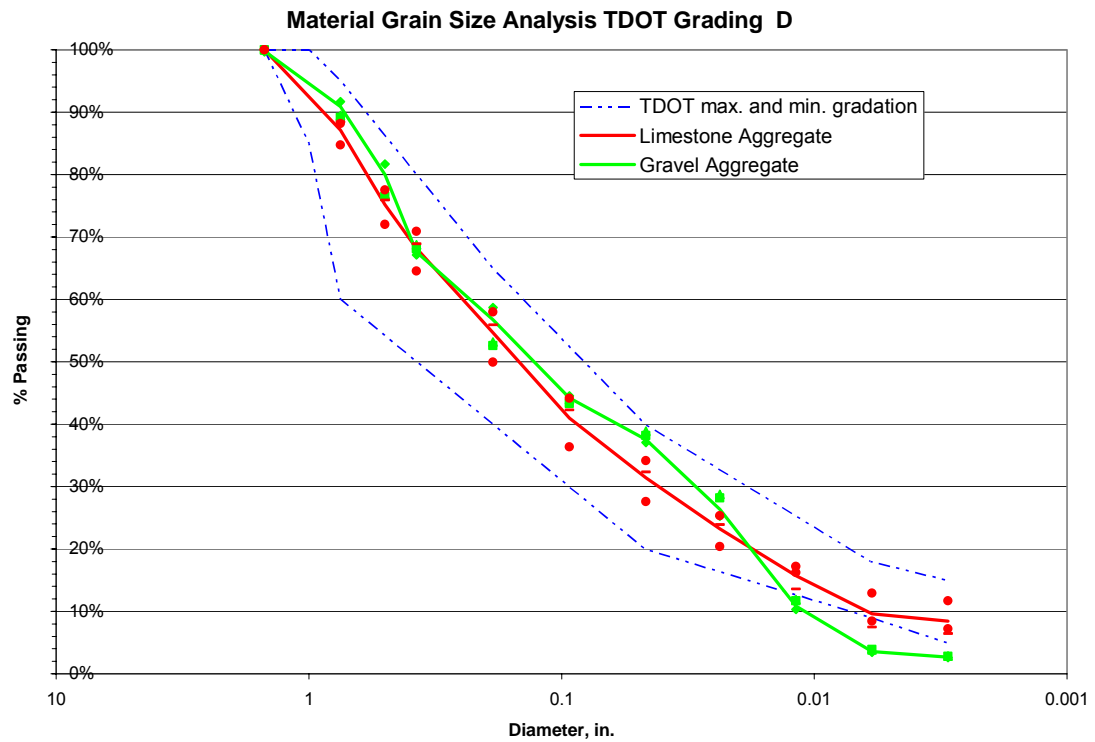
The gravel base material used for this project came from Martin-Marietta Aggregate’s quarry located in McNairy County, Tennessee. This site was chosen due to the fact it is located in the Coastal Plain physiographic region. The West



Figure 2-1 Aggregates used in testing (a) Limestone (b) Gravel

Tennessee Coastal Plain is defined as the area west of the Tennessee River divide and to the east of the loess hills that flank the Mississippi River Valley. This area is known as an area of relatively low relief. Published geologic information indicates the materials at the Martin-Marietta quarry consist of high level alluvial deposits. The high level deposits are characterized by iron-stained gravel, sand, silt, and clay. These deposits are variable in thickness but generally less than 60 feet thick.”

To classify the materials, both were sieved according to ASTM C136-06 (2006), Standard Test Method for Sieve Analysis of Fine and Coarse Aggregates. Grain size distribution curves were created for both materials and can be seen in Figure 2-2. It can be seen that the limestone material lies within the TDOT requirements for maximum and minimum particle size based on TDOT Specification 309 (2006) Aggregate-Cement Base and TDOT Specification 312 (2006) Aggregate-Lime-Fly Ash Stabilized Base course. Both are aggregates that meet the conditions of TDOT Specifications 903.05 (2006) Aggregate for Mineral Aggregate Base and Surface Courses and TDOT Specification 903.15 (2006) Aggregate for Aggregate-Cement Base Course. Atterberg Limits of the portion of the dry soil passing the #40 sieve are given in Table 2-1. These were obtained using ASTM D4318-05 (2005). The Limestone base material is classified as SW-SC, well graded sand with clay and gravel, based on ASTM D 2487-06 (2006). According to the AASHTO Classification system (1993) this same material is A-2-4(0), silty or clayey gravel and sand, which corresponds to a material that has an excellent to good rating as a subgrade. The West Tennessee gravel material is an SP- poorly graded sand with gravel, according to the Unified Soil Classification System and is A-2-6(0) according to AASHTO (1993). Again, this is a silty or clayey gravel and sand that is an excellent to good subgrade. According to MEPDG Table 2.2.51, an A-2-4 material has a typical Resilient Modulus range from 28,000 to 37,500 psi, an SW-SC material has a typical resilient modulus range from 21,500 to 31,000 psi, an A-2-6 material has a typical Resilient Modulus range from 21,500 to 31,000 psi, and an SP material has a typical resilient modulus range from 24,000 to 33,000 psi. All of these values are for the unbound material, so it is safe to assume bound base test values will be much higher.



**Figure 2-2 Grain Size Distribution of Limestone and Gravel Aggregates.**

**Table 2-1 Atterberg Limits obtained from portion passing #40 sieve (after Kilday, 2008)**

Atterberg Limits Summary			
	Liquid Limit	Plastic Limit	Plastic Index
Clarksville Limestone Base	22	13	10
West Tennessee Gravel Base	31	20	11

## ***2.2 Stabilizers/Binders***

Three different binders were added to the aggregates to create the stabilized samples. Cement was used with both types of aggregates while both lime and fly ash were used with the limestone aggregate. Type I Portland Cement from Buzzi Unicem, USA, Signal Mountain plant was used for binding the limestone and gravel aggregates at a rate of 3% by weight of the dry material. (1lb dry aggregate would be mixed with 0.03 lb cement) This cement content was chosen as per TDOT Specification 309.06-Cement Application, Mixing and Spreading of Aggregate-Cement Base Course, where the specified cement content is 3-5%. It is important to note that 3% gives the low end of the strength for this base material. Class F Fly ash and Lime were added to the limestone aggregate at a rate of 11% and 3.5%, respectively, by dry weight as per TDOT Specification 312.03- Proportioning of Aggregate-Lime-Fly Ash Stabilized Base Course (1lb dry aggregate would be mixed with 0.035 lb lime and .11 lb fly ash). Chemical components of the cement and class F fly ash used are presented in Tables C-1 and C-2 in Appendix C (Tinsley, 2007).

## ***2.3 Moisture Density***

Aggregates were oven dried, passed through a  $\frac{3}{4}$  inch sieve and stored in the laboratory in separate containers until needed for testing. Since the sample size was to be 6" diameter by 12" height cylinders, larger particles were removed for testing purposes. Dry aggregates were mixed with their specified amount of stabilizer (cement or lime and fly ash) and the water content varied to determine the maximum dry density (unit weight) and optimum moisture content from standard Proctor tests. Moisture-Unit Weight relationships were determined for each material using AASHTO T 99-01, Moisture Density Relations Using a 2.5-kg (5.5-lb) Rammer and a 305-mm (12-in.) Drop- Method D, with the exception that the dry stabilizing material was thoroughly mixed with the dry aggregate prior to the addition of the water. Unit weight plays an important role in the strength of bound materials. (cite Appendix paper here@#%). For a certain material, an increase in unit weight typically means an increased strength. The addition of water, up to a certain amount (optimum moisture content, will help materials compact and move around, becoming more dense and allowing more particle interlocking. Water also initiates and fuels the chemical processes that give the stabilized materials their extra strength.

The relationships with water and dry unit weight for the materials in this study are shown in Figure 2-3 and the maximum dry unit weight and optimum moisture content are shown in Table 2-2. Both the limestone-cement and limestone-fly ash-lime have similar maximum dry unit weights, but the variation with water content is different. Limestone with fly ash and lime can be seen to have a high dry unit weight before any water is added and then a decrease with the addition of water and then the typical moisture-density curve exhibited by most soils. Fly ash

feels very fluid-like to the bare hands and flows fairly well. This, along with the large amount of fines relative to the cement treated limestone, allows the limestone fly ash mix to compact well. The water must be added to provide for hydration. In spite of the difference in the moisture-unit weight curves, both limestone bases showed little variation of optimum water content or maximum dry unit weight. Gravel Cement has a higher water content and a lower dry unit weight than the two limestone bases. Based on the maximum dry unit weight and optimum moisture content shown in Table 2.2 for the untreated base materials, the additives have only a minor effect on the moisture density curves.

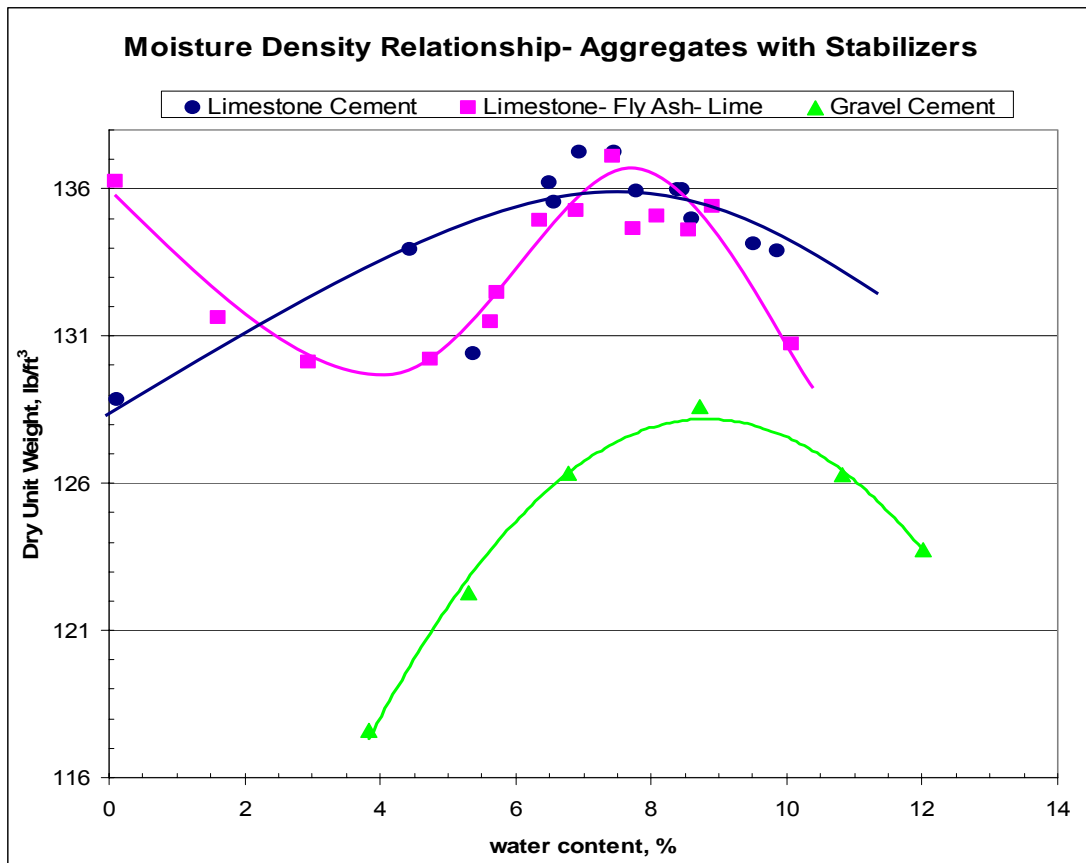


Figure 2-3- Moisture Density Curves

**Table 2-2 Optimum Moisture Content and Maximum Dry Unit Weight**

	Optimum Moisture Content	Maximum Dry Unit Weight, lb/ft <sup>3</sup>
Gravel Cement	8.8%	128
Limestone Cement	7.8%	136
Limestone, Fly Ash, and Lime	7.6%	137
Gravel*	8.5%	129
Limestone*	9.0%	136

**\* unstabilized properties after Kilday (2008)**

## ***2.4 Equipment***

All equipment used in this study to complete material testing is part of the Geotechnology and Infrastructure Materials Laboratory located in Estabrook Hall, University of Tennessee, Knoxville and listed below. A listing of testing equipment used in this study is available in Appendix C.



### **3 Test Procedure**

Tests were conducted on three combinations of the two different base materials. Materials were oven dried and particles larger than  $\frac{3}{4}$ " were removed. Resilient modulus and unconfined compression samples were constructed in a typical 6" diameter x 12" cylindrical plastic concrete mold. These molds were surrounded by a metal mold of the same height and an extension collar was bolted onto the top to allow for extra material to be compacted and shaved and leveled off later. The metal mold guarded against deformation and provided support around the plastic mold while specimens were compacted with the proctor hammer. CBR test samples were prepared in typical CBR molds with collars as per AASHTO T-193-99(2003), The California Bearing Ratio. Appendix C provides details of the lab equipment.

#### ***3.1 Resilient Modulus Specimen Preparation***

Using the optimum moisture content, maximum unit weight, and respective binder content as a target, the proportions of all materials were carefully weighed and prepared to make the desired number of specimens for resilient modulus testing. Generally, either 3 or 6 specimens were made at once and material was prepared for CBR and strength testing from the same batches as used for resilient modulus tests. Dry aggregate was loaded into a pre soaked mixer and dispersed, followed closely by the binder. A small amount of the total water was added to keep fine particles from floating away and then the contents were mixed thoroughly. While the contents were stirring, the remainder of the water was added and the mixer was spun until a thorough blend was achieved. Representative samples were taken from the mixer and used to create each specimen. Concrete cylinder molds were filled in 5 equal lifts and compacted with 56 blows from a standard Proctor hammer (5.5lb and 12 in. drop) being applied to each lift. More than enough material was placed in each mold so the collar of the mold could be taken off and the material extending past the top of the mold scarified and the top be leveled off. A thin concrete or lime-fly ash paste was applied to help level the top of the specimen and assume full contact with loading platen. Specimens were then weighed in order to obtain unit weights and moisture content samples were taken from the same portion of the mix from which the samples were taken. Finally, the specimens were capped, numbered, and placed in a humid room for six days. On the sixth day, samples were strong enough to be broken out of molds and then were renumbered and placed back in the humid room until the time of testing.

#### ***3.2 Resilient Modulus Testing***

Samples were removed at the proper time, either 7 or 28 days, and tested according to AASHTO T 307-99(2003). A vacuum was placed on a membrane stretcher to place the membrane around the sample without disturbing it. The sample was then sealed and O-rings placed around the ends and a vacuum was

applied to the sample while the top of the cell was placed on, screwed down, and the entire cell lifted onto the loading frame. Vacuum pressure was released and drain valves opened while confining pressure and initial vertical contact pressure were applied. After the confining pressure stabilized, the specimen was tested according to the schedule in Table 3-1 which shows the targeted stresses applied. Resilient modulus tests are performed over a range of stress states, each producing a different value of the resilient modulus. Sequence 0 was a conditioning sequence run with 500 load applications. The controller directed the hydraulically applied load to get approximately the targeted stresses based on a 6 inch diameter and 28.2740 inch<sup>2</sup> area. The cyclic loading was applied over a period of 0.1 second, followed by a 0.9 second rest interval as specified by AASHTO T 307-99. However, the specified haversine load pulse was approximated by a triangular load pulse. 600 load and displacement readings were taken every second, which provided a complete load-displacement history. The actual applied stress and measured strain used to determine the resilient modulus, rather than the target cyclical stresses were measured. After sequence 0 was run, the cell was vented to equilibrate and then the 3 psi confining stress was applied. Whenever confining stress was increased, enough time was allowed in between tests for the pressure readings to stay constant. After completion of resilient modulus testing, all samples underwent unconfined compression tests.

**Table 3-1 Schedule of testing from AASHTO T-307(2003)**

Sequence No.	Confining Pressure, $S_3$	Max. Axial Stress, $S_{max}$	Cyclic Stress, $S_{cyclic}$	Constant Stress, $0.1S_{max}$	No. of Load Applications
	psi	psi	psi	psi	
0	15	15	13.5	1.5	500-1000
1	3	3	2.7	0.3	100
2	3	6	5.4	0.6	100
3	3	9	8.1	0.9	100
4	5	5	4.5	0.5	100
5	5	10	9.0	1.0	100
6	5	15	13.5	1.5	100
7	10	10	9.0	1.0	100
8	10	20	18.0	2.0	100
9	10	30	27.0	3.0	100
10	15	10	9.0	1.0	100
11	15	15	13.5	1.5	100
12	15	30	27.0	3.0	100
13	20	15	13.5	1.5	100
14	20	20	18.0	2.0	100
15	20	40	36.0	4.0	100

### ***3.3 Unconfined Compression***

Unconfined Compression tests were run on all 6" diameter by 12" height samples following resilient modulus testing to determine their Unconfined Compressive Strength (UCS). These tests are easy, quick, and inexpensive to run and are used to give an approximate modulus for some materials. ASTM D 1633-00, Standard Test Methods for Compressive Strength of Molded Soil-Cement Cylinders, was followed for all UCS tests regardless of material. Method B was followed, except cylinders were 6" in diameter and 12" in height, as opposed to the 2.8" in diameter and 5.6" in height samples specified. When resilient modulus testing was finished, each sample was carefully taken to the UCS machine and its membrane removed. Two neoprene end caps were used to ensure the load was spread over a more representative area, in case samples were not completely flat on the top or bottom. The sample and end caps were then placed on the Universal Testing Machine. The sample was loaded in the same direction as the resilient modulus test. The machine was programmed to load the sample at a rate of 0.05 inch/min (displacement controlled test). UCS is only concerned with the ultimate load a sample undergoes, but for purposes of this study, the displacement measurements were recorded in addition to the load measurements in an effort to derive a modulus relationship. Specimens were loaded until a peak load was reached and then decreased to 97% of the peak. Once the compression phase was over, samples were unloaded at a constant -0.05 inch per minute until a load no longer existed, with both loads and displacements recorded. To investigate the effect of resilient modulus testing on the strength, 7 and 28 day unconfined compression and unloading tests were also run on samples that did not undergo resilient modulus testing. These samples were prepared in the exact same way as the resilient modulus samples.

### ***3.4 California Bearing Ratio***

California Bearing Ratio (CBR) tests were performed alongside Resilient Modulus and Unconfined Compression tests. The CBR is a simple and inexpensive test that many state highway departments use for correlation with other tests, such as resilient modulus. Tests were conducted in general accordance with AASHTO T-193-99(2003), The California Bearing Ratio. Materials were weighed and prepared in the same way as the Resilient Modulus specimens. Materials were compacted in a CBR mold with an extension collar in three flights of equal height. Each flight was compacted with a standard proctor hammer (5.5lb. and 12in. drop height) using 56 blows per layer. After compaction, the collar was removed, excess material was scraped off the top and any remaining voids were filled with fines. The sample and mold were then weighed to obtain a unit weight and representative moisture samples were taken. After samples were prepared and weighed, a CBR platen with 10lb surcharge ring was placed on the top surface of the material and sample was placed in a humid room. After 6 days, the entire sample, mold, platen, and weights were submerged in buckets with water approximately 1 inch over the top of the mold. The samples

were left to soak for one day. On the seventh day, samples were removed from the buckets and allowed to drain for 30 minutes prior to CBR load testing. The platen was removed and the ring of surcharge weights was placed back on the sample. A CBR piston with a 3 inch cross sectional area was placed in the middle of the surcharge rings, ensuring it was in contact with the surface of the material prior to testing. The Universal Testing Machine loaded each sample until the piston had penetrated the material 0.4 inches. This was done at a rate of 0.05 inch per minute.

## 4 Test Results

### 4.1 Resilient Modulus

For each specimen that was tested for resilient modulus, sixteen large data files were created. Each data file stored time, load, and two different displacement readings for the entire sequence. Every second, six hundred data points are collected from each linear variable differential transformer, or LVDT, and the load cell. This is an adequate amount to define the load pulse that is intended to mimic a moving wheel load. Typical stress and strain data are shown for a time of one second in Figure 4-1. The tenth of a second load pulse and nine-tenth second rest specified by AASHTO T-307 are shown. This loading is repeated 100 times per sequence. Resilient Modulus is defined as the following:

$$M_r = \frac{S_{cyclic}}{\epsilon_r} \quad (1)$$

Where

$M_r$  = Resilient Modulus

$S_{cyclic}$  = cyclic (resilient) axial stress = cyclic axial load/ initial cross-sectional area of specimen

$\epsilon_r$  = resilient (recovered) strain due to  $S_{cyclic}$  = resilient axial deformation/ original specimen length

Because the modulus of aggregates is so dependent on the level of applied stress, the test is performed over a range of stresses to measure the resilient response. For a given stress state or test sequence, the resilient modulus was obtained by finding the maximum and minimum loads each cycle and their corresponding displacements. These values were then used to determine the cyclic stress and resilient strain. The last 10 resilient moduli from each sequence were averaged together to give a representative resilient modulus for that stress state. Figure 4-2 shows the last 10 cycles of sequence 15 for a 28 day Limestone fly ash and lime sample D6. This is typical data obtained from a resilient modulus test and offers a visual interpretation of resilient modulus. A report was generated for each sequence that stated the last 10 resilient moduli and corresponding deviator stresses. The average deviator stress was used along with the known confining pressure for each sequence to calculate octahedral shear stress and bulk stress.

Where:

$$\begin{aligned} \tau_{oct} &= \text{octahedral shear stress} \\ &= \frac{1}{3} \sqrt{(\sigma_1 - \sigma_2)^2 + (\sigma_1 - \sigma_3)^2 + (\sigma_2 - \sigma_3)^2} \end{aligned}$$

$$= \frac{\sqrt{2}}{3} \sigma_d \quad \text{for } M_r \text{ test on cylindrical specimen.}$$

$\theta$  = bulk stress =  $\sigma_1 + \sigma_2 + \sigma_3 = \sigma_d + 3\sigma_3$  for  $M_r$  test on cylindrical specimen.

$\sigma_1$  = major principal stress

$\sigma_2$  = intermediate principal stress =  $\sigma_3$  or confining pressure for  $M_r$  test on cylindrical specimen.

$\sigma_3$  = minor principal stress/ confining pressure

$\sigma_d$  = deviator stress

In some cases, data was missing from the data logger and gave false modulus. Each sequence was scrutinized and when this happened the 9 best sequences were averaged. After each sequence was analyzed, all 15 sequences were put together to generate a model for each sample individually based on octahedral shear stress and bulk stress. Summaries of all samples' resilient modulus testing can be found in Appendix B.

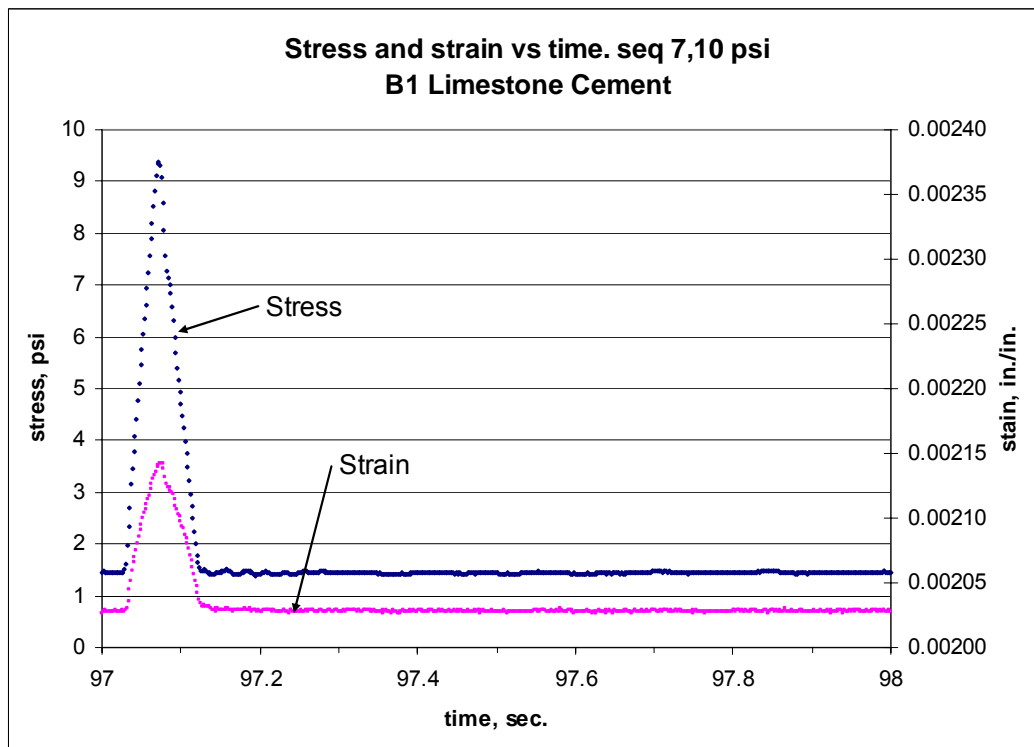


**Figure 4-1 Typical 1 second stress-strain response from Resilient Modulus Testing**

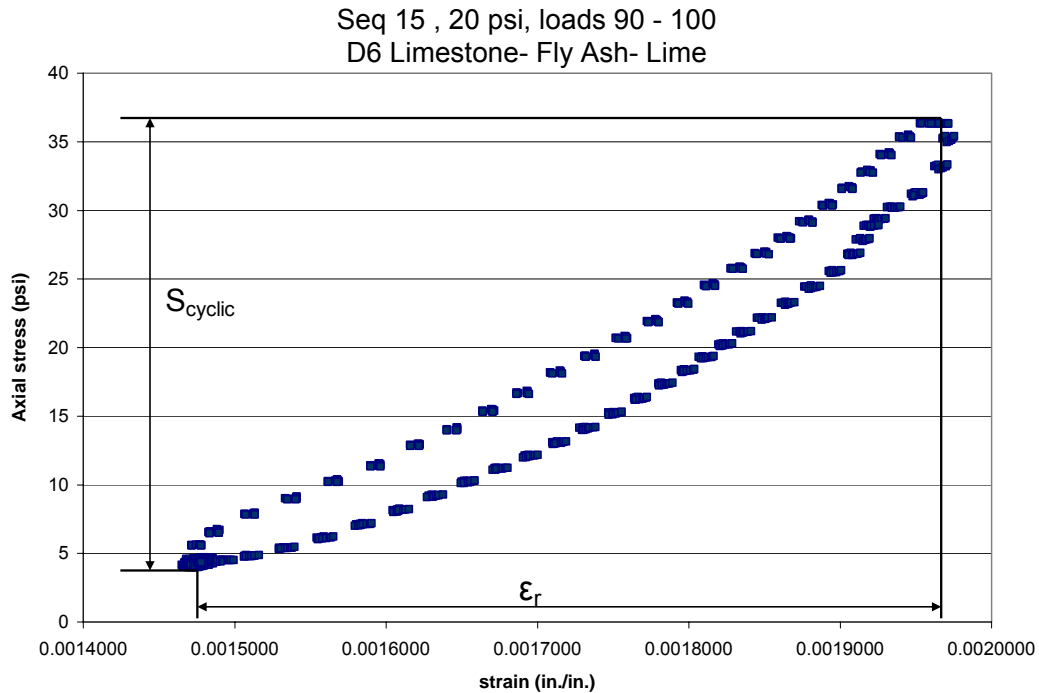


**Figure 4-2 Typical Final 10 Cycles of Resilient Modulus Test**

## ***4.2 Unconfined Compressive Strength***

Results of Unconfined Compressive Strength (UCS) testing can be found below in Table 4-1. UCS was taken to be the ultimate load experienced by each sample divided by its initial area. Six samples of each material were tested after resilient modulus testing at 7 day strength, three samples of each material were tested after resilient modulus testing at 28 day strength, three samples of each material were tested without resilient modulus testing at 7 day strength, and three samples of each material were testing without resilient modulus at 28 day strength. The average of each of these groups is what is reported in Table 4-1. Individual UCS test summaries can be found in Table C-1 and C-2 in the Appendix. Three limestone-fly ash-lime samples were made and cured for 28 days in a 100° F water bath to see if the materials conformed to TDOT specification 312-02. These three samples are included in Table 7-2

**Table 4-1 Unconfined Compression and CBR Test Results**

	Unconfined Compression Test				CBR  (n=6)
	7 day (psi) with RM          no RM (n=6)          (n=3)		28 day (psi) with RM          no RM (n=3)          (n=3)		
Gravel-Cement	182	237	345	310	503
Limestone-Cement	213	267	408	306	527
Limestone-Fly Ash Lime	157	158	255	281	568

**n= number of specimens tested**

### ***4.3 California Bearing Ratio***

CBRs were only tested after 7 day curing. 6 samples of each aggregate and binder mixture were tested for California Bearing Ratio at maximum dry density and optimum moisture content. The average of each material is reported in Table 4-1. CBR is expressed as the ratio of stress at a penetration of 0.2 inches to standard stress of 1500 psi. This value was always greater than the ratio of stress at a penetration of 0.1 inches to standard stress of 1000 psi. Individual CBR test summaries can be found in Table C-3 in Appendix C.



## 5 Discussion of Results

As discussed previously, the resilient modulus varies as a function of bulk stress and octahedral shear stress. A typical resilient modulus-deviator stress relationship for the three treated base materials is shown in Figure 5-1, while Figure 5-2 shows the resilient modulus- bulk stress response. A general increase in resilient modulus with deviator stress can be seen in Figure 5.1. The effect of confining pressure is evident from Figure 5.1 and is also represented in Figure 5.2 through the bulk stress.

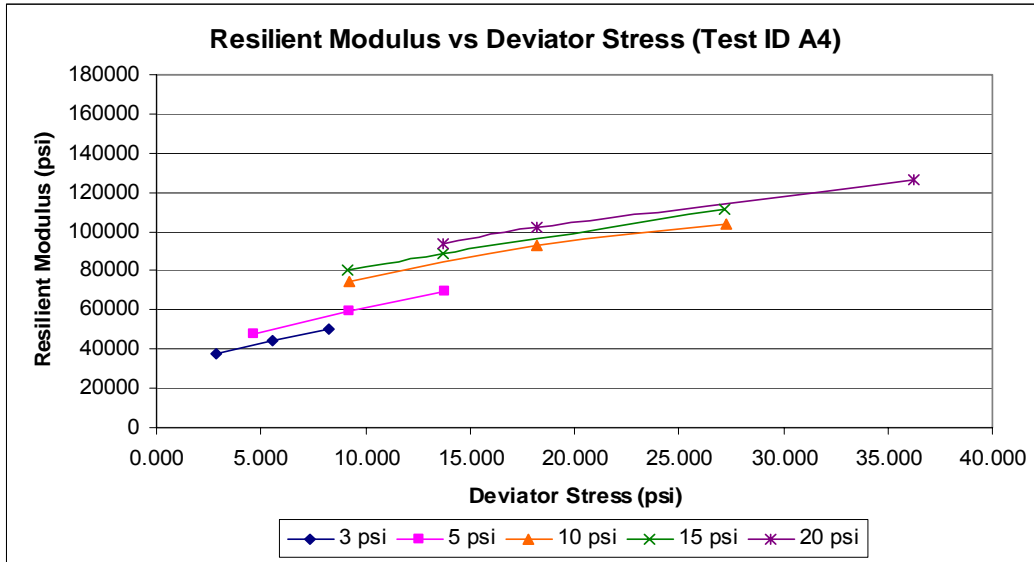
Each sample was modeled with the suggested 2003 Mechanistic-Empirical Pavement Design Guide (MEPDG) equation for the resilient modulus,  $M_r$ , of the base materials as given in equation 2.

$$M_r = k_1 P_a \left( \frac{\theta}{P_a} \right)^{k_2} \left( \frac{\tau_{oct}}{P_a} + 1 \right)^{k_3} \quad (2)$$

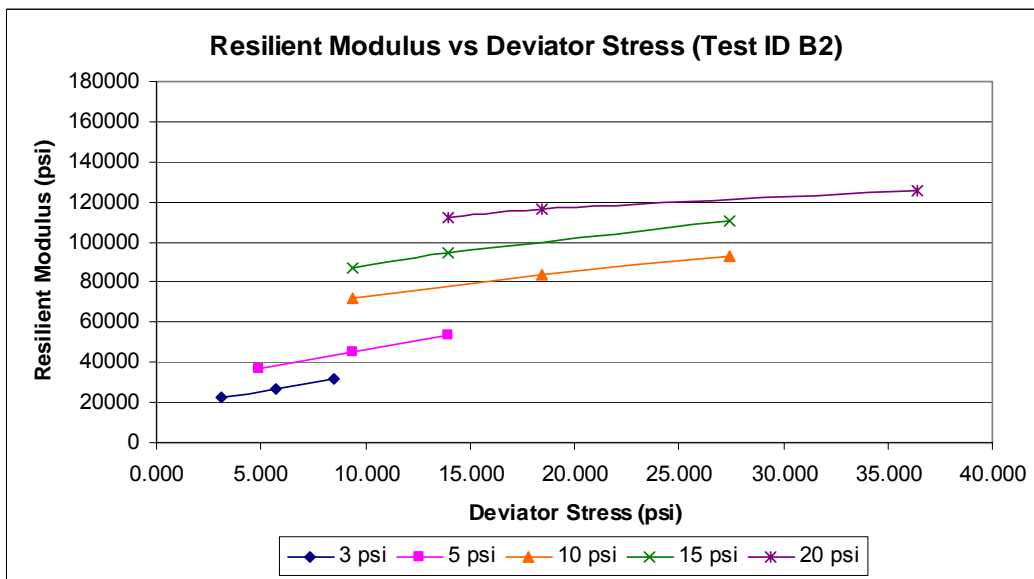
Where

$M_r$	=	resilient modulus
$\theta$	=	bulk stress = $\sigma_1 + \sigma_2 + \sigma_3$
$\tau_{oct}$	=	octahedral shear stress
	=	$\frac{1}{3} \sqrt{(\sigma_1 - \sigma_2)^2 + (\sigma_1 - \sigma_3)^2 + (\sigma_2 - \sigma_3)^2}$
$P_a$	=	normalizing stress (atmospheric pressure)
$k_1, k_2, k_3$	=	regression constants (obtained by fitting resilient modulus test data to equation)
$\sigma_1$	=	major principal stress
$\sigma_2$	=	intermediate principal stress = $\sigma_3$ for $M_r$ test on cylindrical specimen.
$\sigma_3$	=	minor principal stress/ confining pressure

A summary of the model constants each sample tested is presented in Table 5-1 including the individual modeling coefficients  $k_1$ ,  $k_2$ , and  $k_3$ . A high coefficient of determination,  $r^2$ , for each sample suggests that the stabilized base materials are well represented by the mechanistic-empirical model (every sample except two, C1 and C6, are above 0.90). When modeled as an individual material the coefficients of determination are considerably less, but still are believed to be reliable.

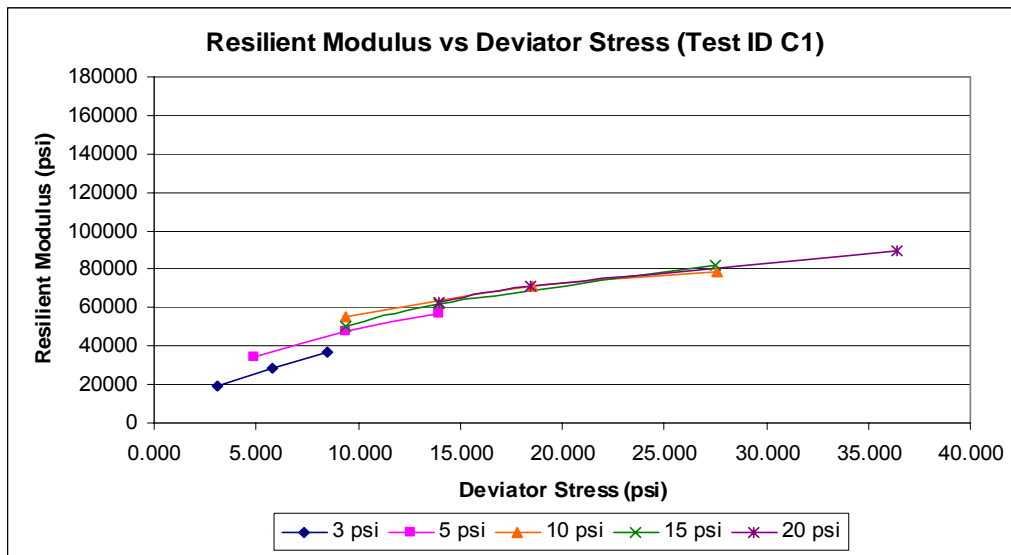


(a)



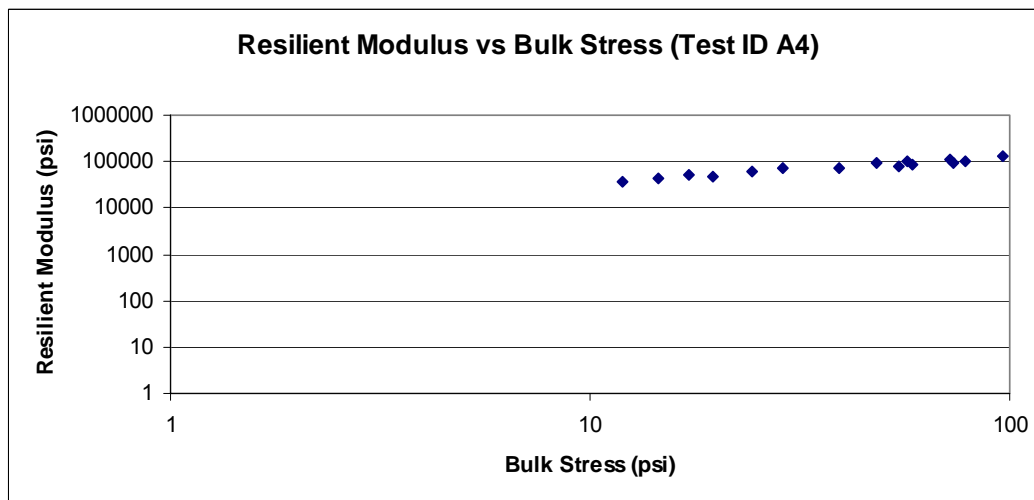
(b)

**Figure 5-1 Typical resilient modulus vs. deviator stress for (a) gravel-cement, (b) limestone-cement, and (c) Limestone-fly ash-lime samples.**



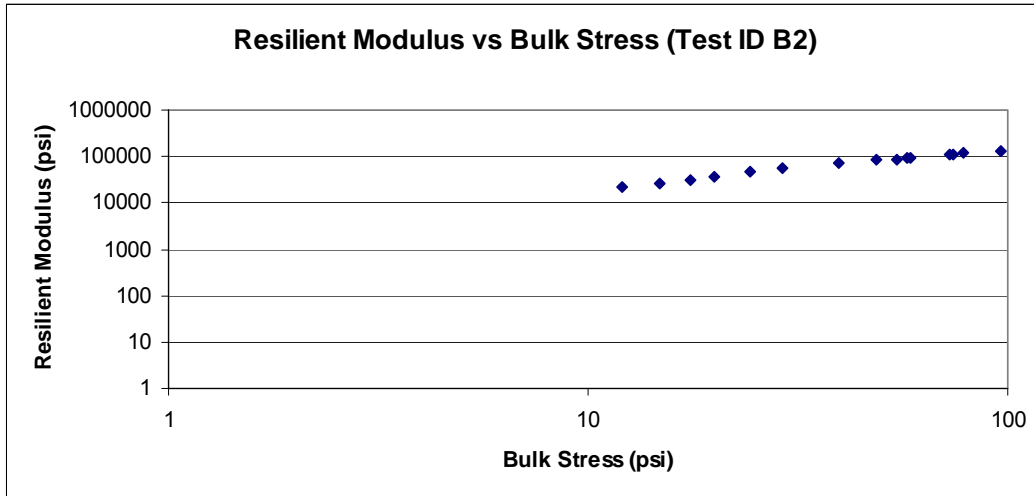
(c)

Figure 5-1 cont'd- Typical resilient modulus vs. deviator stress for (a) gravel-cement, (b) limestone-cement, and (c) Limestone-fly ash-lime samples.

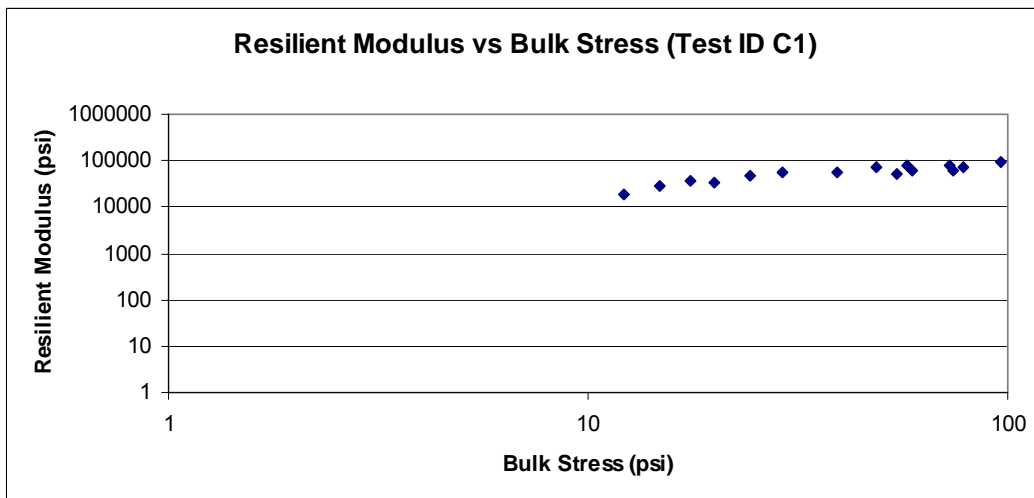


(a)

Figure 5-2 Typical resilient modulus vs. bulk stress for (a) gravel-cement, (b) limestone-cement, and (c) limestone-fly ash-lime samples.



(b)



(c)

**Figure 5-2 cont'd -Typical resilient modulus vs. bulk stress for (a) gravel-cement, (b) limestone-cement, and (c) limestone-fly ash-lime samples.**

**Table 5-1 Overall Summary of Resilient Modulus Samples**

Sample No.	Material	Target Conditions	w%	Dry Unit Wt., lb/ft <sup>3</sup>	Strength, psi	Model Parameters ME design guide equation			
						k <sub>1</sub>	k <sub>2</sub>	k <sub>3</sub>	r <sup>2</sup>
A1	Gravel-Cement	optimum	8.28%	132.0	184	3079.730	0.394	0.498	0.931
A2		optimum	8.11%	130.8	212	1562.452	0.271	1.761	0.932
A3		optimum	8.71%	130.2	172	1202.578	0.971	0.469	0.973
A4		optimum	9.14%	130.5	171	2790.655	0.403	0.570	0.987
A5		optimum	8.88%	128.5	194	1306.887	1.433	-0.495	0.973
A6		optimum	8.92%	132.3	158	1443.905	0.587	0.822	0.952
4A1		optimum	8.55%	128.7	341	2003.444	0.468	0.222	0.980
4A2	Limestone-Cement	optimum	7.76%	127.8	317	1464.756	1.006	-0.065	0.990
4A3		optimum	7.34%	128.8	376	2953.090	0.782	-0.111	0.980
B1		optimum	7.03%	138.5	193	1592.736	0.784	0.437	0.926
B2		optimum	6.94%	137.8	173	1955.028	0.892	-0.137	0.992
B3		optimum	8.14%	133.9	210	2402.817	0.658	0.069	0.966
B4		optimum	8.15%	134.5	212	1593.053	1.180	-0.396	0.949
B5		optimum	7.76%	136.2	230	3796.166	0.472	-0.066	0.977
B6		optimum	7.30%	137.3	258	2784.585	0.804	-0.142	0.962
4B1	Limestone-Fly Ash Lime	optimum	7.31%	138.8	418	2592.266	0.773	-0.091	0.979
4B2		optimum	6.88%	140.4	430	2913.109	0.642	0.004	0.972
4B3		optimum	7.91%	137.4	376	2394.377	0.391	0.572	0.992
C1		optimum	6.99%	139.0	149	1780.476	0.377	0.893	0.898
C2		optimum	7.15%	139.6	164	2437.056	0.396	0.605	0.967
C3		optimum	7.25%	138.5	229	1376.407	1.191	-0.247	0.914
C4		optimum	7.30%	139.3	128	1932.406	0.352	1.092	0.909
C5	Limestone-Fly Ash Lime	optimum	7.20%	139.5	142	2205.087	0.522	0.699	0.905
C6		optimum	7.14%	140.3	127	1894.927	0.617	0.415	0.877
4C1		optimum	7.29%	138.3	204	2009.565	0.348	0.614	0.980
4C2		optimum	7.33%	138.2	258	1443.606	0.664	0.810	0.964
4C3		optimum	6.78%	138.5	304	1609.028	0.308	0.684	0.927

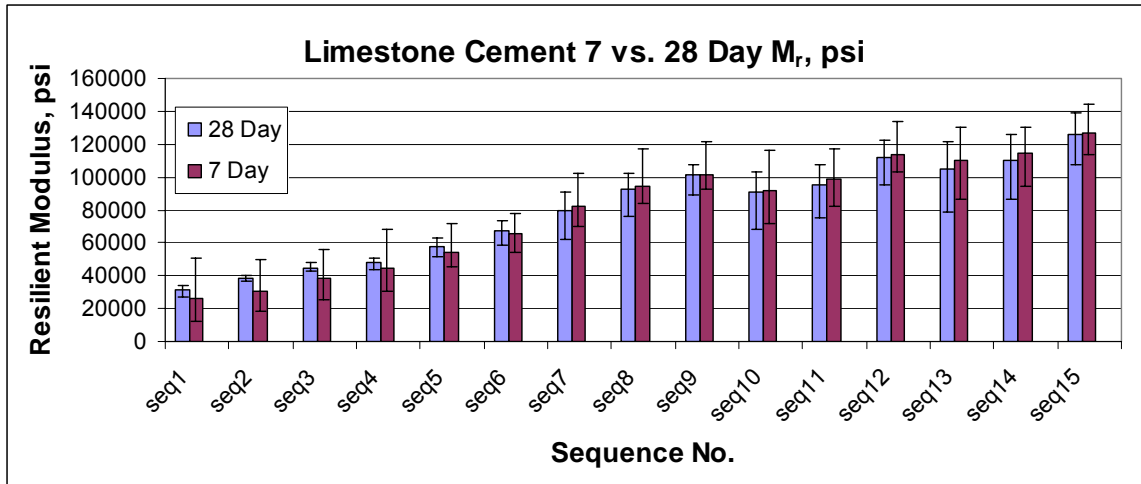
Equation 2 shows just how much resilient modulus is dependent on stress states. The major and minor principal stresses play an important role and care needs to be taken when estimating these parameters. As you go deeper in the pavement, a higher bulk stress and octahedral shear stress based on geostatic stresses will be encountered, leading to a resilient modulus that varies with depth. In the 2003 MEPDG,  $k_1$ ,  $k_2$ , and  $k_3$  are the inputs, not the resilient modulus or layer coefficient for base materials. The new design guide goes on to describe  $k_1$ ,  $k_2$ , and  $k_3$  further:

“Coefficient  $k_1$  is proportional to Young’s modulus. Thus, the values for  $k_1$  should be positive since  $M_r$  can never be negative. Increasing the bulk stress,  $\theta$ , should produce a stiffening or hardening of the material which results in a higher  $M_r$ . Therefore, the exponent  $k_2$ , of the bulk stress term for the above constitutive equation should also be positive. Coefficient  $k_3$  is the exponent of the octahedral shear stress term. The values for  $k_3$  should be negative since increasing shear stresses will produce a softening of the material (i.e. a lower  $M_r$ ).” (MEPDG, 2003)

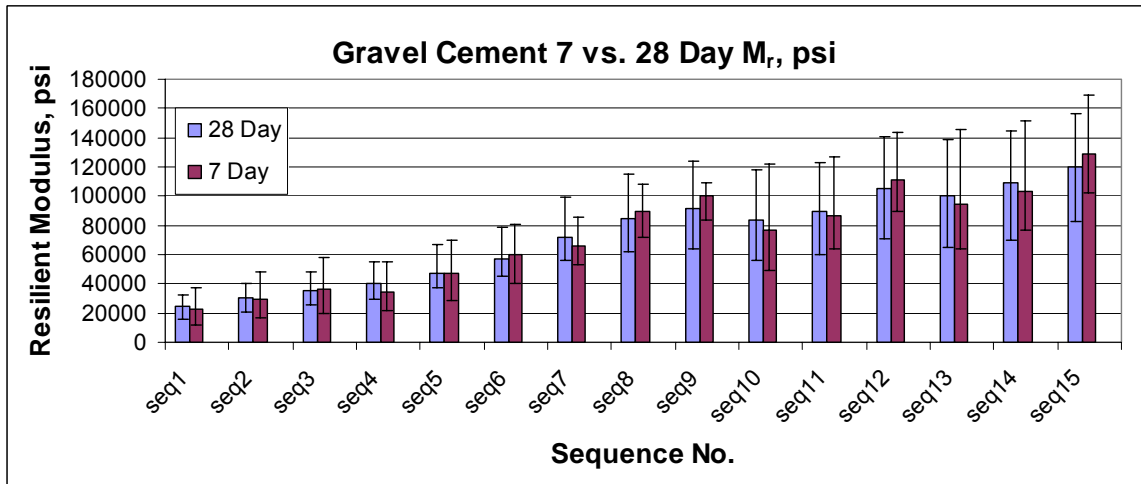
A similar relation of the coefficients to the stress terms can be seen from the materials tested in this study with the exception of the  $k_3$  term. The above description was describing the response of unbound granular materials. The  $k_3$  term for bound granular materials can be seen to have both positive and negative values, within a range of about  $\pm 1$  and approximately centered on 0.

Six samples of each material were tested at a 7 day cure and three samples of each material were tested at 28 day cure. Figure 5-3 shows the comparison of 7 and 28 day experimental resilient modulus results for the three base materials tested. The mean is shown by the bars, with the range of each group of tests shown by the tick marks and lines. There is very little difference in the two curing periods for limestone and cement and the disparity could be attributed to the difference in the number of samples tested. Likewise, there is little difference between 7 and 28 day strength for the gravel cement, and, although the ranges of moduli are slightly greater, they are greater for both 7 and 28 day curing times. On the other hand, the limestone, fly ash, and lime samples behave differently than the samples stabilized with cement. Fig 5-3(c) shows the 28 day moduli to be consistently less than the 7 day samples. This could be due to extended exposure to the air during its curing time, resulting in an erosion of the chemical bonds built up by the lime and fly ash, which is an effect called carbonation (Little, 2000).

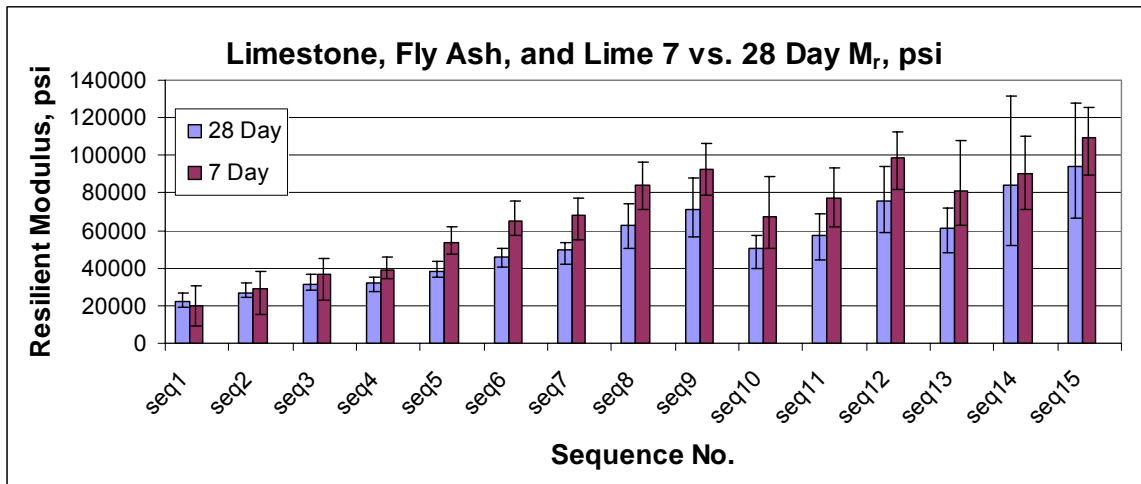
Both the cement treated gravel and cement treated limestone were modeled with both the 7 day and 28 day samples together, as no significant difference was observed from the resilient moduli of the two curing periods. Limestone with fly ash and lime showed discrepancies between the 7 day and 28 day curing periods. The 28 day samples generally showed a decrease in modulus compared to the 7 day, especially in the sequences with higher stresses. Because it was assumed



(a)



(b)



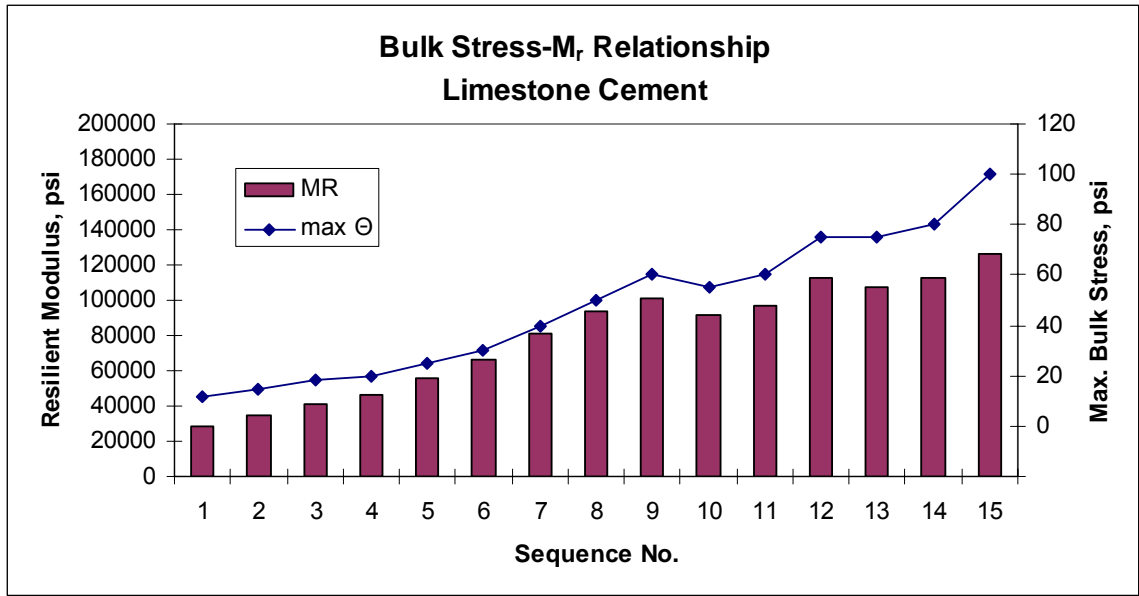
(c)

**Figure 5-3 - Resilient modulus comparison of 7 and 28 day samples of (a)Limestone cement, (b) Gravel Cement, and (c) Limestone, fly ash, and lime.**

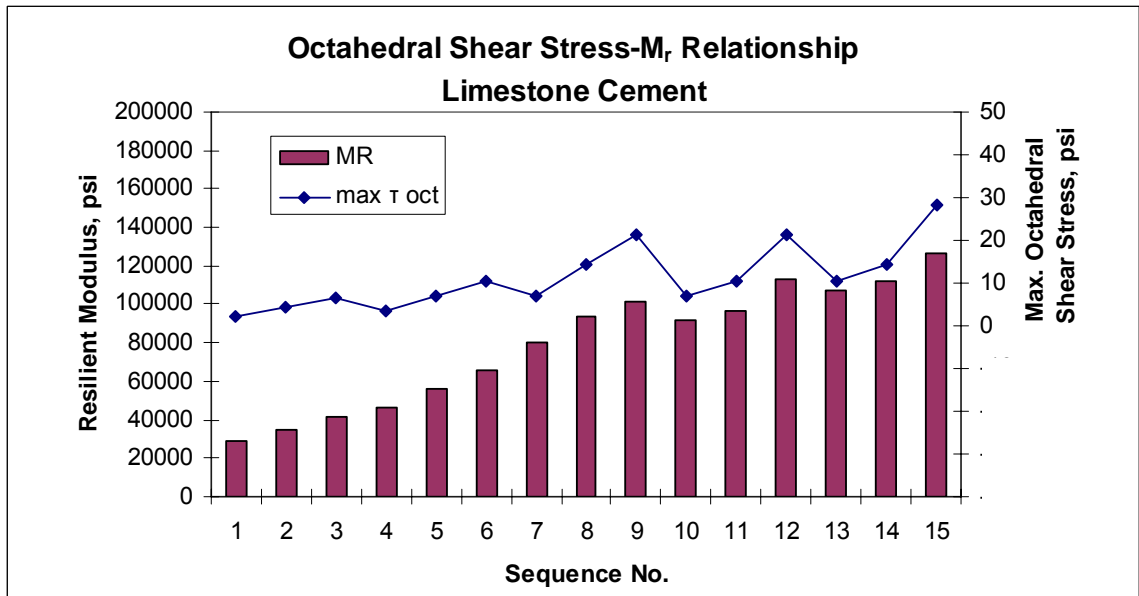
that the curing affected the 28 day resilient modulus of the limestone with fly ash and lime samples, the model parameters were generated solely from 7-day sample data.

Figure 5-4(a) shows the relationship between the overall mean resilient modulus of all 9 (7 and 28 day) limestone cement samples for each sequence and the ideal, or target, maximum bulk stress,  $\theta$ , that should be experienced from the samples on each sequence. This depicts a good correlation between the two as the general shape of the bar chart is nearly outlined by the line graph. Sequences 10 and 13 specifically are significant because these two points represents two of the 5 changes in confining pressure and the decrease in overall bulk stress goes along with a decrease in resilient modulus. Figure 5-4(b) shows the same relation of resilient modulus but this time it is depicted along with theoretical maximum octahedral shear stress. The general shape of the two is the same, but it can be seen that the resilient modulus is not as strongly correlated to the shear stress. The groupings of three sequences with the same confining pressure and changes in confining pressure are even more evident in the depiction of octahedral shear stress/bulk stress, Figure 5-4(c). The theoretical maximum bulk stress and octahedral shear stresses come from the earlier definitions and the AASHTO T 307 guidelines for loading for each sample. These stresses are shown in Table 3-1. It should be noted that each sequence and each sample were not necessarily tested at the exact target cyclic and constant stress, but the actual stress values were used for the calculation of resilient modulus and the development of the mechanistic-empirical model. Deviations from the target stresses originated from the load controlling module, but since the resilient modulus is a function of stress state, this had no effect on the resulting model parameters.



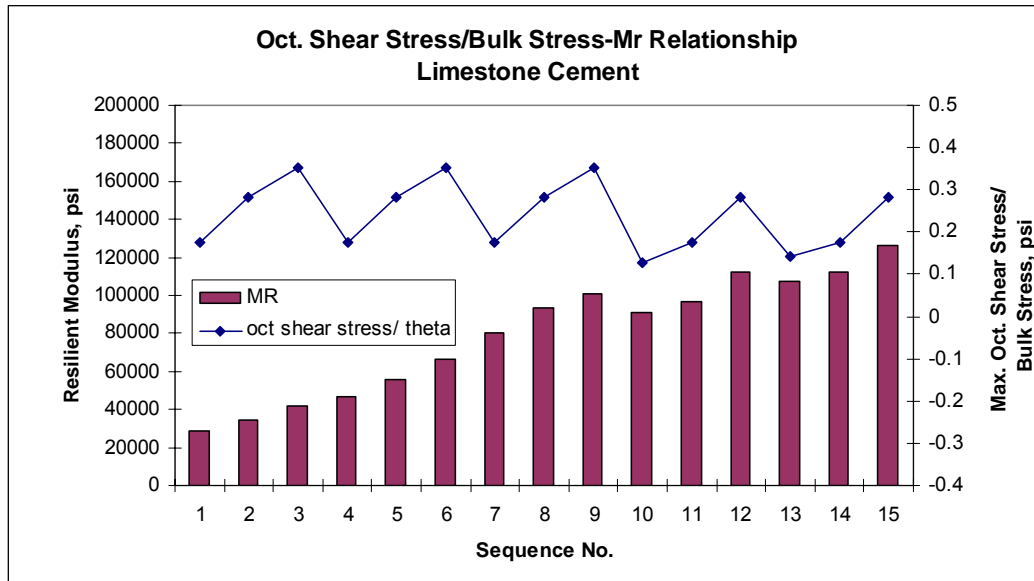


(a)



(b)

Figure 5-4 Typical relationship of resilient modulus with (a) bulk stress, (b) octahedral shear stress, and (c) octahedral shear stress/ bulk stress.



(c)

**Figure 5-4 cont'd - Typical relationship of resilient modulus with (a) bulk stress, (b) octahedral shear stress, and (c) octahedral shear stress/ bulk stress.**

## 6 Analysis

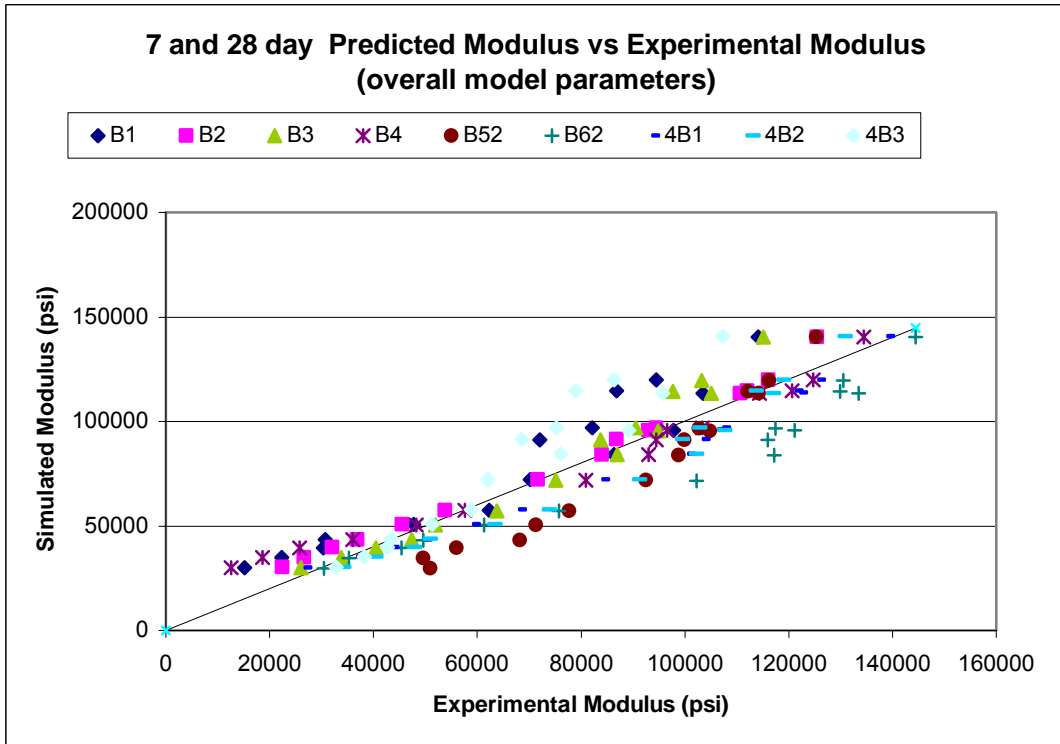
### 6.1 Overall MEPDG models for Resilient Modulus

Older pavement design equations, such as those proposed by Rada and Witczak and the 1993 AASHTO Pavement Design Guide, among others use only bulk stress to model resilient modulus. The 2003 MEPDG however uses both octahedral shear stress and bulk stress to model it. Both models were investigated and the newer model gave a higher  $r^2$  value for every sample as would be expected by the addition of a variable. The lowest individual  $r^2$  from the MEPDG model was 0.877 and the overall average from 27 resilient modulus tests was 0.954. The single stress state bulk stress model used a different definition of resilient modulus than is proposed in the 2003 MEPDG. Until recently, the resilient modulus was defined as the deviator stress divided by resilient strain. Inconsistent definitions make it hard to compare current moduli to those obtained in the 80s and 90s. Once again, the resilient modulus used in this paper was the cyclic stress divided by the resilient strain. The model is defined in terms of three variables,  $k_1$ ,  $k_2$ , and  $k_3$ . A summary of all individual model parameters as well as the goodness of fit and other soil properties is given in Table 5-1. The development of each equation and relation of tested value to predicted value can be found in Appendix B for each sample that underwent resilient modulus testing.

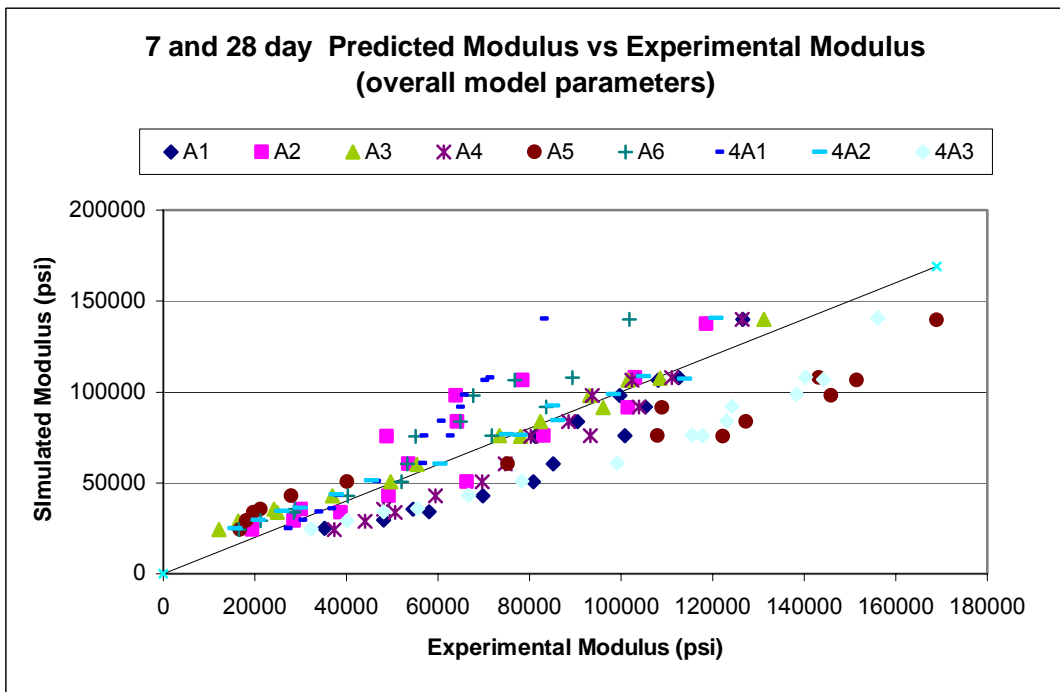
An overall resilient modulus model was created for each material. For all limestone-cement and gravel-cement samples, both 7 and 28 days test samples were used to obtain an overall model. For the limestone-fly ash- lime samples, only the 7 day tests were used. The characteristic coefficients for each material and the coefficients of correlation,  $r^2$ , are listed in Table 6-1. As expected, the  $r^2$  for the overall models are somewhat lower than the  $r^2$  for each of the individual tests as represented in Table 5-1. However, the overall models have coefficients of correlations from 0.77 to 0.84 which suggests good performance. Figure 6-1 compares the overall MEPDG material model with the experimental test results for each of the three materials.

**Table 6-1 Overall model equations for each material**

	$k_1$	$k_2$	$k_3$	$r^2$
Limestone-Cement	2364.025	0.734	0.021	0.844
Gravel-Cement	1855.515	0.702	0.409	0.767
Limestone-Fly Ash-Lime	1906.295	0.576	0.579	0.813

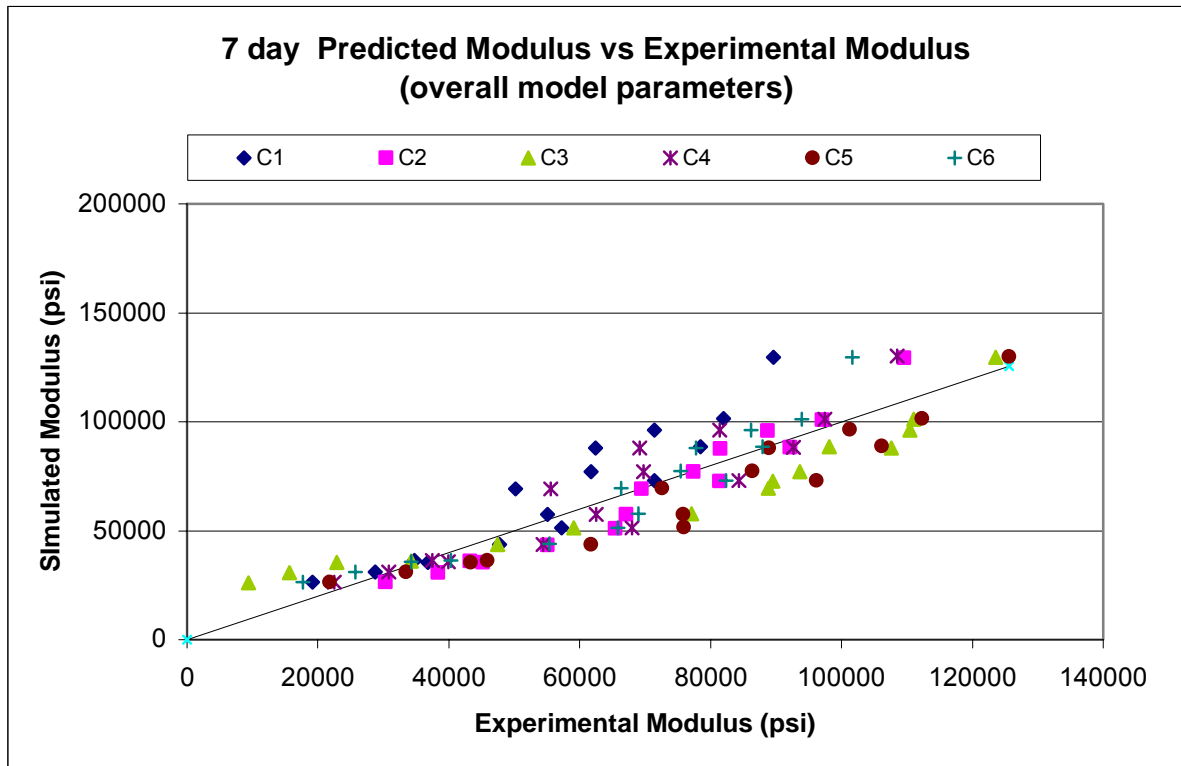


(a.) Limestone and Cement



(b.) Gravel and Cement

**Figure 6-1 Experimental results vs. Overall models for (a.) Limestone and cement, (b.) Gravel Cement, and (c.) Limestone, Fly Ash, and Lime**



(c.) Limestone, Fly Ash, and Lime

Figure 6-1 – Cont'd (c.) Limestone, Fly Ash, and Lime

## 6.2 Layer Coefficients

In the 1993 AASHTO Pavement design guide, resilient modulus for untreated base material was used to obtain a structural layer coefficient,  $a_2$ , as defined in equation 3.

$$a_2 = 0.249(\log_{10} E_{BS}) - 0.977 \quad (3)$$

Where

$E_{BS}$  = Resilient Modulus

$a_2$  = structural layer coefficient for base

In this method of pavement design developed from the AASHTO road test in 1962,  $a_2$  was able to be predicted by resilient modulus, CBR, Texas Triaxial, or R-value testing. A nomograph was developed to relate all these to one another. Similar to the untreated base, a nomograph was developed that related 7 day unconfined

compressive strength and resilient modulus to the same structural layer coefficient,  $a_2$ . A resilient modulus of approximately 100,000 psi correlates to a structural coefficient of 0.26. The standard makes no mention about amount of cement or other types of binder. (AASHTO, 1993)

With the new 2003 model of resilient modulus, a layer coefficient is no longer needed; only  $k_1$ ,  $k_2$ , and  $k_3$  need to be put in. MEPDG software takes into account these parameters and other material properties to model the pavement. However, an attempt is made here to obtain a layer coefficients for the three base materials tested. In general, if you go deeper in the base layer, the resilient modulus will increase. Using the 1993 equation, this would give a varying layer coefficient with depth. To more easily digest the results, the stress conditions calculated at the middle of the pavement layer were used to obtain the predicted modulus from the developed equations. Finite Element and Layered Elastic theory were used to determine the stresses in the pavement layers.

There is a fundamental difference between stresses induced in the laboratory tests and the stresses the base layers are exposed to in the field. The pavement layers in the field are connected in a theoretically “infinite” horizontal layer. A wheel load only compresses a small area of this layer and creates bending stress. The laboratory samples are not exposed to this same type of stress due to its size and loading. The test setup mimics some important features of the real world loading but simply can not mimic others. A constant horizontal stress is applied by the confining pressure to act like geostatic horizontal stress that actually increases with depth. The confining pressure is also not able apply additional horizontal stress, whether it be positive or negative, that would be due to bending. The size of the samples also do not allow for bending since the vertical load is applied over the entire horizontal area. The resilient modulus modeling of these tests only take into account the horizontal stress due to confining pressure. In some cases in the field, the bending stress applies a tension and decreases the horizontal stresses and therefore the bulk stress, and leads to a weaker modulus from the model. The stresses were calculated in the middle of the layer to neglect as much of the bending stress as possible.

Typical pavement thicknesses for an interstate and a state road were considered for this investigation. Figure 6-2 shows a schematic layout for the three different pavement sections considered. The “thick” pavement is a typical design for Interstates in Tennessee, the “medium” is a typical design for a State route in Tennessee, and the “thin” is a smaller pavement created just to see the additional effect of modulus and layer coefficient based on depth of asphalt. All subgrades are assumed to be infinitely thick in relation to the other two layers. Except the base layer modulus which was thrice iterated, all material properties were kept the same for all three cases and initial conditions are summarized in Table 6-2. Each pavement section investigated was subject to a circular load with a radius of 6 inches and pressure of 100 psi to mimic a semi truck wheel. Stresses were

investigated directly under the center of this loading. ADINA-AUI 2007 900 node version finite element software and linear elastic response was used for this investigation. Each section was modeled as a half space with axisymmetric, 9-node elements. Vertical boundaries were allowed only vertical translation and that bottom horizontal boundary was fixed in all directions and rotations. A no-friction contact surface was placed between the asphalt layer and the base material where stresses were in question. A representative finite element mesh is pictured in Figure 6-3, showing the contact surface, mesh and loading. After vertical and horizontal stresses were obtained for the middle of the base layer, and resilient moduli were calculated using the individual model parameters, the process was repeated with the only change being the modulus of the base, and then the layer coefficients were obtained using equation 3. The final modulus of the base layer and layer coefficients after three iterations are shown in Table 6-3. The stresses obtained appear to correspond to the lower half of the range of stresses under which the resilient modulus test is conducted (sequences 1 to 7 from Table 3-1).

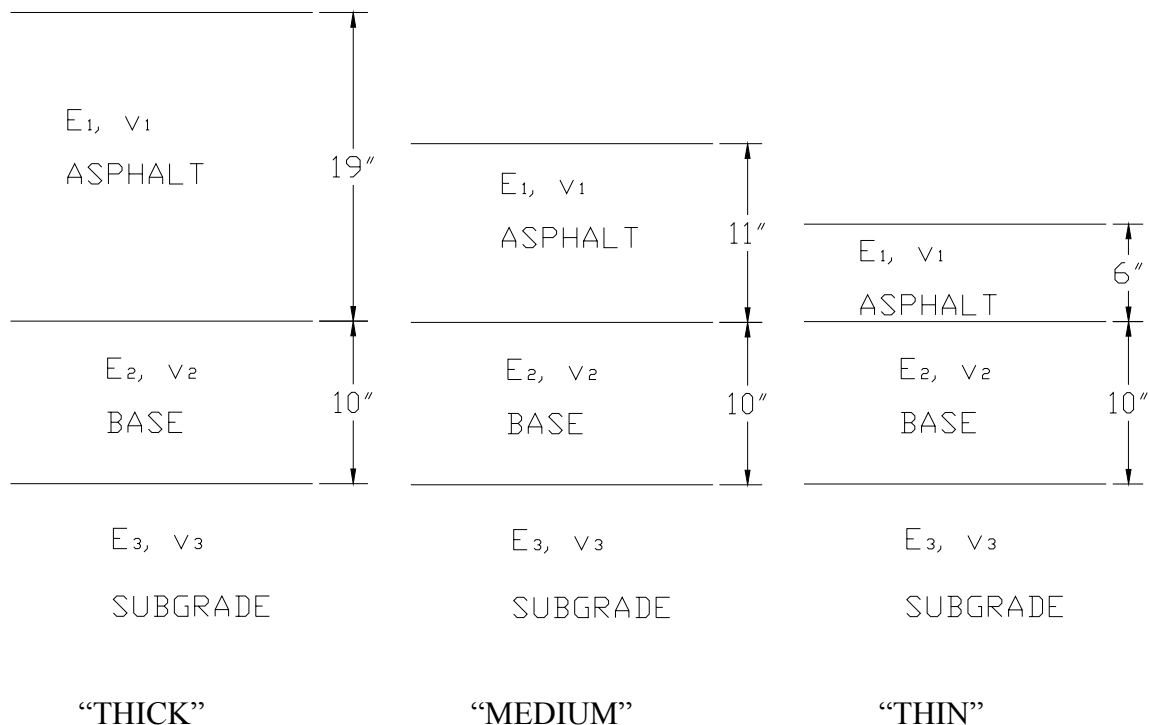


**Figure 6-2 Pavement Thicknesses Considered for Finite Element Models**

**Table 6-2 Initial Layered Material Properties and Stresses at Mid-layer of Base**

	$E_1$ , psi	$\nu_1$	$H_1$ , in.	$E_2$ , psi	$\nu_2$	$H_2$ , in.	$E_3$ , psi	$\nu_3$	$H_3$ , in.	$\sigma_1$ , psi	$\sigma_3$ , psi
Thick	400000	0.35	19	60000	0.35	10	15000	0.45	" $\infty$ "	7.167	3.459
Medium	400000	0.35	11	60000	0.35	10	15000	0.45	" $\infty$ "	10.357	3.764
Thin	400000	0.35	6	60000	0.35	10	15000	0.45	" $\infty$ "	22.051	5.304

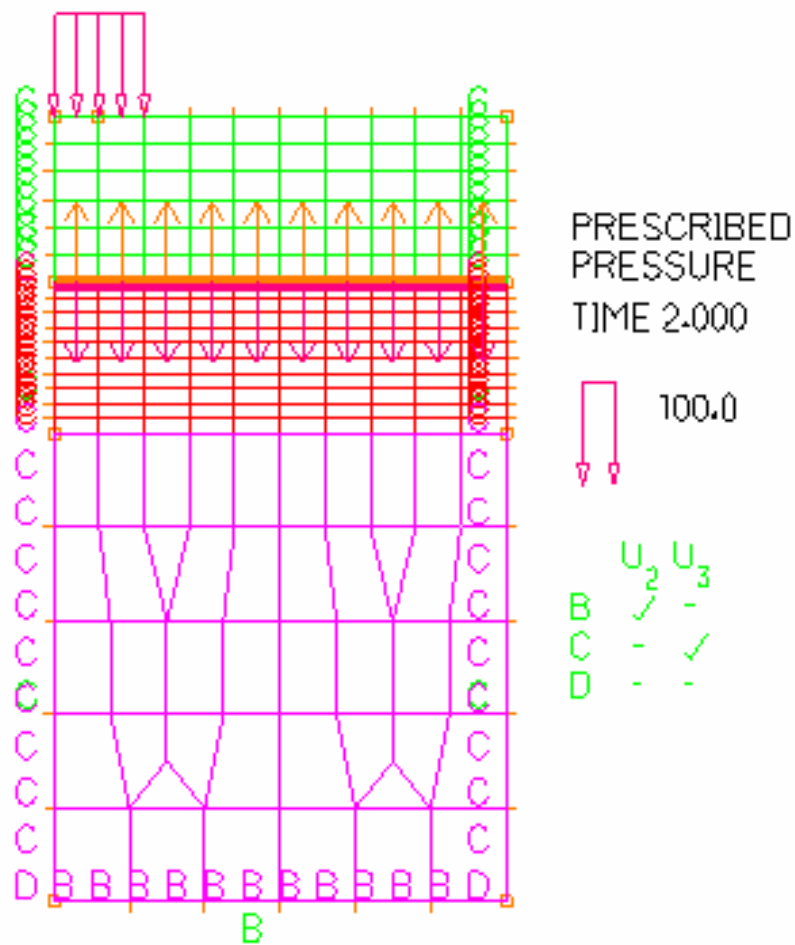


**Figure 6-3 Finite Element Mesh of Medium Pavement (ADINA-AUI 8.4, 2007)**



**Table 6-3 Modeled Moduli and Layer Coefficients for Pavements**

	Limestone-cement		Gravel Cement		Limestone fly ash lime	
	$M_R$	$a_2$	$M_R$	$a_2$	$M_R$	$a_2$
Thick	33090	0.15	26928	0.13	28478	0.13
Medium	38473	0.16	31386	0.14	32836	0.15
Thin	63457	0.22	56349	0.21	56293	0.21

**Table 6-4 Standard TDOT Base Layer Coefficients**

Material	Layer Coefficient, $a_2$
Limestone (unbound)	0.14
Gravel (unbound)	0.13
Limestone & Cement	0.23
Gravel & Cement	0.23
Limestone with Lime and Fly Ash	0.28

The Tennessee Department of Transportation currently uses fixed standard layer coefficients for pavement design. These values, for both bound and unbound base materials, are summarized in Table 6-4. Layer coefficients generated for bound base materials from resilient modulus-stress state relations and Equation 3 are drastically smaller than the accepted coefficients in use by TDOT today. They are about the same as the coefficient of unbound gravel. Clearly, using a higher stress state will lead to a higher resilient modulus and therefore a higher layer coefficient using equation 3. It is difficult to use the 2003 MEPDG resilient modulus modeling parameters to obtain a layer coefficient that is used for the 1993 Pavement Design Guide due to the fact that many of the latter's relationships are empirically obtained from studies and tests conducted nearly 40 years ago at the AASHO road test in Ottawa, Illinois (Van Til, 1972).

### ***6.3 Correlations to Resilient Modulus and Layer Coefficients***

An attempt was made to correlate simpler tests to resilient modulus and layer coefficients. 48 Unconfined Compression Tests, on samples that had and had not undergone resilient modulus testing and 18 CBR tests were used with empirical correlations to obtain resilient modulus and base layer coefficients. Table 6-5 is a summary of predicted moduli and layer coefficients based on CBR values and Table 6-6 is a summary of the predicted moduli generated based on UCS.

Several different approximate models are used in these tables. First, using stress strain data from UCS tests, a hyperbolic relationship between stress and strain

was assumed to find an initial tangent modulus.. Using this same data, a visual modulus was estimated by finding an approximately linear part of the stress strain curve during the UCS tests.

Also, the 2003 MEPDG suggests correlations between UCS and resilient modulus for lime stabilized soil and lime cement fly ash (Table 2.2.42). These relationships are also shown in Table 6-6. The range of these predicted values from the various methods are very encouraging as they are approximately the range of values obtained from resilient modulus testing for each sample (Appendix B). Also, the low end of the range corresponds with the moduli obtained from the constitutive equations with generated parameters from testing and stresses experienced during sequence 3 of resilient modulus testing which is about the same stress states as the middle of the base layer experiences in “thick” pavement aforementioned.

Figure 6-4 shows a summary of predicted resilient moduli and layer coefficients. The range of all the values can easily be seen as well as the many methods used for predicted and estimating the layer moduli and coefficients. It is also easy to see how they compare to the standard values TDOT uses currently. The dashed line is Equation 3 plotted out.

**Table 6-5 Predicted Moduli and Layer Coefficients based on CBR**

	Actual CBR	Predicted based on AASHTO T193		Predicted based on Rada & Witczak	
		$M_r$	$a_2$	$M_r$	$a_2$
Gravel- Cement	503	136928	0.302	178786	0.331
Limestone- Cement	527	140964	0.305	187088	0.336
Limestone- Fly Ash Lime	568	147954	0.310	201783	0.344

**Table 6-6 Predicted Resilient Moduli Based on UCS (units = psi)**

		UCS		Hyperbolic Model				Visually Estimated Modulus		Lime Cement Fly Ash Relation		Lime stabilized Soils Relation		Range		$\sigma_1 = 12$  $\sigma_2 = \sigma_3$  pred $M_R$ at seq 3
				Predicted UCS		Initial Modulus				ASTM C 593		ASTM D 5102				
				Mean	Std. Dev.	Mean	Std. Dev.			Predicted E based on $q_u$		Predicted $M_r$ based on $q_u$				
		Mean	Std. Dev.	Mean	Std. Dev.	Mean	Std. Dev.	Mean	Std. Dev.	Mean	Std. Dev.	Mean	Std. Dev.	Min	Max	
Gravel- Cement	7 Day	200	34	348	146	134039	60521	46035	10951	100056	17124	34794	4247	34794	134039	34682
	28 Day	328	28	707	236	108522	38626	46056	3261	163750	14088	50590	3494	46056	163750	35353
Limestone- Cement	7 Day	231	40	329	109	76758	21053	33229	9046	115389	19923	38596	4941	33229	115389	38327
	28 Day	357	65	559	212	121269	13329	49944	7310	178500	32410	54248	8038	49944	178500	45399
Limestone- Fly Ash- Lime	7 Day	157	31	212	69	75669	29132	30525	8454	78500	15439	29448	3829	29448	78500	36464
	28 Day	268	38	368	61	138948	35208	45081	11373	134000	18950	43212	4700	43212	138948	32130

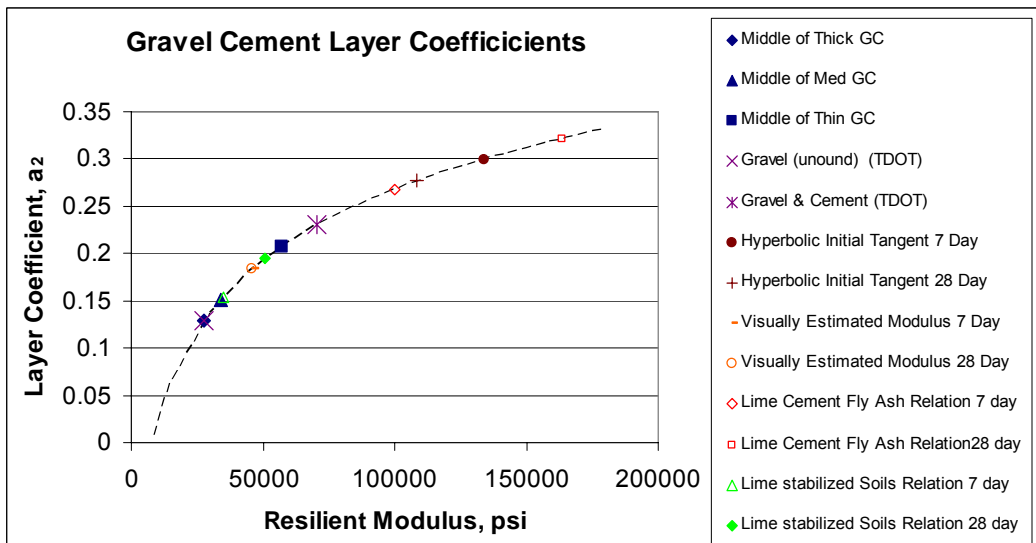
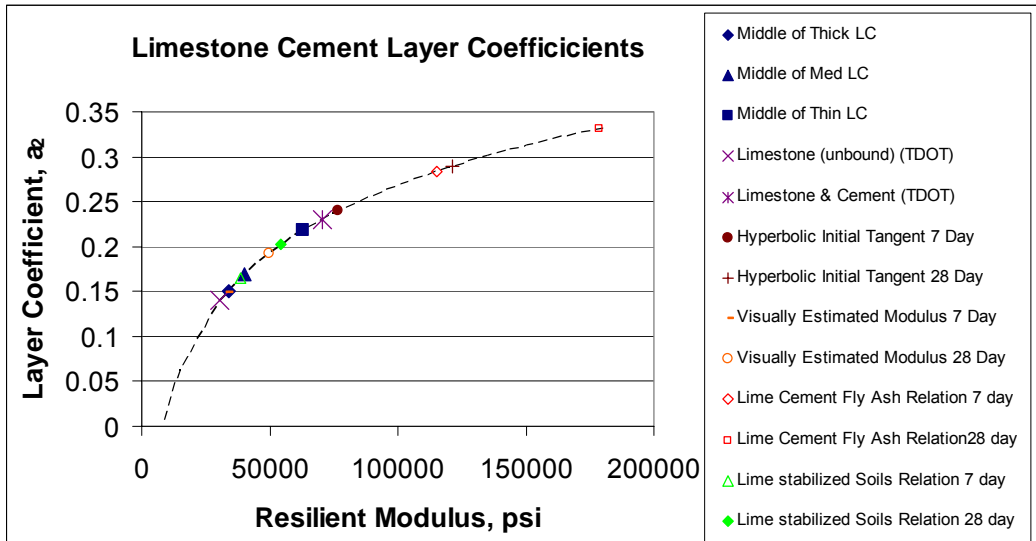
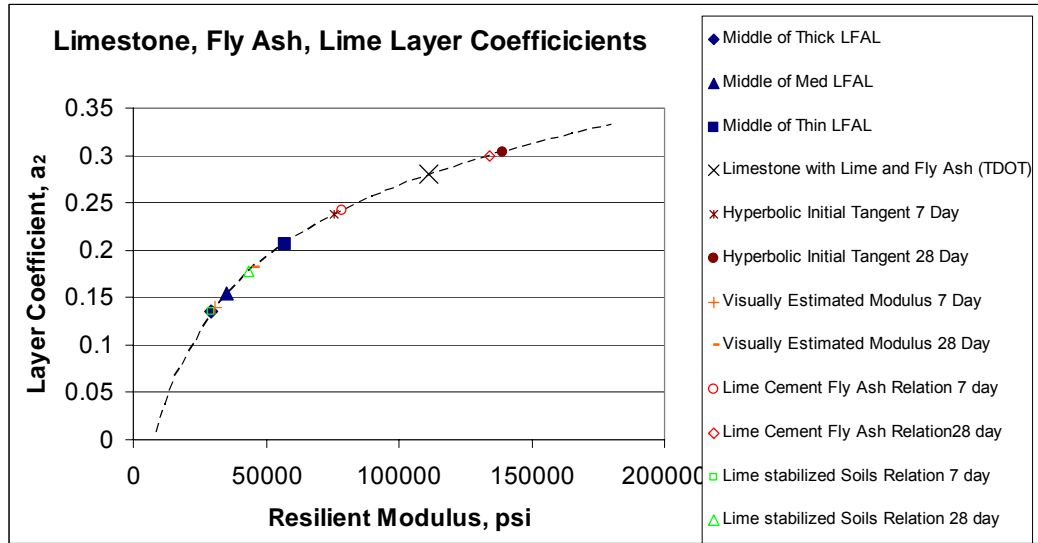


**Figure 6-4 Layer Coefficients for (a) Limestone Cement, (b) Gravel Cement, and (c) Limestone Fly ash Lime**



(c)

Figure 6-4 cont'd - Layer Coefficients for (a) Limestone Cement, (b) Gravel Cement, and (c) Limestone Fly ash Lime

## **7 Summary and Conclusions**

Laboratory resilient modulus tests have been conducted on bound base materials typically used in the state of Tennessee: Limestone cement, gravel cement, and limestone-fly ash-lime. Tests were analyzed based on Level 1 input for the 2003 MEPDG and coefficients for input into MEPDG software were obtained for each of the three stabilized base materials. To provide a conservative estimate of response, the cement bound materials were tested on the low end of the range allowed (3% out of the specified 3-5% cement content). These materials would be expected to have higher resilient modulus values if a larger amount of cement were used. The materials combined with lime and fly ash had slightly lower resilient modulus values than expected which could be due to the curing process or dysfunctional lime. Tests conducted at 28 days for these samples were ignored and only the 7 day resilient modulus tests were used to model the limestone-fly ash-lime combination.

It was difficult to correlate resilient modulus tests with layer coefficient because stress states in typical thick TDOT pavement layers were lower than expected. Better correlations existed between UCS and CBR tests with resilient modulus. These empirical relations gave ranges of moduli that were typically recorded during the lab testing and layer coefficients that were comparable to those that are currently in use by TDOT. Currently it is not suggested that TDOT change its layer coefficients for bound base materials based on the tests in this report. However, should the 2003 MEPDG ever be implemented by TDOT, it is suggested that the coefficients contained herein be used.

## **REFERENCES**

AASHTO Guide for Design of Pavement Structures. AASHTO, Washington, D.C., 1993.

AASHTO T307-99 (2003). Determining the Resilient Modulus of Soils and Aggregate Materials.

ADINA-AUI, 900 nodes version 8.4, 1994-2007. Adina R & D, inc. F

ASTM C136-06. Standard Test Method for Sieve Analysis of Fine and Course Aggregates. Annual Book of ASTM Standards. American Society for Testing and Materials. Easton, MD, 2006

ASTM C593. Standard Specification for Fly Ash and Other Pozzolans for Use with Lime for Soil Stabilization. Annual Book of ASTM Standards. American Society for Testing and Materials. Easton, MD, 2006

ASTM D1633-00. Standard Test Methods for Compressive Strength of Molded Soil-Cement Cylinders. Annual Book of ASTM Standards. American Society for Testing and Materials. Easton, MD, 2000.

ASTM D2487-06. Standard Practice for Classification of Soils for Engineering Purposes (Unified Soil Classification System). Annual Book of ASTM Standards. American Society for Testing and Materials. Easton, MD, 2006

ASTM D4318. Standard Test Methods for Liquid Limit, Plastic Limit, and Plasticity of Soils. Annual Book of ASTM Standards. American Society for Testing and Materials. Easton, MD, 2000.

ASTM D5102-04. Standard Test Methods for Unconfined Compressive Strength of Soil-Lime Mixtures. Annual Book of ASTM Standards. American Society for Testing and Materials. Easton, MD, 2004.

Elias, Mohammed B. and Titi, Hani H. Evaluation of Resilient Modulus Model Parameters for Mechanistic-Empirical Pavement Design. Transportation Research Record: Journal of The Transportation Research Board, No. 1967, Transportation Research Board of the National Academies, Washington, D.C., 2006, pp.89-100.

Guide for Mechanistic-Empirical Design of New and Rehabilitated Pavement Structures. Final Report. Prepared for NCHRP by ARA, inc. ERES Consultants Division, Champaign, Illinois, March, 2004.



Khazanovich, Lev, Celauro Clara, Chadbourn, Bruce, Zollars, John, and Dai, Shongtao. Evaluation of Subgrade Resilient Modulus Predictive Model for Use in Mechanistic-Empirical Pavement Design Guide. Transportation Research Record: Journal of the Transportation Research Board, No. 1947, Transportation Research Board of the National Academies, Washington, D.C., 2006. pp. 155-166.

Kilday, Derek. "Resilient Moduli of Tennessee Base Materials". Forthcoming Masters Thesis. University of Tennessee, Knoxville, 2008.

Kongsukprasert, Lalana, Tatsuoka, Fumio, and Tateyama, Masaru. Several Factors Affecting the Strength and Deformation Characteristics of Cement-Mixed Gravel. Soils And Foundations. Vol. 45, No. 3. pp. 107-124, June 2005. Japanese Geotechnical Society.

Konrad, J.M. 2006. The Use of Tangent Stiffness to Characterize the Resilient Response of Unbound Crushed Aggregates. Canadian Geotech. Journal. Vol. 43, 2006. 1117-1130.

Lim, Seungwook and Zollinger, Dan G. Estimation of the Compressive Strength and Modulus of Elasticity of Cement-Treated Aggregate Base Materials. Transportation Research Record, Vol. 1837. p. 30-38. Paper No. 03-4448.

Little, Dallas, N. Evaluation of Structural Properties of Lime Stabilized Soils and Aggregates, Vol. 3: Mixture Design and Testing Protocol for Lime Stabilized Soils, Prepared for the National Lime Association, March, 2000.  
<http://www.lime.org>

NCHRP 1-37A. Guide for Mechanistic-Empirical Design of New and Rehabilitated Pavement Structures. Final Report. Ara Inc., ERES Consultants Division. Transportation Research Board. National Research Council. Washington, D.C., March, 2004.

Standard Specifications for Road and Bridge Construction. Tennessee Department of Transportation. March 1, 2006.  
<http://www.tdot.state.tn.us/construction/specs.htm> Accessed October 18, 2007.

TDOT Specification 309. Standard Specifications for Road and Bridge Construction. Tennessee Department of Transportation, Nashville, TN, 2006.

TDOT Specification 312. Standard Specifications for Road and Bridge Construction. Tennessee Department of Transportation, Nashville, TN, 2006.

TDOT Specification 903. Standard Specifications for Road and Bridge Construction. Tennessee Department of Transportation, Nashville, TN, 2006.

Tinsley, Andrew. Parametric Study of the Effects of Water to Cementitious Materials Ratio and Cementitious Materials Content on the Durability Properties of High Performance Concrete. M.S Thesis, University of Tennessee, Knoxville, August, 2007.

White, Gregory W. and Gnanendran, Carthigesu T. The Influence of Compaction Method and Density on the Strength and Modulus of Cementitiously Stabilised Pavement Materials. The International Journal of Pavement Engineering, Vol. 6, No. 2, June, 2005, p. 97- 110.

## **APPENDICES**

## **A. APPENDIX A**

### **Literature Review**

Lim, Seungwook and Zollinger, Dan G. Estimation of the Compressive Strength and Modulus of Elasticity of Cement-Treated Aggregate Base Materials. Transportation Research Record, Vol. 1837. p. 30-38. Paper No. 03-4448.

Experiments were done on 189 samples of cement treated aggregate base (CTAB)(4% and 8% cement). Cement content, coarse aggregate content, and fine aggregate content were investigated. Some samples were conventional crushed limestone base. CTAB generally has higher cement and coarse aggregate contents and an elastic slab like performance. Tensile strength and flexural strength were 10 -25 % of unconfined compressive strength (UCS). (Generally accepted is 10% for design). Modulus is hard to get from tests, so a relationship between modulus and UCS is desired. Maximum aggregate size was  $\frac{3}{4}$ ". 4" by 8" Samples tested at 1, 3, 7, and 28 days. Recycled concrete samples were weaker than base samples probably due to high optimum moisture content and therefore a high water/cement ratio. Cement content appears to be the most influencing factor for the strength development regardless of aggregate type. A new time dependent model of compressive strength is proposed with new coefficients based on 28 day compressive tests. Modulus was investigated using initial secant at 25% of the ultimate stress. A revamped ACI equation for modulus is derived that is more conservative and more applicable to base materials. Typical modulus values are given and can be used to compare my results.

---

White, Gregory W. and Gnanendran, Carthigesu T. The Influence of Compaction Method and Density on the Strength and Modulus of Cementitiously Stabilised Pavement Materials. The International Journal of Pavement Engineering, Vol. 6, No. 2, June, 2005, p. 97- 110.

Density has a significant effect on strength and modulus. Compaction method had no effect. Australian practice is to determine OMC and MDD density of aggregate itself and then add a percent or two. Samples compacted with standard, modified, and gyratory compaction. In their lit review a reduction of UCS was observed when time between adding water and compaction increased. In their lit review shows increasing RM with time. Used slag-lime binder for tests in 85 to 15 by dry mass ratio. Mixed with 7% binder to aggregate dry weight. Adding binder increased OMC and had mixed effects on MDD. Recycled material had enough fines already and addition of binder led to a decrease in MDD. New material as improved by addition of binder so MDD stayed the same or slightly increased. Recycled could also be less angular and rounded interlocking less. Compaction method is concluded not to be a significant determinant of strength or modulus, when compared at equal densities.

---

Mohammad, Louay N., Herath, Ananda, Rasoulia, Masood, and Zhongjie, Zhang. Laboratory Evaluation of Untreated and Treated Pavement Base Materials: Repeated Load Deformation Test. Transportation Research Record: Journal of the Transportation Research Board, No. 1967, Transportation Board of the National Academies, Washington, D.C., 2006, pp.78-88.

Pavement performance depends on resilient modulus as well as permanent deformation and other factors. A permanent deformation test is needed. Many factors affect permanent deformation including: material type, gradation, moisture content, dry unit weight, and deviator stress. Lab tests were run on treated and untreated samples taken from the field. Samples were 6" in diameter by 12" in height, compacted in 6 layers using vibratory hammer. Samples were sealed with polythene bags and left for 28 days curing in humid room. Non traditional resilient modulus testing was done. Confining and cyclic stresses weren't changed, only additional cycles were performed. One material showed high resilient modulus values but permanent deformation showed it was unstable under reported loading (the permanent deformation vs. number of load curve never leveled off). Even materials with same resilient modulus had drastically different permanent strains, showing resilient modulus test alone is not enough to model pavement design. Permanent deformation tests ordered the materials as performers in the same order as resilient modulus (non typical RM). There could be possible differences in the loads applied during tests of each material.

---

Konrad, J.-M. The Use of Tangent Stiffness to Characterize the Resilient Response of Unbound Crushed Aggregates. Canadian Geotechnical Journal. No. 43 pp.1117-1130, 2006. Published on the NRC Research Press Website at <http://cgj.nrc.ca> on 22 November, 2006.

Granular unbound samples are tested in this study. Poisson's ratio is known to vary with stress level in granular material. Most models use constant Poisson's ratio. 4" in diameter by 8" height samples. Samples made in 2 half molds with membrane with 25 blows per layer and 6 layers. 0.2 hertz loading with load cell inside triaxial cell. The same sample can be used over a variety of stress paths as long as the maximum deviator stress does not exceed 60% of the peak shear strength of the material. This study claims RM is secant modulus and non-unique and that tangent modulus is a better measure. This paper has little to contribute to my research. .

---

Van Til, C.J., McCullough, B.F., Vallerger, B.A., and Hicks, R.G. Evaluation of AASHO Interim Guides for Design of Pavement Structures. National Cooperative Highway Research Program Report 128. Highway Research Board, Washington, D.C. 1972

This report shows a summary of a questionnaire of all 50 state transportation organizations. Layer coefficients for cement treated base course varied from 0.12 to 0.30 depending on organization. . Layer coefficients for lime treated base course varied from 0.05 to 0.30 depending on organization. "It was decided as a result of Coffman that layered elastic theory could be used as a first step in determining variations of structural layer coefficients." Typical pavement moduli used for analysis: Asphaltic concrete- 150,000(summer) to 900,000 psi, Aggregate base- 15,000-30,000 psi, subgrade-3,000 to 15,000 psi. 4500 lb, 70 psi dual wheel load were used with layered elastic theory. Charts are given for determination of  $a_2$  based on other material properties for both untreated and treated base. These are the same charts used in the 1993 design guide! Original AASHO road test data suggested 0.15-0.23 for cement treated base and 0.15- 0.30 for lime treated base. These are either established from the road test or estimated with engineering judgement. These numbers are applicable only to the materials and environmental conditions at the AASHO road test. Arizona revised AASHO coefficients and they were generally lower. Cement treated base- 0.15 to 0.29. Untreated base varied from 0.06 to 0.14

---

Lominac, John Kent. Adaptation and Correlation of the Tennessee Method of Flexible Pavement Design to the AASHO Interim Guide. Masters Thesis. University of Tennessee, 1973.

"The structural number is an index number derived from an analysis of traffic and roadbed soil conditions. Layer coefficients are empirical relationships between structural number and layer thickness which expresses the relative ability of a material to function as a structural component of the pavement. " Tennessee specific values are needed based on AASHO Interim Pavement Design Guide. There are many environmental and geologic differences between Illinois and Tennessee. CBR was selected to obtain soil support index numbers. "This value has no theoretical or rational relationship to engineering characteristics of soils." Limestone base and sandy subbase materials were tested and were from all parts of Tennessee. A relationship similar to the layer coefficient  $a_2$  from 1993 PDG is given.  $SSV = 5.77\log(CBR) - 2.65$ . Calculated layer coefficients for surface: 0.4-0.44, base: 0.1-0.30, and subbase: 0.04-0.11. Static and dynamic CBR tests were done to correlate to soil structure value, SSV. An attempt to correlate Modulus of Elasticity from Triaxial tests to layer coefficient was undertaken. A nomograph was created relating Modulus, CBR, and layer coefficient.

---

Huang, Yang H. Pavement Analysis and Design, Second Edition. Pearson-Prentice Hall, Upper Saddle River, New Jersey, 2004.

Base course is used to control pumping, frost action, drainage, and reduce critical stress in concrete, and subbase can be used as filter. Typical values for cement treated materials and lime fly ash materials – 0.15. It is recommended that layer coefficient be based on resilient modulus. Typical values of theta are from 5 to 30 psi, depending on depth of base layer, asphalt concrete thickness, and roadbed soil resilient modulus.

---

Shao, Y. and Monkman, S. Carbonated Cementitious Materials and Their Role in CO<sub>2</sub> Sequestration. From “ Measuring, Monitoring, and Modeling Concrete Properties. Ed. M.S. Konsta-Gdoutos, 353-359. Springer, Netherlands, 2006.

Carbonation of concrete materials can create early strength and sequester excess carbon dioxide. 5 % of global carbon dioxide emissions come from cement production. A lot of cement is being produced and due to global warming an effort is being led to use other cementitious materials such as fly ash, or use other methods to control carbon dioxide emissions. Carbonation was done for 2 hours and a water to cementitious ratio of 0.15 was used. Rectangular samples were made of only cementitious paste and no aggregates. Three point bending tests and compressive strength tests were performed directly after two hour carbonation. Loose and compacted samples were also tested to see if porosity affects the absorption of CO<sub>2</sub>. Hydrated samples were also made and tested at 7 days. Loose samples reached distinctively higher temperatures when under pressure for 2 hours( carbonation is an exothermic reaction). Cement samples carbonated for 2 hours had higher compressive strengths then samples hydrated for 7 days. Fly ash and lime were considerably less than the cement samples and also had about twice the carbonation degree as the cement samples.

---

Khunthongkeaw, J and Tangtermsirikul, S. Model for Simulating Carbonation of Fly Ash Concrete. Journal of Materials in Civil Engineering, ASCE September/October 2005. pp 570-578.

A model for carbonation of concrete with and without fly ash is proposed and seems to be accurate. This paper is good for describing concrete reactions and not much more. May not be what is needed for this report, but it is still informative. If fly ash is used with cement, the rate of carbonation increases. Fly ash consumes calcium hydroxide (CH) that is produced in cement hydration.

---



Rada, Gonzalo, and Witczak, Matthew W. Comprehensive Evaluation of Laboratory Resilient Moduli Results for Granular Materials. Transportation Research Record, Vol. 810, pp 23-33.

A database of unbound granular material resilient moduli from 10 different agencies (271 test results) is compiled and different factors and their effects are probed. Here, resilient modulus is the ratio of cyclic deviator stress to resilient axial strain and it is modeled as  $M_r = k_1 \cdot \sigma_v^k$ . There was a poor relationship between resilient modulus and USCS of AASHTO soil classification. Different characteristics investigated were: aggregate type, degree of saturation, loading conditions, percent compaction, and aggregate degradation. Loading conditions has little effect on resilient modulus response. Degree of saturation plays an important part in resilient modulus response. At about 80-85% saturation, granular materials are unstable and fail in this test.  $k_1$  and  $k_3$  vary with saturation and not in the same way for all materials. Crusher run and other base material's  $k_1$  is improved by about 60% when the compactive effort goes from standard to modified. (12300 to 56200 lb/ft<sup>2</sup>). The most important factors on resilient modulus are stress state, saturation, and density. Bulk stresses for highway bases in a typical pavement range from 20 to 40 psi. The Hueklom and Foster relation of CBR to resilient modulus corresponds to a bulk stress of almost 400 psi. and new relationship of resilient modulus and cbr is proposed, this time with bulk stress added.

$$MR = CBR \cdot (490 \log(\sigma_v) - 243).$$

---

**B. APPENDIX B**  
**Laboratory Test Results**

**7-1 Summary of Resilient Modulus/ UCS Tests**

Sample No.	Material	Target Conditions	Water Content, %	Dry Unit Wt., lb/ft <sup>3</sup>	Strength, psi	Model Parameters ME design guide equation for M <sub>r</sub>			
						k <sub>1</sub>	k <sub>2</sub>	k <sub>3</sub>	r <sup>2</sup>
A1	Gravel-Cement	optimum	8.28%	132.0	184	3079.730	0.394	0.498	0.931
A2		optimum	8.11%	130.8	212	1562.452	0.271	1.761	0.932
A3		optimum	8.71%	130.2	172	1202.578	0.971	0.469	0.973
A4		optimum	9.14%	130.5	171	2790.655	0.403	0.570	0.987
A5		optimum	8.88%	128.5	194	1306.887	1.433	-0.495	0.973
A6		optimum	8.92%	132.3	158	1443.905	0.587	0.822	0.952
4A1		optimum	8.55%	128.7	341	2003.444	0.468	0.222	0.980
4A2		optimum	7.76%	127.8	317	1464.756	1.006	-0.065	0.990
4A3		optimum	7.34%	128.8	376	2953.090	0.782	-0.111	0.980
B1	Limestone-Cement	optimum	7.03%	138.5	193	1592.736	0.784	0.437	0.926
B2		optimum	6.94%	137.8	173	1955.028	0.892	-0.137	0.992
B3		optimum	8.14%	133.9	210	2402.817	0.658	0.069	0.966
B4		optimum	8.15%	134.5	212	1593.053	1.180	-0.396	0.949
B5		optimum	7.76%	136.2	230	3796.166	0.472	-0.066	0.977
B6		optimum	7.30%	137.3	258	2784.585	0.804	-0.142	0.962
4B1		optimum	7.31%	138.8	418	2592.266	0.773	-0.091	0.979
4B2		optimum	6.88%	140.4	430	2913.109	0.642	0.004	0.972
4B3		optimum	7.91%	137.4	376	2394.377	0.391	0.572	0.992
C1	Limestone-Fly Ash Lime	optimum	6.99%	139.0	149	1780.476	0.377	0.893	0.898
C2		optimum	7.15%	139.6	164	2437.056	0.396	0.605	0.967
C3		optimum	7.25%	138.5	229	1376.407	1.191	-0.247	0.914
C4		optimum	7.30%	139.3	128	1932.406	0.352	1.092	0.909
C5		optimum	7.20%	139.5	142	2205.087	0.522	0.699	0.905
C6		optimum	7.14%	140.3	127	1894.927	0.617	0.415	0.877
4C1		optimum	7.29%	138.3	204	2009.565	0.348	0.614	0.980
4C2		optimum	7.33%	138.2	258	1443.606	0.664	0.810	0.964
4C3		optimum	6.78%	138.5	304	1609.028	0.308	0.684	0.927

**Note: Sample No. XN, where X= material type, n = specimen number. A = Gravel-cement, B= Limestone cement, C = Limestone-fly ash lime, 4AN, 4BN, 4CN = 28 day specimens**

**7-2 UCS Test Results on Samples That Did Not Undergo RM Testing**

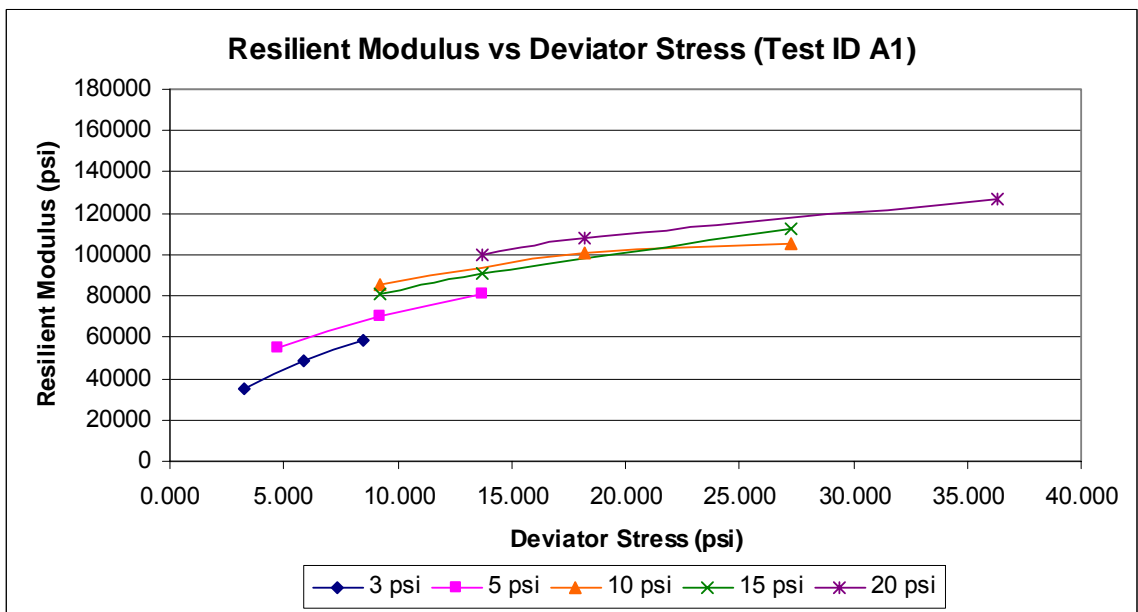
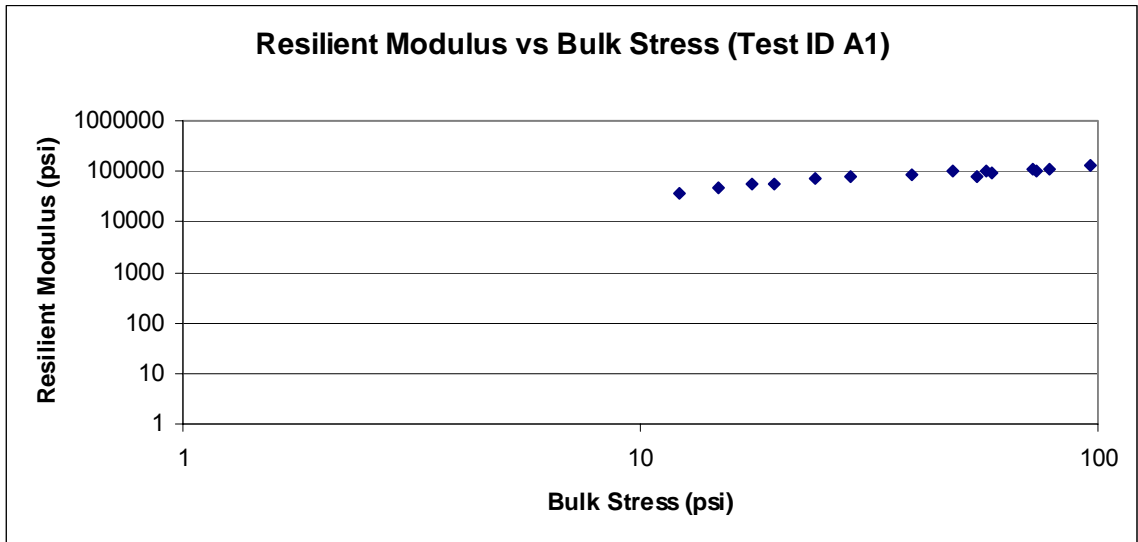
Sample No.	Material	Target Conditions	W%	Dry Unit Wt., lb/ft <sup>3</sup>	Strength, psi
4V4	Gravel-Cement	7 days No RM	9.86%	128.6	267
4V5			8.90%	130.1	230
4V6			10.33%	127.5	213
4V1		28 days no RM	9.16%	126.3	314
4V2			7.78%	125.4	323
4V3			8.90%	124.4	294
4W4	Limestone-Cement	7 days no RM	5.62%	131.4	234
4W5			6.53%	138.9	304
4W6			7.74%	138.0	263
4W1		28 days noRM	7.26%	139.3	314
4W2			6.69%	139.7	259
4W3			6.89%	140.1	345
L1	Limestone-Fly Ash Lime	7 days no RM	7.98%	136.6	143
L2			7.76%	136.9	162
L3			7.16%	138.1	169
D1		28 days noRM	7.63%	138.2	255
D3			7.23%	138.5	304
D4			7.00%	139.2	283
Y1		28 days no RM	7.74%	135.5	336
Y2			7.37%	136.0	359
Y3			100 deg. 7.33%	135.6	385

**7-3 CBR Test Results**

Sample No.	Material	Target Conditions	Water Content, %	Dry Unit Wt., lb/ft <sup>3</sup>	% compaction	CBR
E1	CBR, Gravel-Cement	optimum	8.12%	128.6	100%	438.9
E2		optimum	7.96%	128.1	100%	543.2
E3		optimum	9.83%	126.1	98%	539.9
E4		optimum	8.30%	128.9	101%	490.7
E5		optimum	8.27%	128.5	100%	558.9
E6		optimum	8.61%	127.3	99%	447.5
F1	CBR, Limestone-Cement	optimum	7.25%	136.3	101%	635.2
F2		optimum	6.79%	137.6	102%	687.2
F3		optimum	6.81%	135.0	100%	415.4
F4		optimum	7.07%	136.0	100%	582.4
F5		optimum	9.31%	130.4	96%	413.8
F6		optimum	7.49%	132.1	98%	425.3
H1	CBR, Limestone-Fly Ash Lime	optimum	7.32%	138.8	101%	523.2
H2		optimum	7.38%	140.1	102%	555.4
H3		optimum	7.39%	138.7	101%	553.3
H4		optimum	7.28%	137.8	101%	544.1
H5		optimum	6.77%	139.1	102%	547.3
H6		optimum	6.79%	141.0	103%	684.1

*a. Gravel and cement, 7 days*

**i. A1**



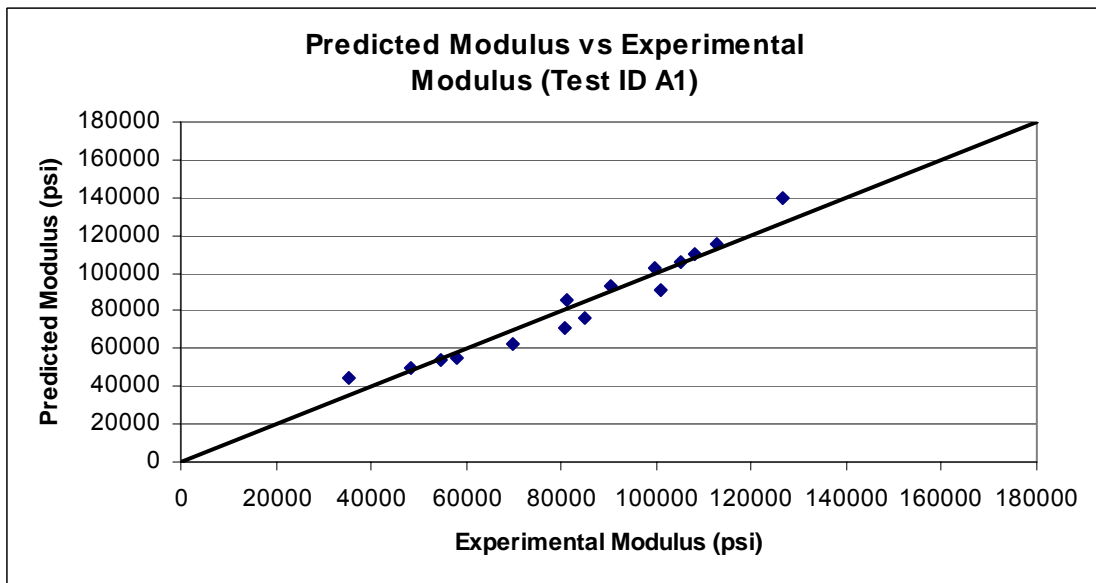
# A1

Sequence Number	Experimental Resilient Modulus	Deviator Stress	Confining Pressure	Bulk Stress	Octahedral Shear Stress	log (M <sub>r</sub> /P <sub>a</sub> )	log (Bulk Stress/P <sub>a</sub> )	log((T <sub>oct</sub> /P <sub>a</sub> )+1)	Regression Predicted Modulus
1	35300	3.225	3	12.225	1.520	3.380	-0.080	0.043	44215
2	48171	5.868	3	14.868	2.766	3.515	0.005	0.075	49553
3	58057	8.519	3	17.519	4.016	3.597	0.076	0.105	54713
4	54590	4.698	5	19.698	2.214	3.570	0.127	0.061	54482
5	69774	9.197	5	24.197	4.335	3.676	0.216	0.112	62663
6	80824	13.739	5	28.739	6.477	3.740	0.291	0.159	70714
7	85106	9.229	10	39.229	4.350	3.763	0.426	0.113	75832
8	100791	18.213	10	48.213	8.586	3.836	0.516	0.200	90900
9	105295	27.290	10	57.290	12.865	3.855	0.591	0.273	105821
10	81258	9.192	15	54.192	4.333	3.743	0.567	0.112	86087
11	90555	13.708	15	58.708	6.462	3.790	0.601	0.158	93663
12	112638	27.248	15	72.248	12.845	3.884	0.692	0.273	115905
13	99660	13.713	20	73.713	6.464	3.831	0.700	0.158	102456
14	108075	18.239	20	78.239	8.598	3.866	0.726	0.200	110030
15	126606	36.331	20	96.331	17.126	3.935	0.816	0.335	139502

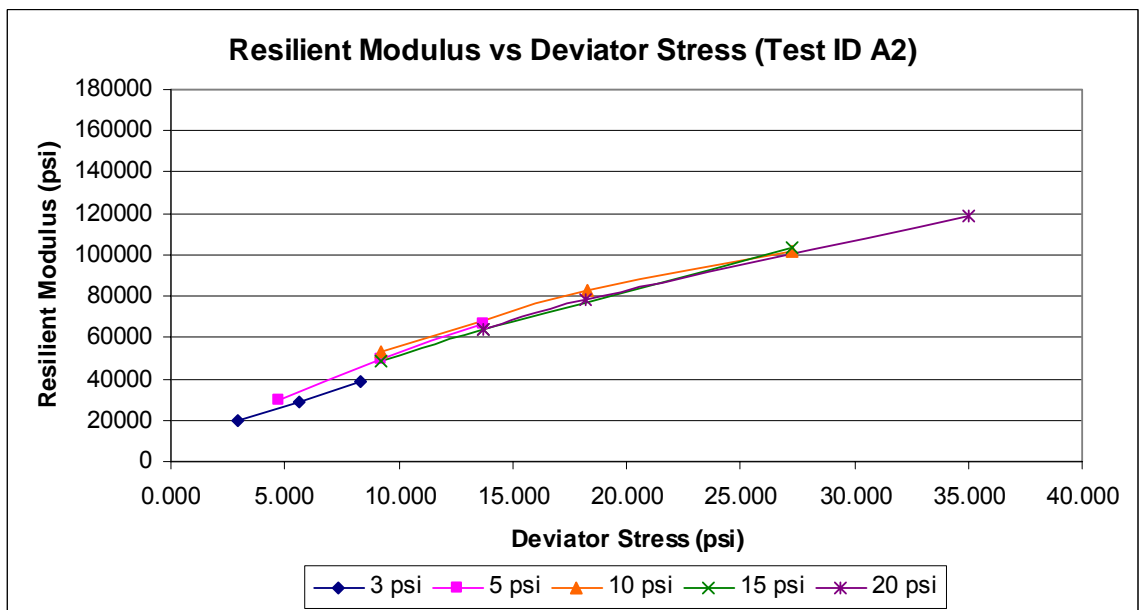
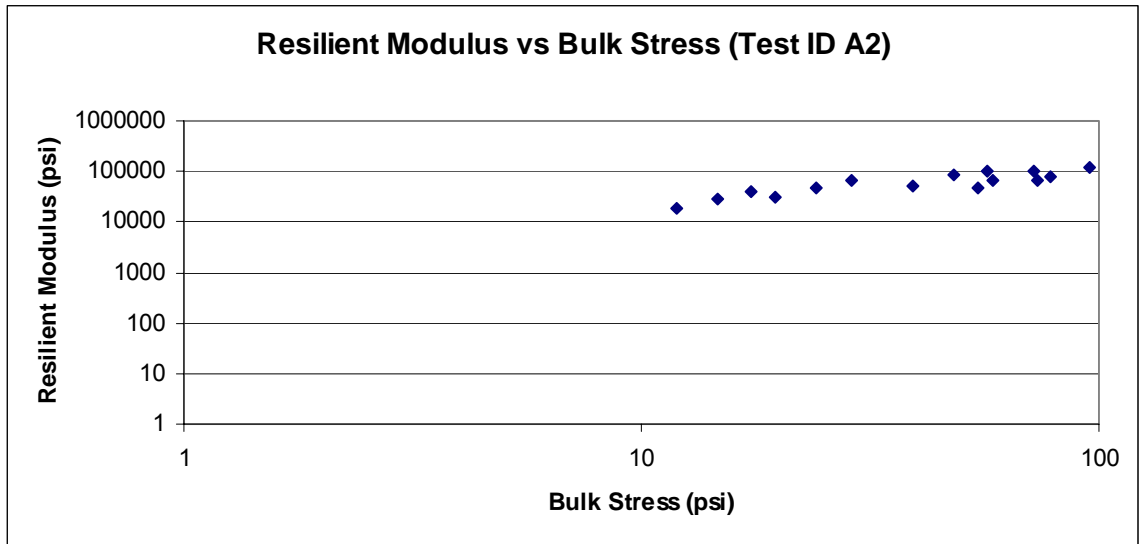
## Equation of Model:

$$M_r = k_1 P_a \left( \frac{\theta}{P_a} \right)^{k_2} \left( \frac{\tau_{oct}}{P_a} + 1 \right)^{k_3}$$

k <sub>1</sub>	3079.730
k <sub>2</sub>	0.394
k <sub>3</sub>	0.498
R <sup>2</sup>	0.931



A2





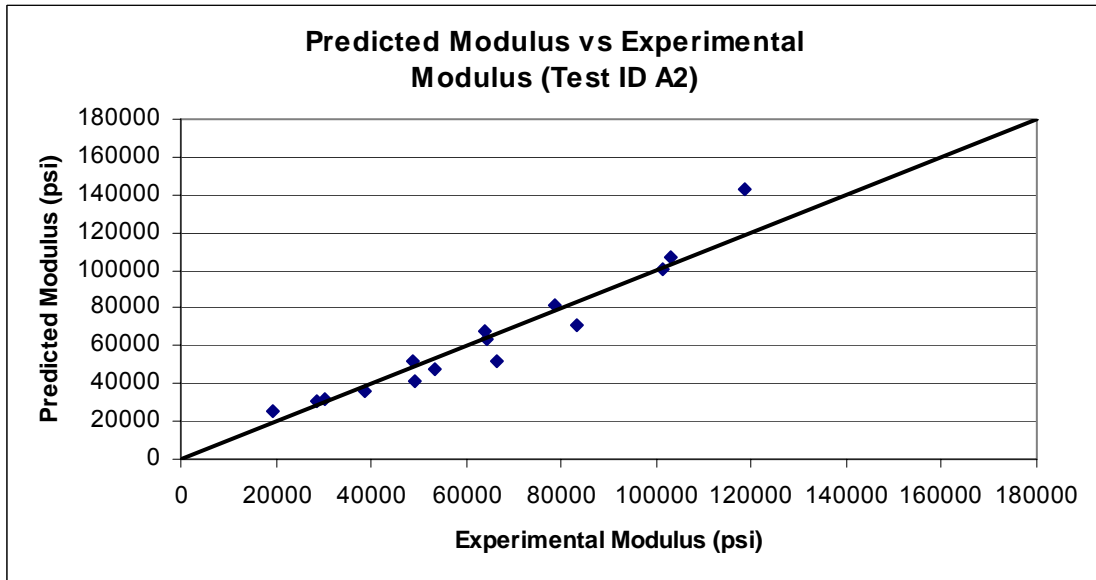
## A2

Sequence Number	Experimental Resilient Modulus	Deviator Stress	Confining Pressure	Bulk Stress	Octahedral Shear Stress	log (M <sub>r</sub> /P <sub>a</sub> )	log (Bulk Stress/P <sub>a</sub> )	log((T <sub>oct</sub> /P <sub>a</sub> )+1)	Regression Predicted Modulus
1	19372	2.921	3	11.921	1.377	3.120	-0.091	0.039	25407
2	28559	5.630	3	14.630	2.654	3.288	-0.002	0.072	30723
3	38804	8.332	3	17.332	3.928	3.422	0.072	0.103	36438
4	30133	4.701	5	19.701	2.216	3.312	0.127	0.061	31837
5	49193	9.204	5	24.204	4.339	3.525	0.217	0.112	41451
6	66250	13.730	5	28.730	6.473	3.654	0.291	0.158	52351
7	53532	9.219	10	39.219	4.346	3.561	0.426	0.112	47271
8	83084	18.258	10	48.258	8.607	3.752	0.516	0.200	71346
9	101532	27.244	10	57.244	12.843	3.839	0.590	0.273	100261
10	48793	9.191	15	54.191	4.333	3.521	0.567	0.112	51536
11	64186	13.726	15	58.726	6.470	3.640	0.602	0.158	63525
12	103091	27.237	15	72.237	12.840	3.846	0.691	0.273	106762
13	63853	13.735	20	73.735	6.475	3.638	0.700	0.158	67589
14	78448	18.214	20	78.214	8.586	3.727	0.726	0.200	81188
15	118655	35.031	20	95.031	16.514	3.907	0.811	0.327	143359

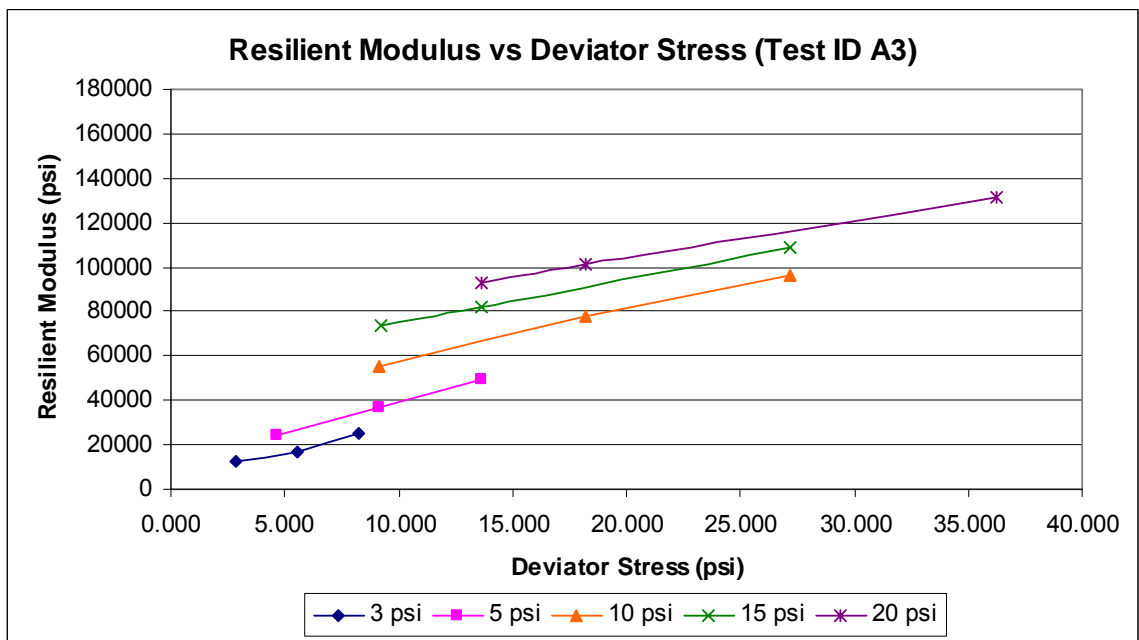
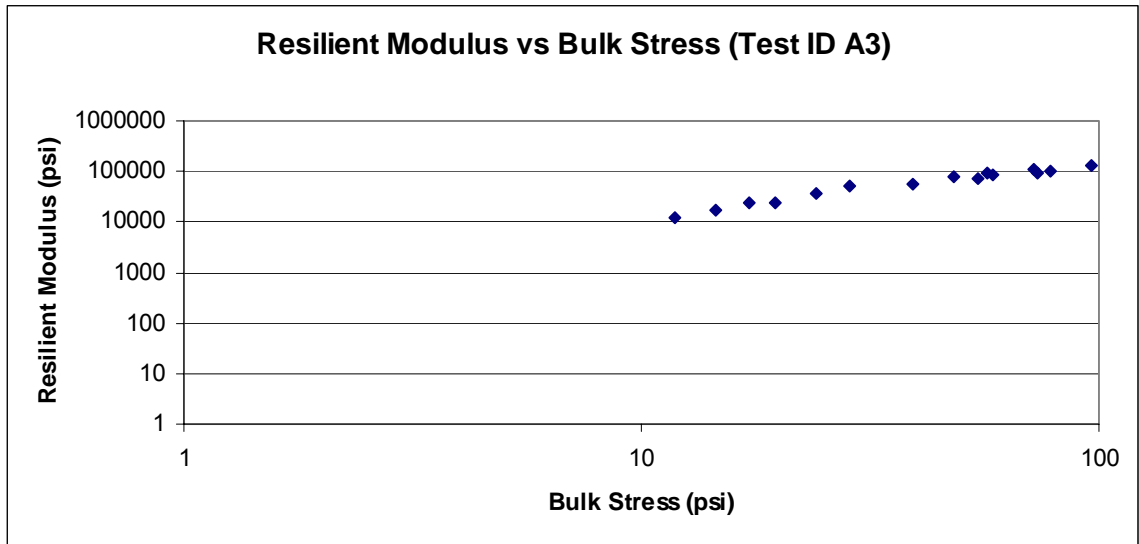
### Equation of Model:

$$M_r = k_1 P_a \left( \frac{\theta}{P_a} \right)^{k_2} \left( \frac{\tau_{oct}}{P_a} + 1 \right)^{k_3}$$

k <sub>1</sub>	1562.452
k <sub>2</sub>	0.271
k <sub>3</sub>	1.761
R <sup>2</sup>	0.932



# A3



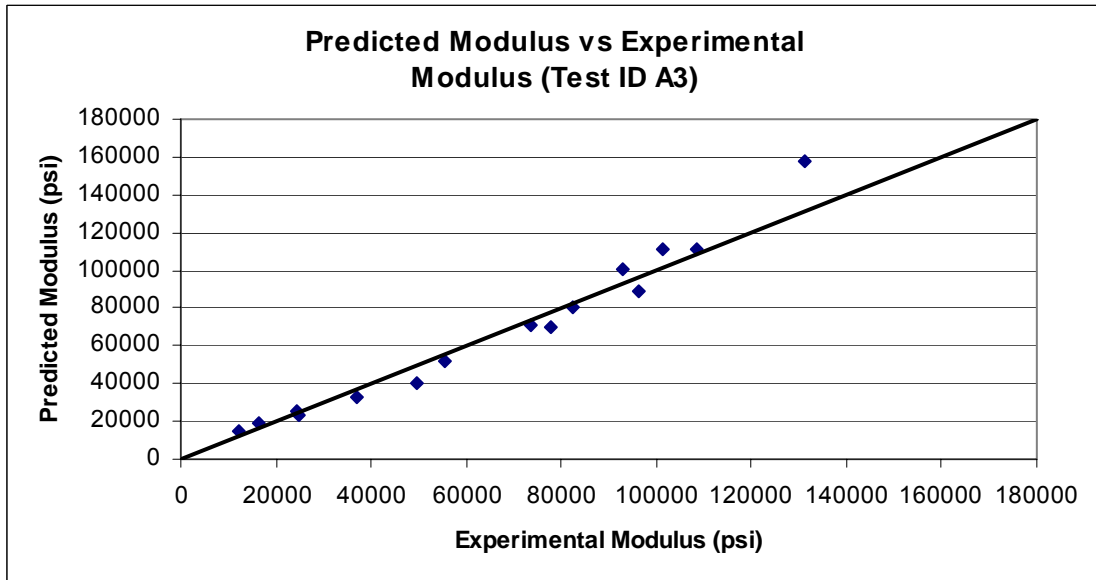
### A3

Sequence Number	Experimental Resilient Modulus	Deviator Stress	Confining Pressure	Bulk Stress	Octahedral Shear Stress	log (M <sub>r</sub> /P <sub>a</sub> )	log (Bulk Stress/P <sub>a</sub> )	log((T <sub>oct</sub> /P <sub>a</sub> )+1)	Regression Predicted Modulus
1	12172	2.870	3	11.870	1.353	2.918	-0.093	0.038	14968
2	16397	5.520	3	14.520	2.602	3.047	-0.005	0.071	18855
3	24901	8.239	3	17.239	3.884	3.229	0.069	0.102	23035
4	24223	4.638	5	19.638	2.186	3.217	0.126	0.060	24994
5	36894	9.163	5	24.163	4.320	3.400	0.216	0.112	32325
6	49635	13.654	5	28.654	6.437	3.528	0.290	0.158	40081
7	55370	9.142	10	39.142	4.310	3.576	0.425	0.112	51628
8	77980	18.179	10	48.179	8.569	3.725	0.516	0.199	69452
9	96149	27.161	10	57.161	12.804	3.816	0.590	0.272	88687
10	73442	9.260	15	54.260	4.365	3.699	0.567	0.113	70993
11	82410	13.650	15	58.650	6.434	3.749	0.601	0.158	80357
12	108526	27.180	15	72.180	12.813	3.868	0.691	0.272	111255
13	93097	13.661	20	73.661	6.440	3.802	0.700	0.158	100276
14	101525	18.194	20	78.194	8.577	3.839	0.726	0.200	111174
15	131168	36.205	20	96.205	17.067	3.951	0.816	0.335	157326

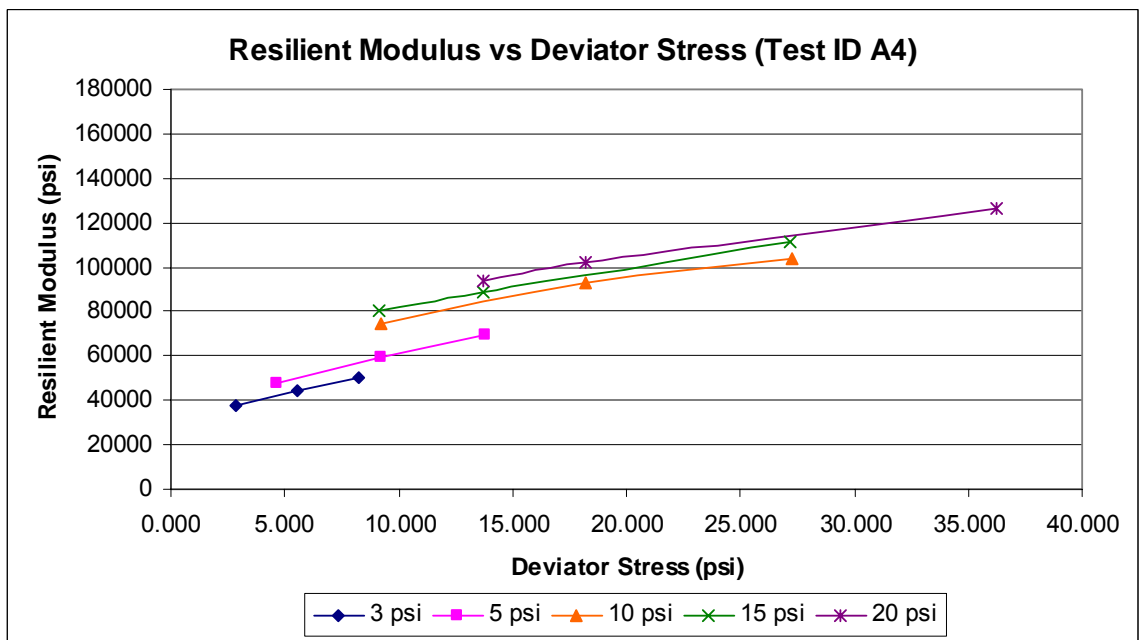
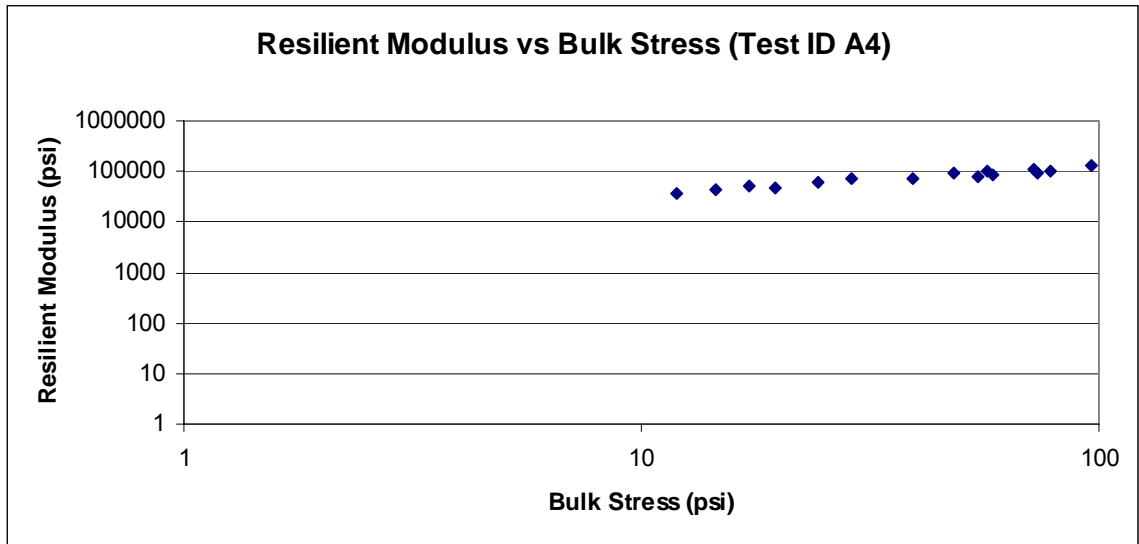
$$M_r = k_1 P_a \left( \frac{\theta}{P_a} \right)^{k_2} \left( \frac{\tau_{oct}}{P_a} + 1 \right)^{k_3}$$

#### Equation of Model:

k <sub>1</sub>	1202.578
k <sub>2</sub>	0.971
k <sub>3</sub>	0.469
R <sup>2</sup>	0.973



## A4



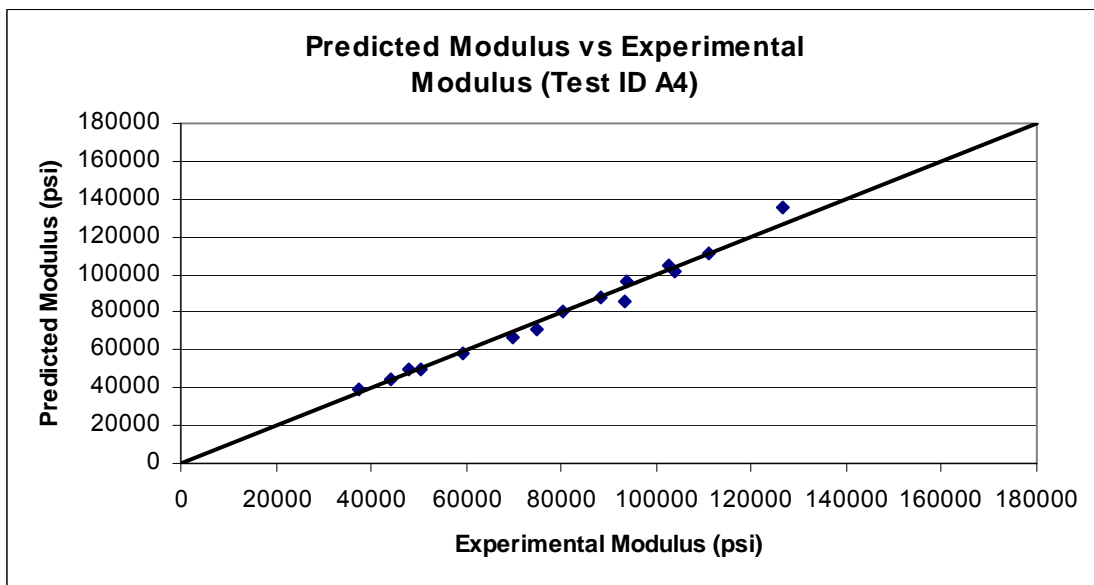
## A4

Sequence Number	Experimental Resilient Modulus	Deviator Stress	Confining Pressure	Bulk Stress	Octahedral Shear Stress	log (M <sub>r</sub> /P <sub>a</sub> )	log (Bulk Stress/P <sub>a</sub> )	log((T <sub>oct</sub> /P <sub>a</sub> )+1)	Regression Predicted Modulus
1	37368	2.896	3	11.896	1.365	3.405	-0.092	0.039	39619
2	44110	5.531	3	14.531	2.607	3.477	-0.005	0.071	44812
3	50623	8.247	3	17.247	3.888	3.537	0.069	0.102	50011
4	48053	4.681	5	19.681	2.207	3.514	0.127	0.061	49974
5	59482	9.222	5	24.222	4.347	3.607	0.217	0.113	58157
6	69654	13.779	5	28.779	6.496	3.676	0.292	0.159	66260
7	74691	9.252	10	39.252	4.361	3.706	0.427	0.113	70692
8	93295	18.235	10	48.235	8.596	3.803	0.516	0.200	86118
9	103880	27.285	10	57.285	12.862	3.849	0.591	0.273	101583
10	80212	9.170	15	54.170	4.323	3.737	0.566	0.112	80408
11	88464	13.713	15	58.713	6.464	3.779	0.601	0.158	88267
12	110985	27.211	15	72.211	12.828	3.878	0.691	0.272	111450
13	93750	13.680	20	73.680	6.449	3.805	0.700	0.158	96694
14	102407	18.217	20	78.217	8.588	3.843	0.726	0.200	104641
15	126417	36.238	20	96.238	17.083	3.934	0.816	0.335	135819

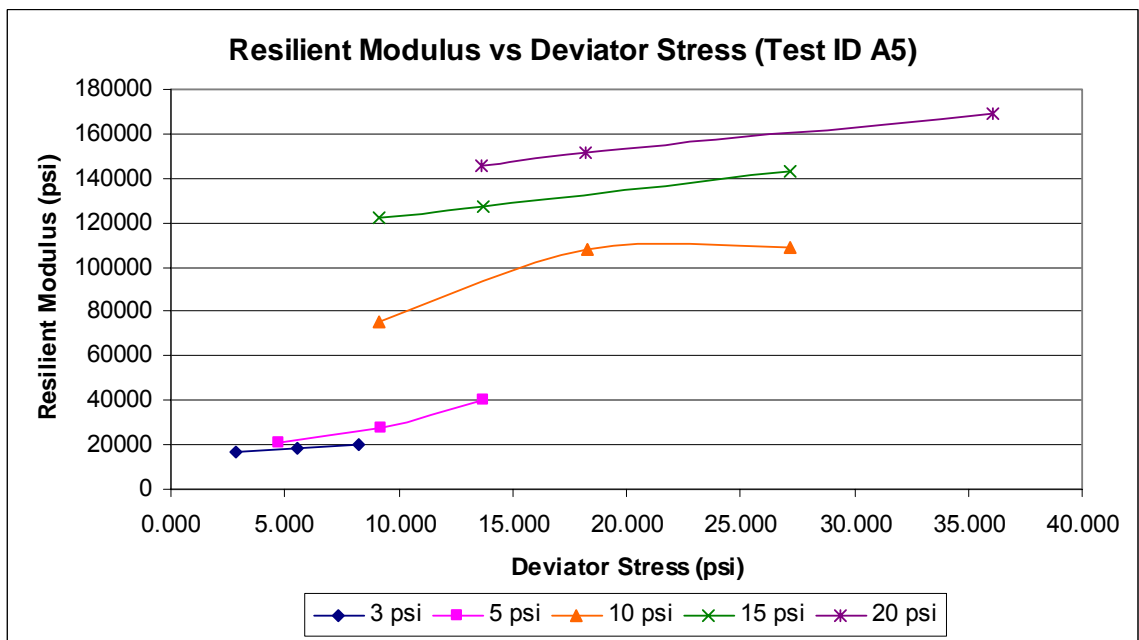
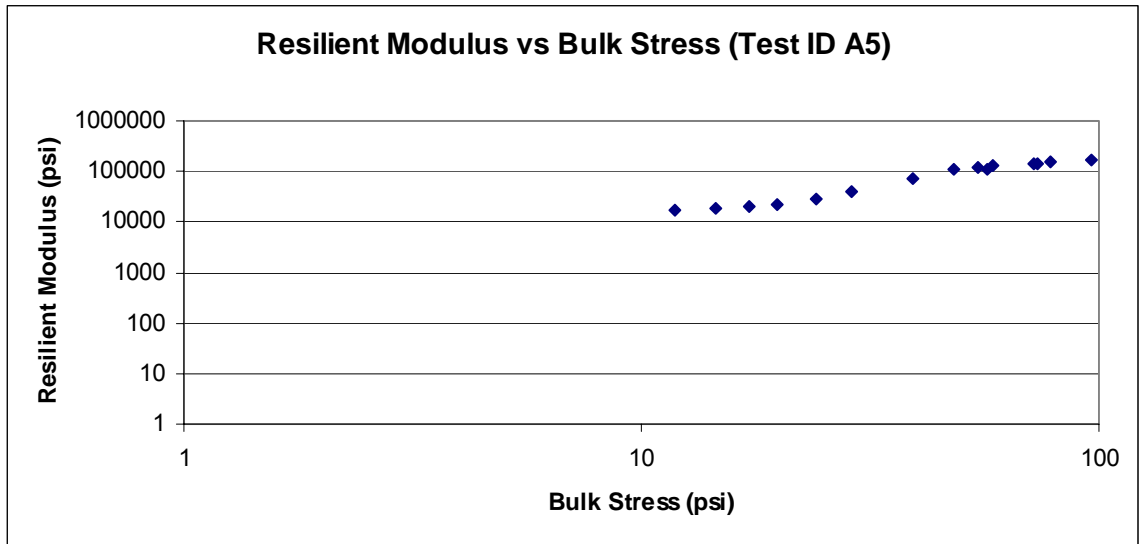
$$M_r = k_1 P_a \left( \frac{\theta}{P_a} \right)^{k_2} \left( \frac{\tau_{oct}}{P_a} + 1 \right)^{k_3}$$

**Equation of Model:**

k <sub>1</sub>	2790.655
k <sub>2</sub>	0.403
k <sub>3</sub>	0.570
R <sup>2</sup>	0.987



A5



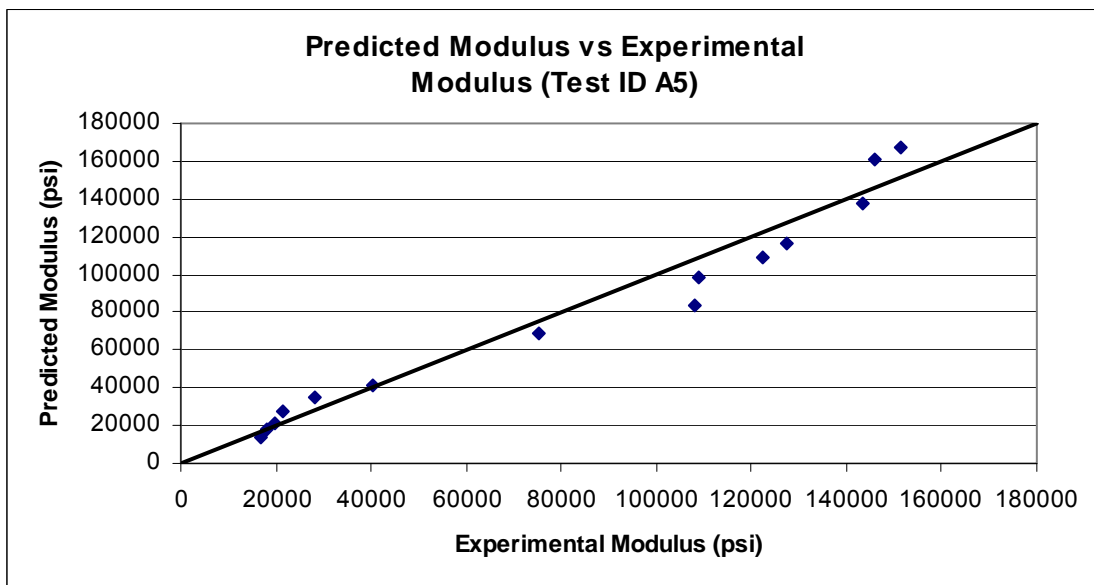
## A5

Sequence Number	Experimental Resilient Modulus	Deviator Stress	Confining Pressure	Bulk Stress	Octahedral Shear Stress	log (M <sub>r</sub> /P <sub>a</sub> )	log (Bulk Stress/P <sub>a</sub> )	log((T <sub>oct</sub> /P <sub>a</sub> )+1)	Regression Predicted Modulus
1	16744	2.880	3	11.880	1.358	3.057	-0.093	0.038	13553
2	18130	5.574	3	14.574	2.628	3.091	-0.004	0.071	17491
3	19684	8.246	3	17.246	3.887	3.127	0.069	0.102	21500
4	21241	4.736	5	19.736	2.232	3.160	0.128	0.061	27315
5	28038	9.199	5	24.199	4.337	3.280	0.216	0.112	34519
6	40196	13.678	5	28.678	6.448	3.437	0.290	0.158	41790
7	75228	9.183	10	39.183	4.329	3.709	0.426	0.112	68861
8	107992	18.276	10	48.276	8.615	3.866	0.516	0.200	83965
9	108985	27.207	10	57.207	12.825	3.870	0.590	0.272	98623
10	122199	9.182	15	54.182	4.328	3.920	0.567	0.112	109553
11	127306	13.695	15	58.695	6.456	3.938	0.601	0.158	116573
12	143219	27.211	15	72.211	12.827	3.989	0.691	0.272	137682
13	145908	13.653	20	73.653	6.436	3.997	0.700	0.158	161447
14	151465	18.174	20	78.174	8.567	4.013	0.726	0.199	167657
15	168934	36.104	20	96.104	17.020	4.060	0.815	0.334	193291

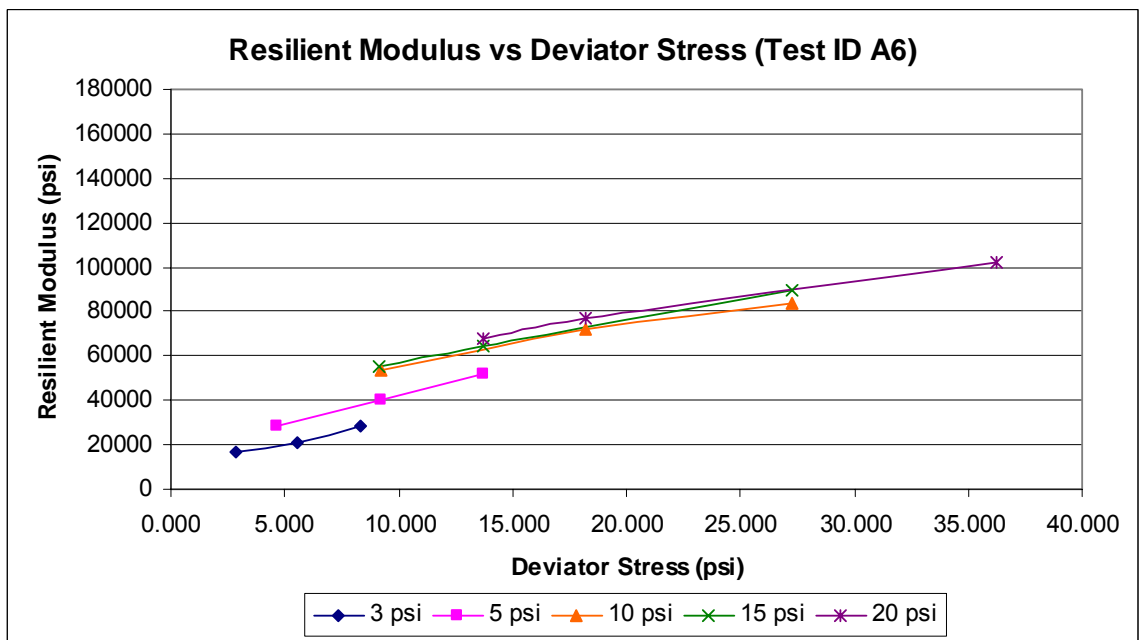
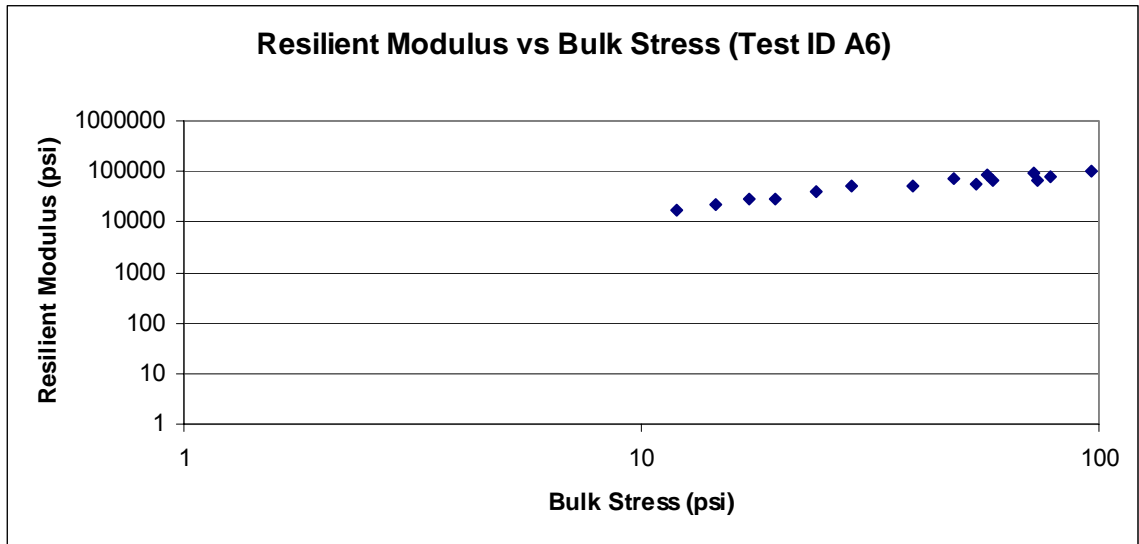
**Equation of Model:**

$$M_r = k_1 P_a \left( \frac{\theta}{P_a} \right)^{k_2} \left( \frac{\tau_{oct}}{P_a} + 1 \right)^{k_3}$$

k <sub>1</sub>	1306.887
k <sub>2</sub>	1.433
k <sub>3</sub>	-0.495
R <sup>2</sup>	0.973



## A6





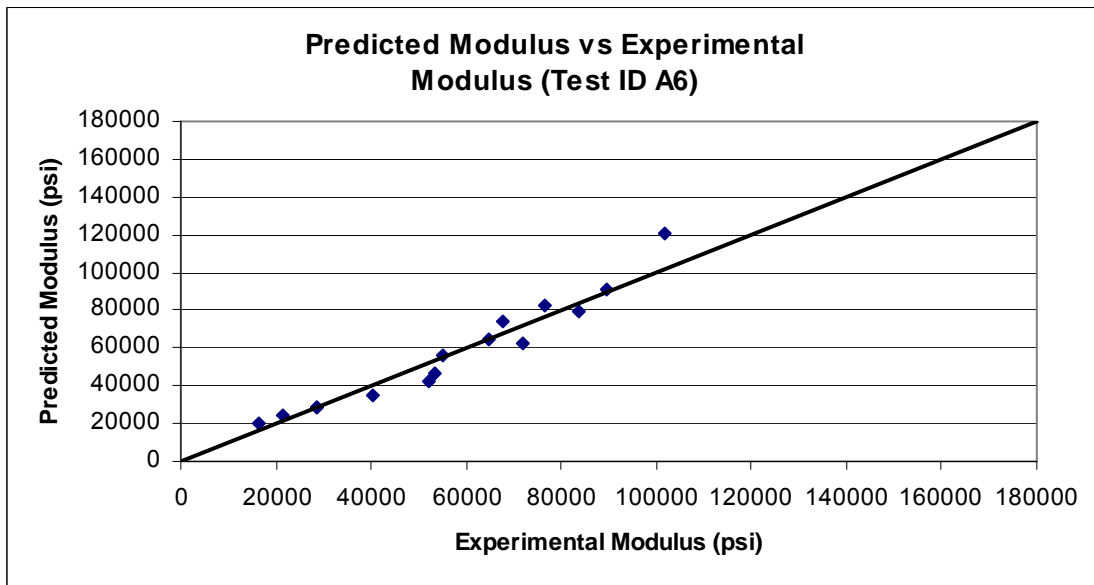
## A6

Sequence Number	Experimental Resilient Modulus	Deviator Stress	Confining Pressure	Bulk Stress	Octahedral Shear Stress	log (M <sub>r</sub> /P <sub>a</sub> )	log (Bulk Stress/P <sub>a</sub> )	log((T <sub>oct</sub> /P <sub>a</sub> )+1)	Regression Predicted Modulus
1	16443	2.893	3	11.893	1.364	3.049	-0.092	0.039	20160
2	21290	5.579	3	14.579	2.630	3.161	-0.004	0.071	24182
3	28540	8.290	3	17.290	3.908	3.288	0.070	0.102	28340
4	28763	4.680	5	19.680	2.206	3.292	0.127	0.061	28262
5	40331	9.196	5	24.196	4.335	3.438	0.216	0.112	35175
6	52036	13.720	5	28.720	6.467	3.549	0.291	0.158	42448
7	53270	9.210	10	39.210	4.342	3.559	0.426	0.112	46720
8	71732	18.211	10	48.211	8.585	3.688	0.516	0.200	62234
9	83667	27.273	10	57.273	12.857	3.755	0.591	0.273	79086
10	55131	9.160	15	54.160	4.318	3.574	0.566	0.112	56424
11	64878	13.723	15	58.723	6.469	3.645	0.601	0.158	64617
12	89429	27.233	15	72.233	12.838	3.784	0.691	0.273	90584
13	67623	13.702	20	73.702	6.459	3.663	0.700	0.158	73813
14	76720	18.188	20	78.188	8.574	3.718	0.726	0.200	82645
15	101844	36.251	20	96.251	17.089	3.841	0.816	0.335	120651

$$M_r = k_1 P_a \left( \frac{\theta}{P_a} \right)^{k_2} \left( \frac{\tau_{oct}}{P_a} + 1 \right)^{k_3}$$

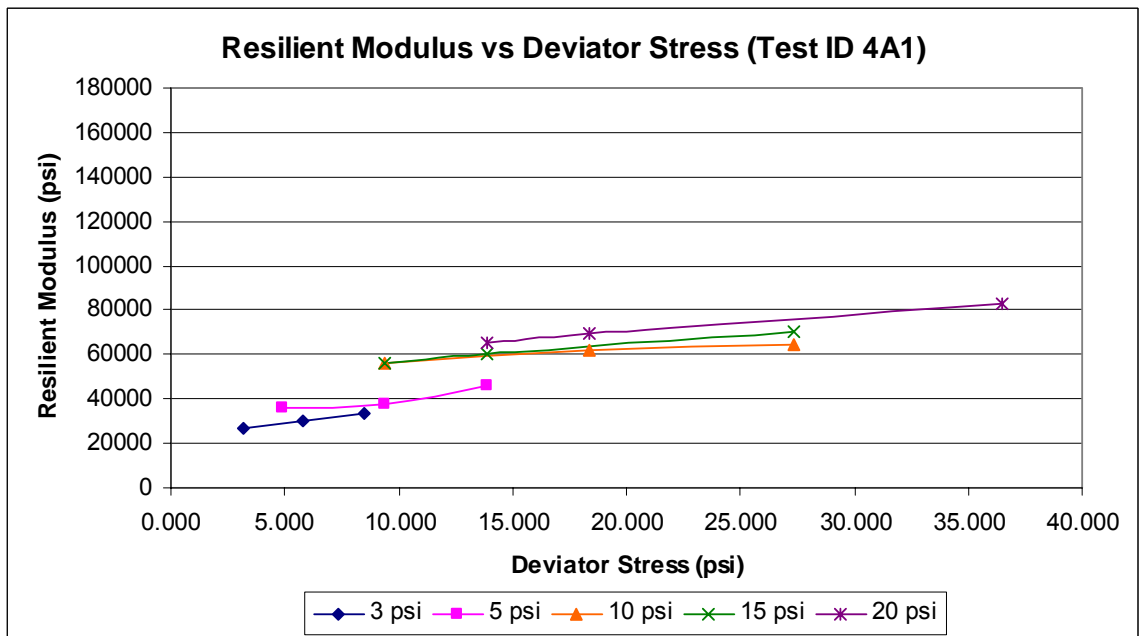
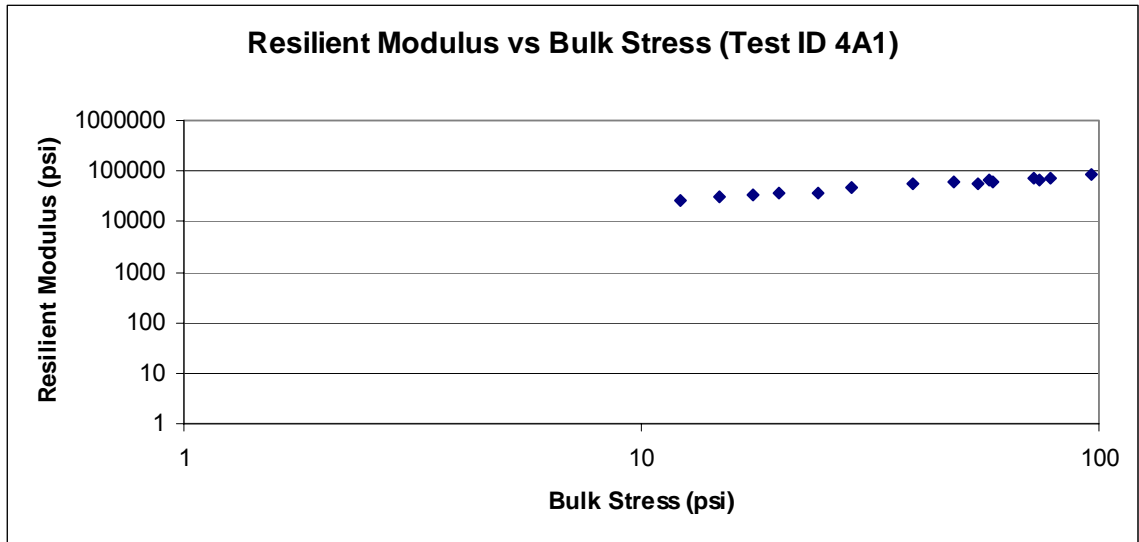
**Equation of Model:**

k <sub>1</sub>	1443.905
k <sub>2</sub>	0.587
k <sub>3</sub>	0.822
R <sup>2</sup>	0.952



Gravel and cement, 28 days

4A1



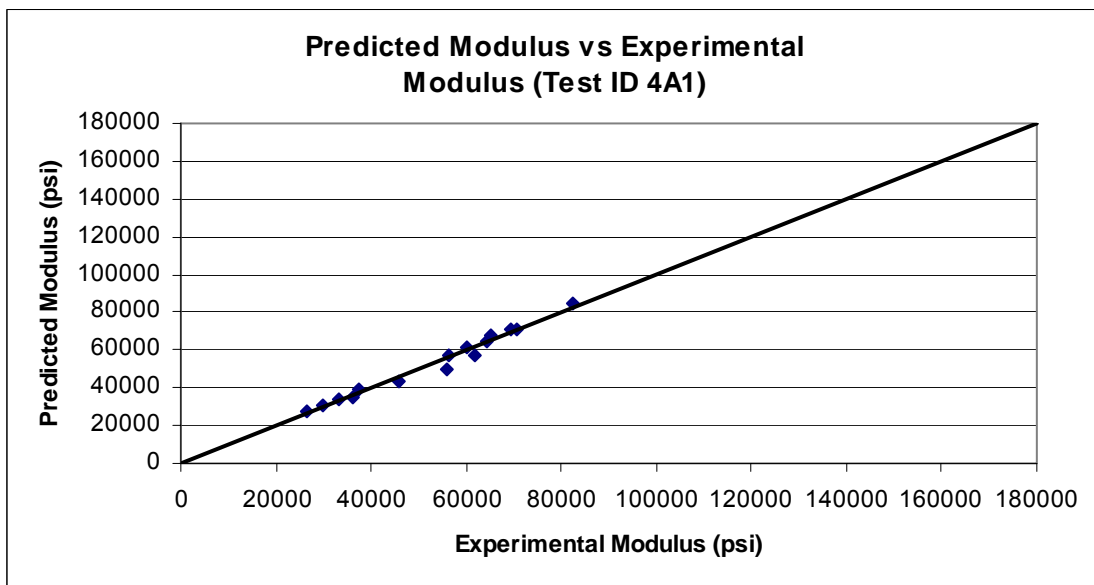
## 4A1

Sequence Number	Experimental Resilient Modulus	Deviator Stress	Confining Pressure	Bulk Stress	Octahedral Shear Stress	log (M <sub>r</sub> /P <sub>a</sub> )	log (Bulk Stress/P <sub>a</sub> )	log((T <sub>oct</sub> /P <sub>a</sub> )+1)	Regression Predicted Modulus
1	26534	3.187	3	12.187	1.502	3.256	-0.081	0.042	27565
2	29819	5.806	3	14.806	2.737	3.307	0.003	0.074	30692
3	33298	8.492	3	17.492	4.003	3.355	0.076	0.105	33704
4	36136	4.934	5	19.934	2.326	3.391	0.132	0.064	35090
5	37532	9.355	5	24.355	4.410	3.407	0.219	0.114	39541
6	45900	13.840	5	28.840	6.524	3.494	0.293	0.160	43805
7	56008	9.385	10	39.385	4.424	3.581	0.428	0.114	49525
8	61927	18.397	10	48.397	8.672	3.625	0.518	0.201	57025
9	64177	27.354	10	57.354	12.895	3.640	0.591	0.274	64062
10	56159	9.356	15	54.356	4.410	3.582	0.568	0.114	57578
11	59949	13.865	15	58.865	6.536	3.610	0.603	0.160	61183
12	70693	27.359	15	72.359	12.897	3.682	0.692	0.274	71426
13	64986	13.882	20	73.882	6.544	3.646	0.701	0.160	68055
14	69508	18.361	20	78.361	8.656	3.675	0.727	0.201	71444
15	82465	36.455	20	96.455	17.185	3.749	0.817	0.336	84377

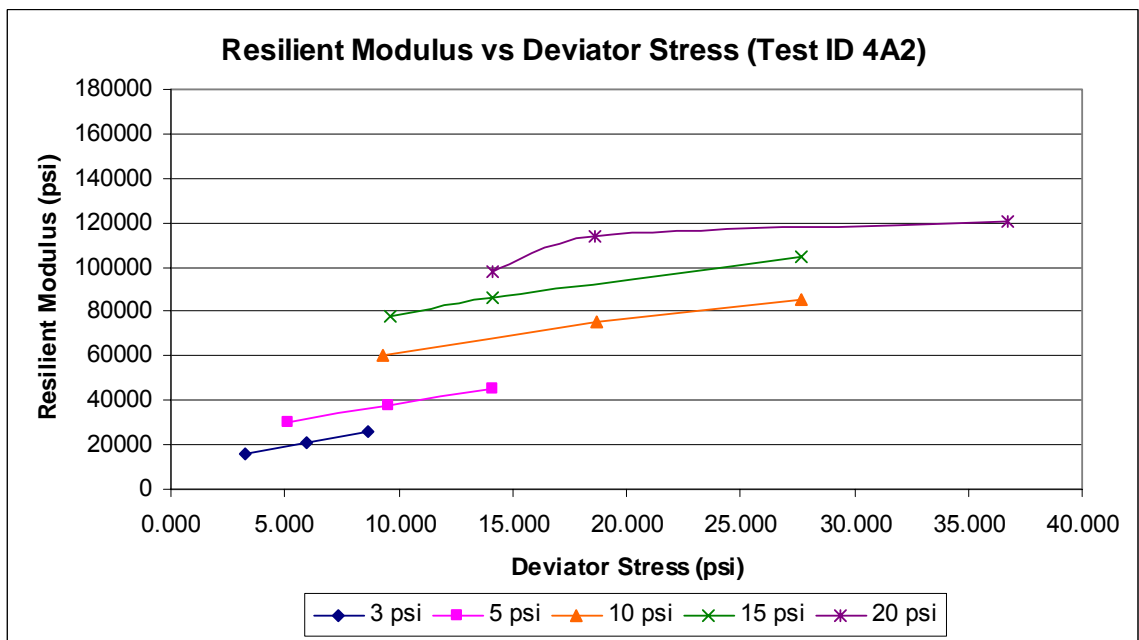
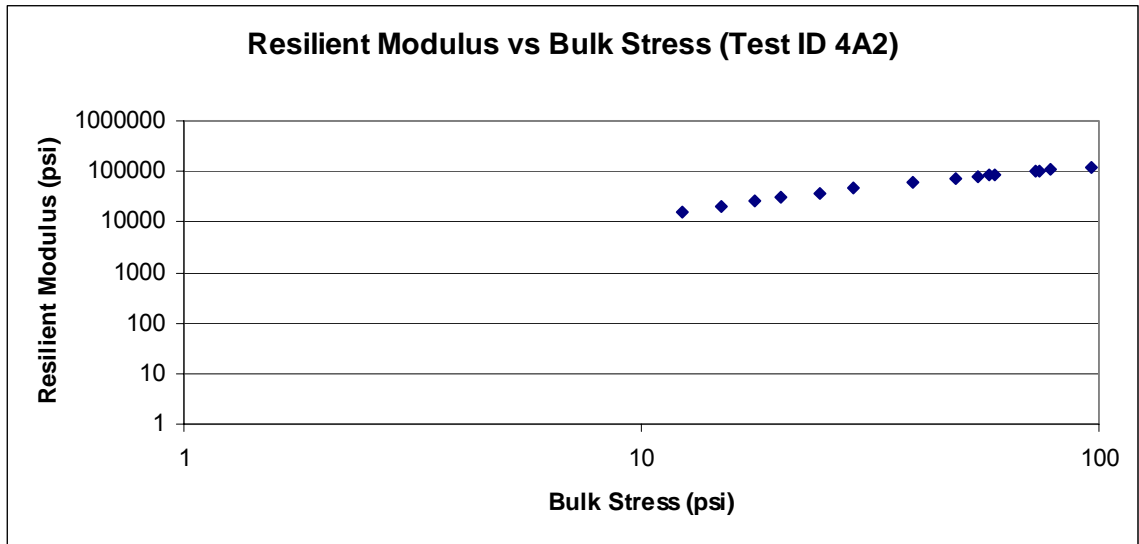
$$M_r = k_1 P_a \left( \frac{\theta}{P_a} \right)^{k_2} \left( \frac{\tau_{oct}}{P_a} + 1 \right)^{k_3}$$

**Equation of Model:**

k <sub>1</sub>	2003.444
k <sub>2</sub>	0.468
k <sub>3</sub>	0.222
R <sup>2</sup>	0.980



## 4A2



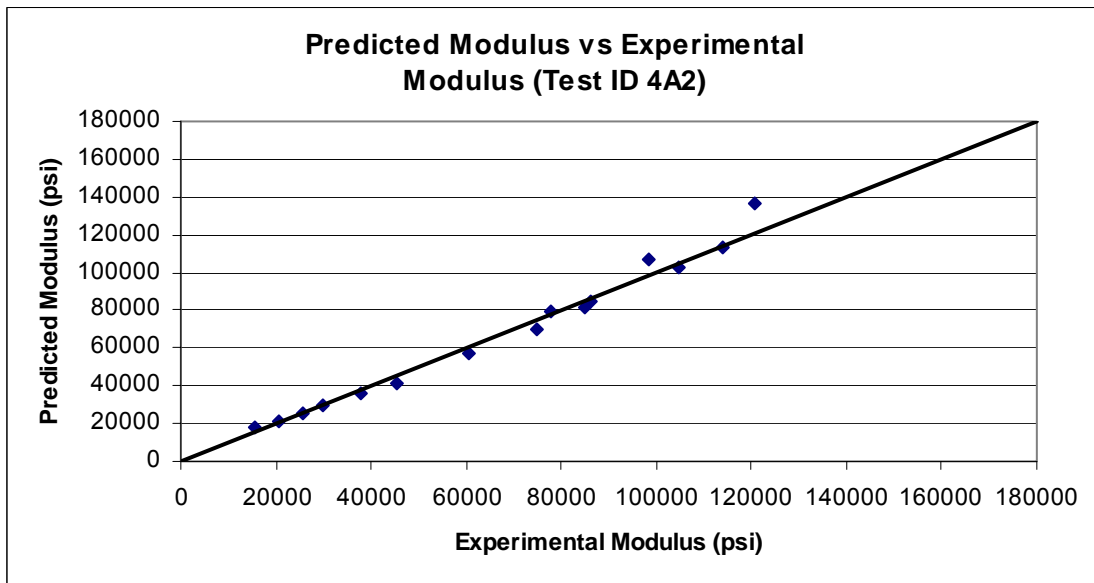
## 4A2

Sequence Number	Experimental Resilient Modulus	Deviator Stress	Confining Pressure	Bulk Stress	Octahedral Shear Stress	log (M <sub>r</sub> /P <sub>a</sub> )	log (Bulk Stress/P <sub>a</sub> )	log((T <sub>oct</sub> /P <sub>a</sub> )+1)	Regression Predicted Modulus
1	15677	3.282	3	12.282	1.547	3.028	-0.078	0.043	17854
2	20740	5.975	3	14.975	2.817	3.149	0.008	0.076	21688
3	25812	8.682	3	17.682	4.093	3.244	0.080	0.107	25516
4	29956	5.108	5	20.108	2.408	3.309	0.136	0.066	29216
5	37764	9.588	5	24.588	4.520	3.410	0.223	0.116	35495
6	45496	14.105	5	29.105	6.649	3.491	0.297	0.162	41770
7	60353	9.286	10	39.286	4.377	3.613	0.427	0.113	56892
8	74962	18.697	10	48.697	8.814	3.708	0.520	0.204	69652
9	84977	27.693	10	57.693	13.055	3.762	0.594	0.276	81711
10	77964	9.598	15	54.598	4.524	3.725	0.570	0.117	79175
11	86198	14.125	15	59.125	6.659	3.768	0.604	0.162	85193
12	104913	27.688	15	72.688	13.052	3.854	0.694	0.276	103084
13	98267	14.114	20	74.114	6.653	3.825	0.703	0.162	106930
14	113906	18.621	20	78.621	8.778	3.889	0.728	0.203	112771
15	120689	36.725	20	96.725	17.312	3.914	0.818	0.338	136123

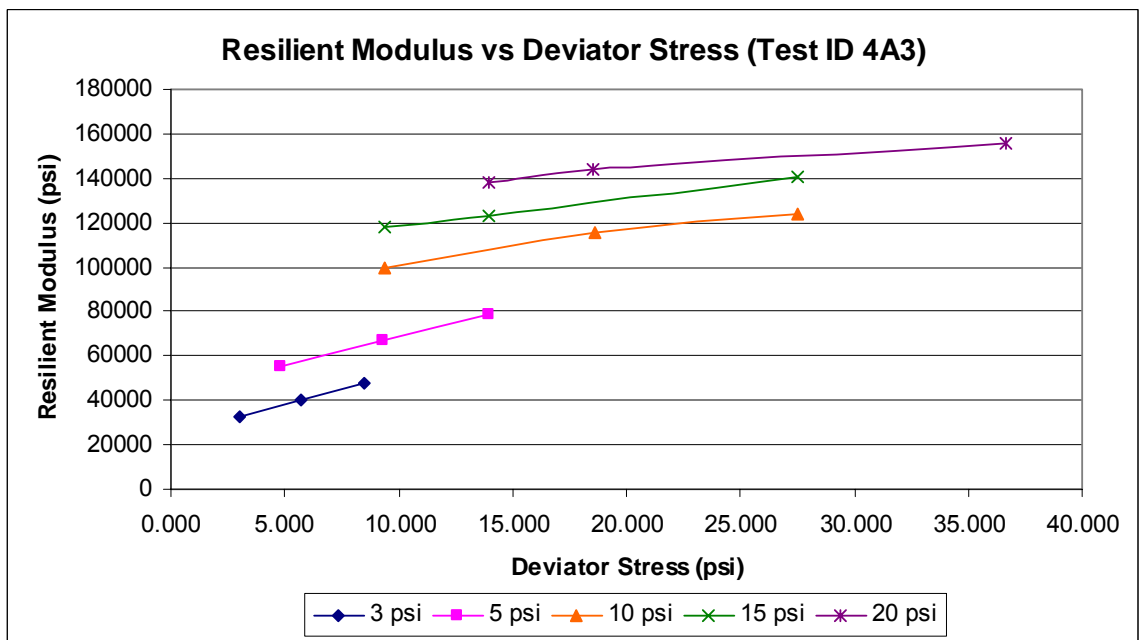
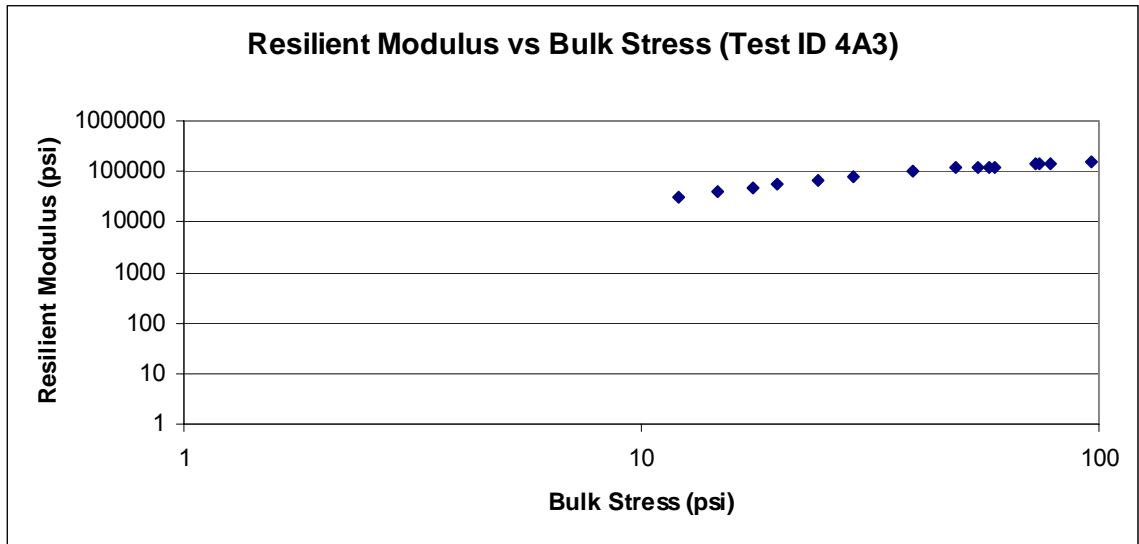
### Equation of Model:

$$M_r = k_1 P_a \left( \frac{\theta}{P_a} \right)^{k_2} \left( \frac{\tau_{oct}}{P_a} + 1 \right)^{k_3}$$

k <sub>1</sub>	1464.756
k <sub>2</sub>	1.006
k <sub>3</sub>	-0.065
R <sup>2</sup>	0.990



### 4A3



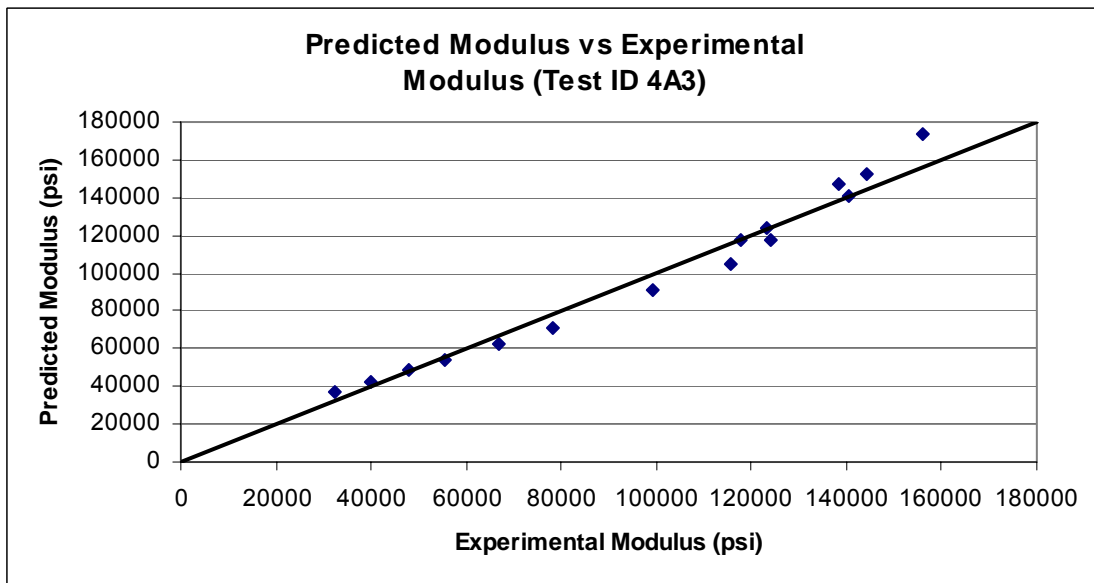
### 4A3

Sequence Number	Experimental Resilient Modulus	Deviator Stress	Confining Pressure	Bulk Stress	Octahedral Shear Stress	log (M <sub>r</sub> /P <sub>a</sub> )	log (Bulk Stress/P <sub>a</sub> )	log((T <sub>oct</sub> /P <sub>a</sub> )+1)	Regression Predicted Modulus
1	32293	3.035	3	12.035	1.431	3.342	-0.087	0.040	36744
2	40154	5.728	3	14.728	2.700	3.436	0.001	0.073	42667
3	48120	8.478	3	17.478	3.997	3.515	0.075	0.104	48391
4	55467	4.842	5	19.842	2.283	3.577	0.130	0.063	54012
5	66680	9.339	5	24.339	4.402	3.657	0.219	0.114	62541
6	78295	13.956	5	28.956	6.579	3.726	0.294	0.161	70786
7	99219	9.399	10	39.399	4.431	3.829	0.428	0.114	91132
8	115455	18.595	10	48.595	8.766	3.895	0.519	0.203	104964
9	124261	27.535	10	57.535	12.980	3.927	0.593	0.275	117600
10	117734	9.389	15	54.389	4.426	3.904	0.568	0.114	117265
11	123109	13.977	15	58.977	6.589	3.923	0.603	0.161	123452
12	140281	27.547	15	72.547	12.986	3.980	0.693	0.275	140971
13	138296	13.965	20	73.965	6.583	3.973	0.702	0.161	147369
14	144181	18.532	20	78.532	8.736	3.992	0.728	0.203	152791
15	156111	36.638	20	96.638	17.271	4.026	0.818	0.337	173600

#### Equation of Model:

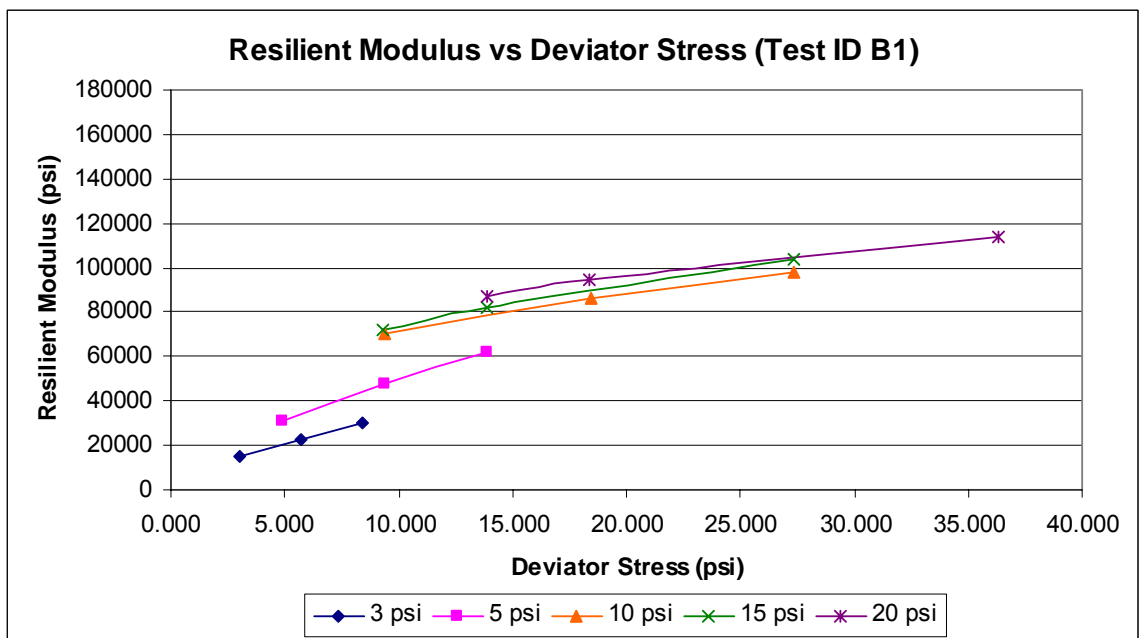
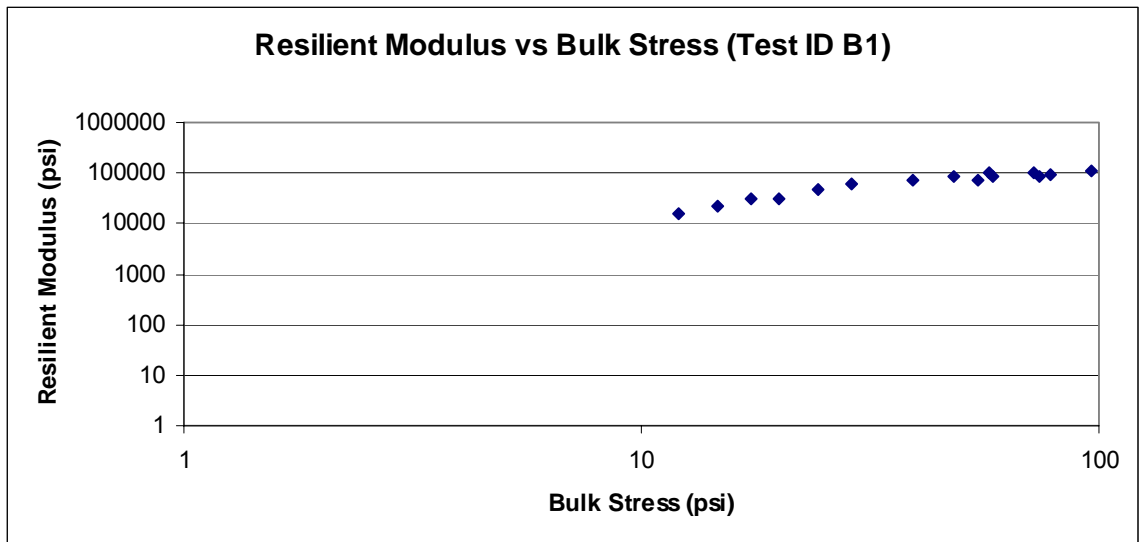
$$M_r = k_1 P_a \left( \frac{\theta}{P_a} \right)^{k_2} \left( \frac{\tau_{oct}}{P_a} + 1 \right)^{k_3}$$

k <sub>1</sub>	2953.090
k <sub>2</sub>	0.782
k <sub>3</sub>	-0.111
R <sup>2</sup>	0.980



**Limestone and cement, 7 days**

**B1**





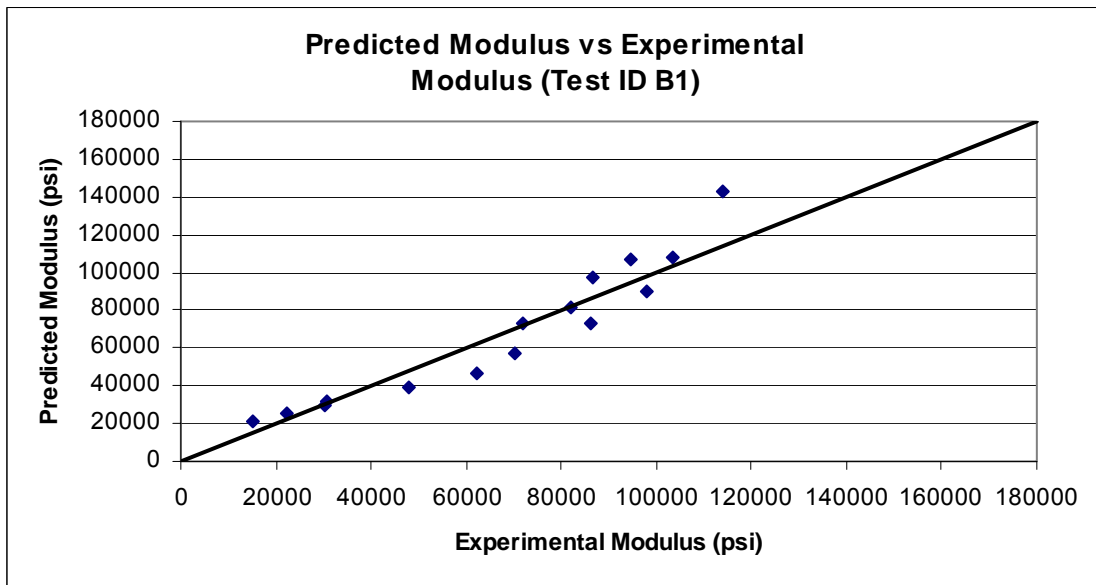
# B1

Sequence Number	Experimental Resilient Modulus	Deviator Stress	Confining Pressure	Bulk Stress	Octahedral Shear Stress	log (M <sub>r</sub> /P <sub>a</sub> )	log (Bulk Stress/P <sub>a</sub> )	log((T <sub>oct</sub> /P <sub>a</sub> )+1)	Regression Predicted Modulus
1	15146	3.004	3	12.004	1.416	3.013	-0.088	0.040	20795
2	22357	5.730	3	14.730	2.701	3.182	0.001	0.073	25243
3	30309	8.438	3	17.438	3.978	3.314	0.074	0.104	29717
4	30730	4.904	5	19.904	2.312	3.320	0.132	0.063	31645
5	47755	9.397	5	24.397	4.430	3.512	0.220	0.114	39067
6	62247	13.896	5	28.896	6.551	3.627	0.294	0.160	46704
7	70165	9.383	10	39.383	4.423	3.679	0.428	0.114	56849
8	86307	18.409	10	48.409	8.678	3.769	0.518	0.201	72954
9	97812	27.361	10	57.361	12.898	3.823	0.591	0.274	89589
10	72036	9.331	15	54.331	4.399	3.690	0.568	0.114	73113
11	82201	13.860	15	58.860	6.533	3.748	0.602	0.160	81531
12	103494	27.381	15	72.381	12.908	3.848	0.692	0.274	107515
13	86828	13.869	20	73.869	6.538	3.771	0.701	0.160	97425
14	94470	18.389	20	78.389	8.669	3.808	0.727	0.201	106416
15	114051	36.356	20	96.356	17.138	3.890	0.817	0.336	143177

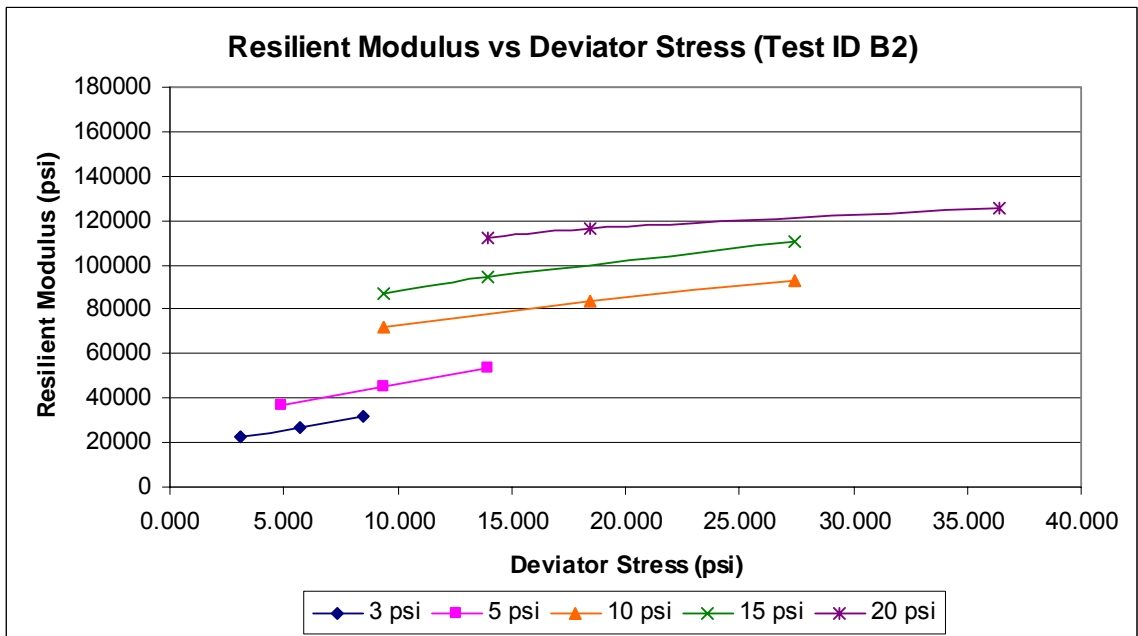
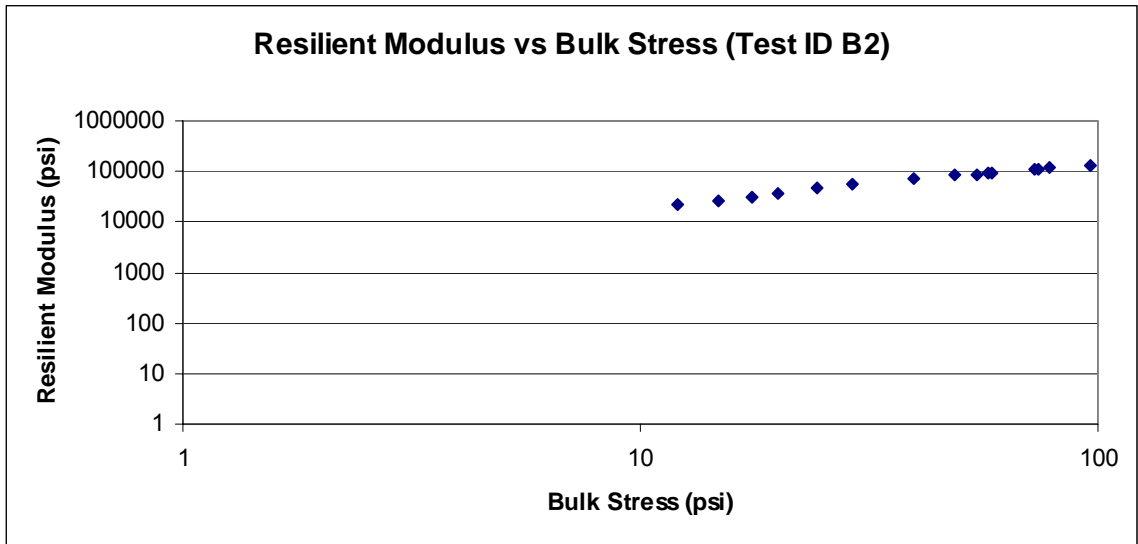
## Equation of Model:

$$M_r = k_1 P_a \left( \frac{\theta}{P_a} \right)^{k_2} \left( \frac{\tau_{oct}}{P_a} + 1 \right)^{k_3}$$

k <sub>1</sub>	1592.736
k <sub>2</sub>	0.784
k <sub>3</sub>	0.437
R <sup>2</sup>	0.926



## B2



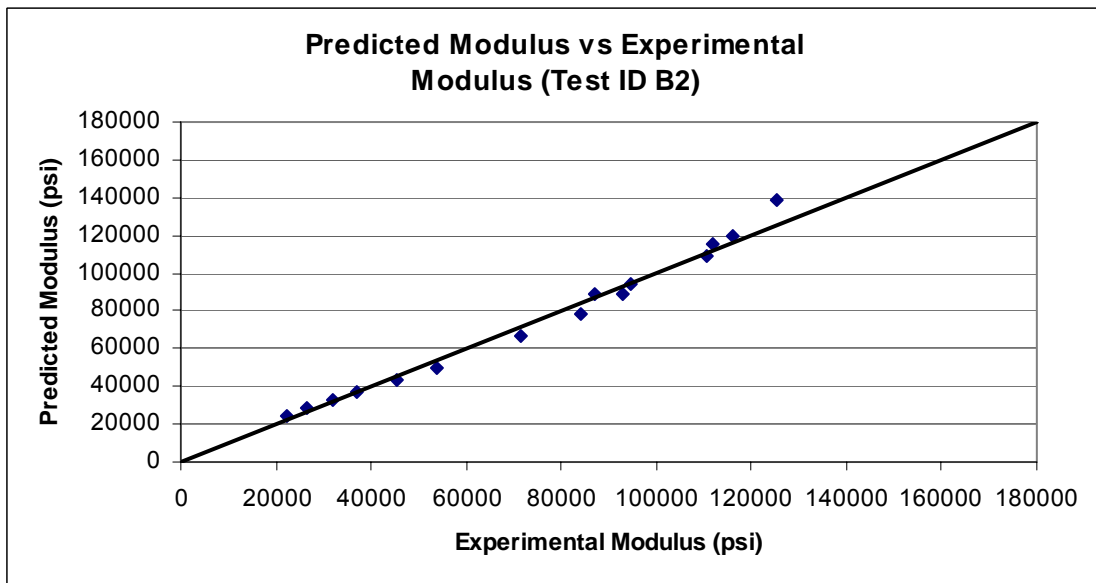
## B2

Sequence Number	Experimental Resilient Modulus	Deviator Stress	Confining Pressure	Bulk Stress	Octahedral Shear Stress	log (M <sub>r</sub> /P <sub>a</sub> )	log (Bulk Stress/P <sub>a</sub> )	log((T <sub>oct</sub> /P <sub>a</sub> )+1)	Regression Predicted Modulus
1	22402	3.114	3	12.114	1.468	3.183	-0.084	0.041	23871
2	26618	5.751	3	14.751	2.711	3.258	0.002	0.074	28169
3	32034	8.474	3	17.474	3.994	3.338	0.075	0.104	32445
4	36858	4.905	5	19.905	2.312	3.399	0.132	0.063	36915
5	45524	9.352	5	24.352	4.409	3.491	0.219	0.114	43492
6	53787	13.945	5	28.945	6.574	3.563	0.294	0.161	49999
7	71687	9.412	10	39.412	4.437	3.688	0.428	0.115	66803
8	84048	18.457	10	48.457	8.701	3.757	0.518	0.202	78143
9	92968	27.434	10	57.434	12.932	3.801	0.592	0.274	88889
10	86869	9.412	15	54.412	4.437	3.772	0.568	0.115	89067
11	94439	13.920	15	58.920	6.562	3.808	0.603	0.160	94253
12	110611	27.443	15	72.443	12.937	3.876	0.693	0.274	109335
13	112016	13.928	20	73.928	6.566	3.882	0.701	0.160	115391
14	116136	18.421	20	78.421	8.684	3.898	0.727	0.202	120057
15	125432	36.412	20	96.412	17.165	3.931	0.817	0.336	138364

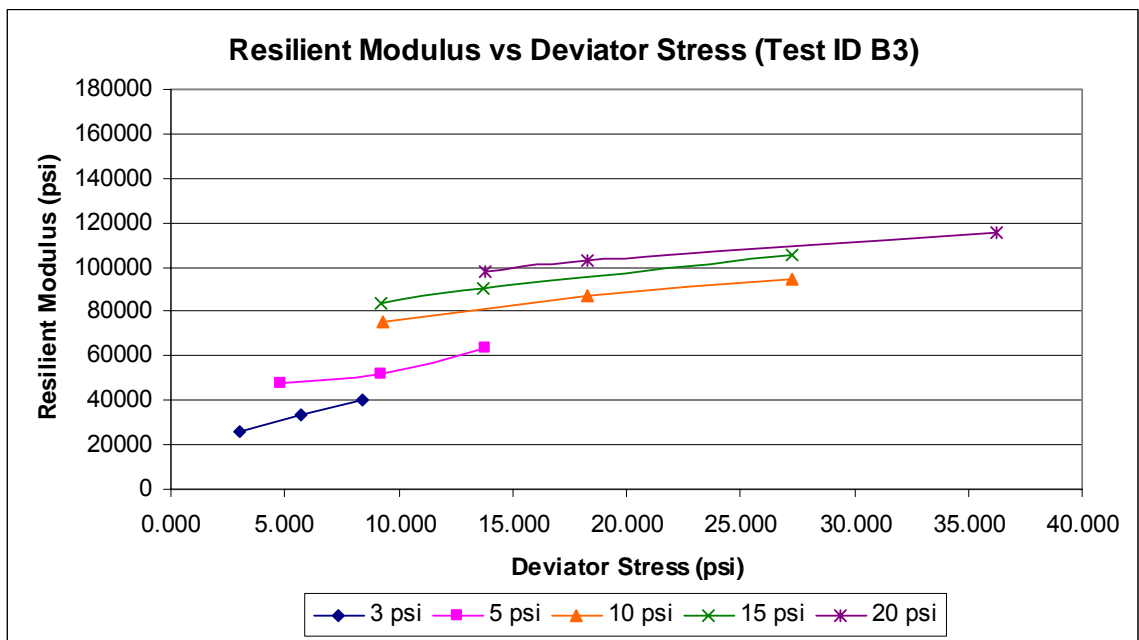
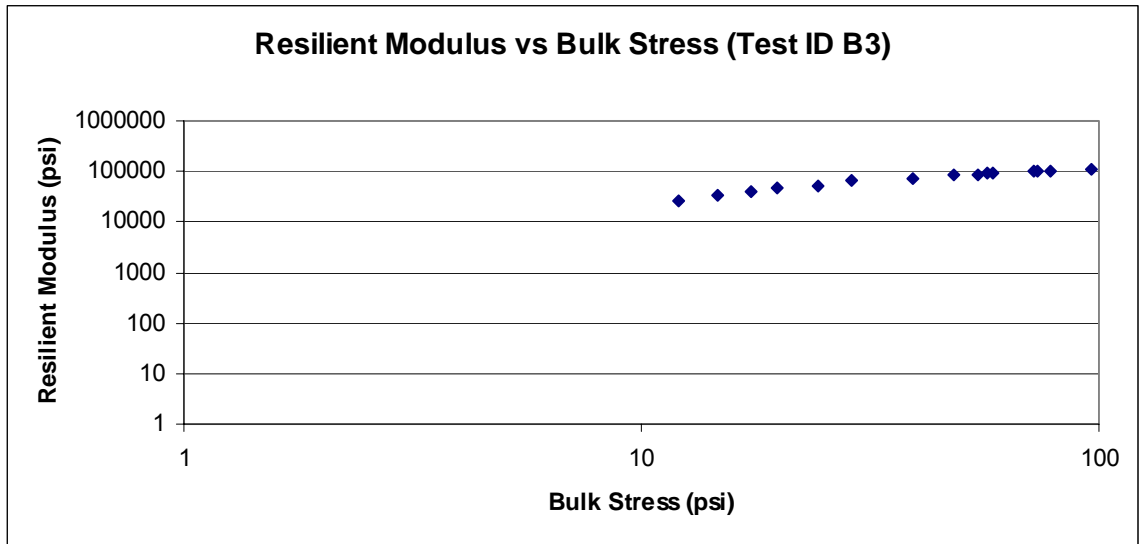
### Equation of Model:

$$M_r = k_1 P_a \left( \frac{\theta}{P_a} \right)^{k_2} \left( \frac{\tau_{oct}}{P_a} + 1 \right)^{k_3}$$

k <sub>1</sub>	1955.028
k <sub>2</sub>	0.892
k <sub>3</sub>	-0.137
R <sup>2</sup>	0.992



### B3



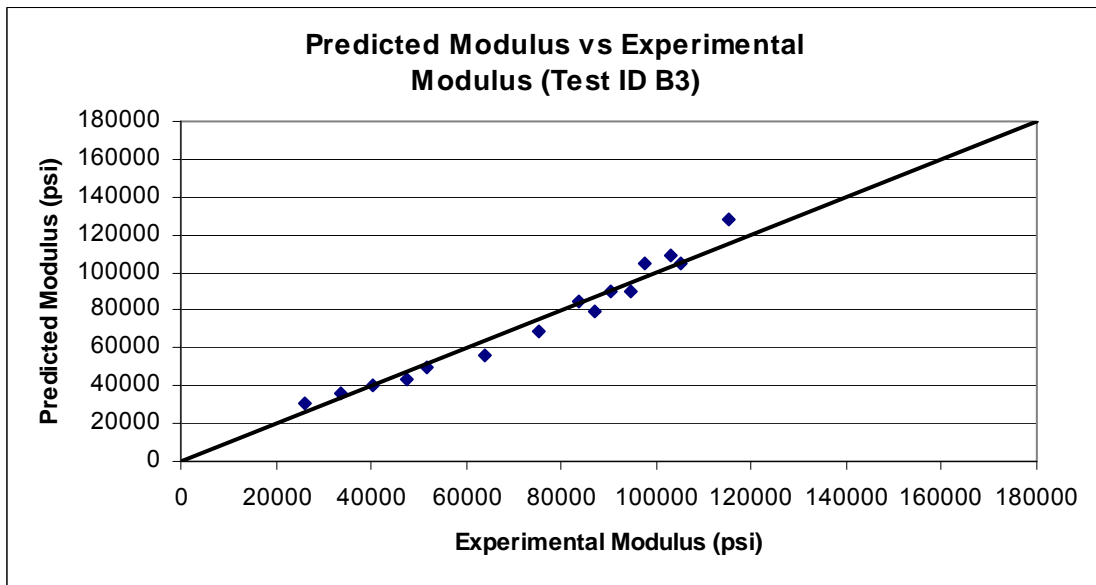
### B3

Sequence Number	Experimental Resilient Modulus	Deviator Stress	Confining Pressure	Bulk Stress	Octahedral Shear Stress	log (M <sub>r</sub> /P <sub>a</sub> )	log (Bulk Stress/P <sub>a</sub> )	log((T <sub>oct</sub> /P <sub>a</sub> )+1)	Regression Predicted Modulus
1	25985	3.057	3	12.057	1.441	3.247	-0.086	0.041	31202
2	33749	5.698	3	14.698	2.686	3.361	0.000	0.073	35726
3	40452	8.391	3	17.391	3.956	3.440	0.073	0.103	40103
4	47392	4.780	5	19.780	2.253	3.508	0.129	0.062	43362
5	51919	9.249	5	24.249	4.360	3.548	0.217	0.113	49982
6	63740	13.760	5	28.760	6.486	3.637	0.291	0.159	56327
7	75082	9.269	10	39.269	4.369	3.708	0.427	0.113	68642
8	86969	18.277	10	48.277	8.616	3.772	0.516	0.200	79725
9	94824	27.249	10	57.249	12.845	3.810	0.590	0.273	90213
10	83751	9.235	15	54.235	4.354	3.756	0.567	0.113	84887
11	90495	13.753	15	58.753	6.483	3.789	0.602	0.159	90129
12	105123	27.264	15	72.264	12.853	3.854	0.692	0.273	105159
13	97727	13.767	20	73.767	6.490	3.823	0.701	0.159	104691
14	103231	18.253	20	78.253	8.604	3.846	0.726	0.200	109549
15	115129	36.245	20	96.245	17.086	3.894	0.816	0.335	128232

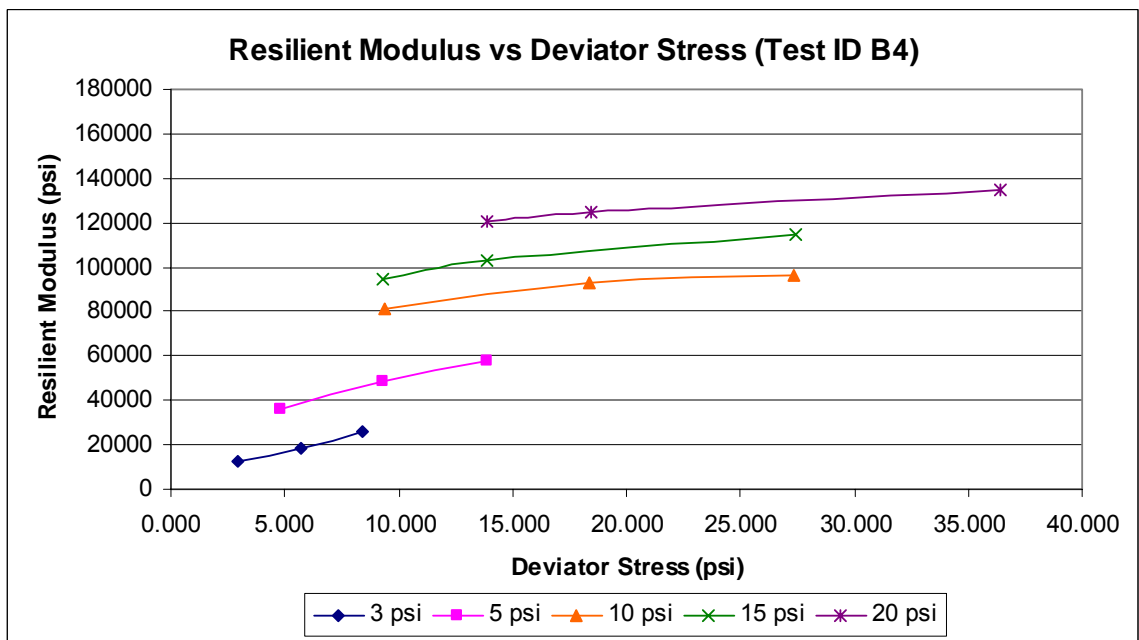
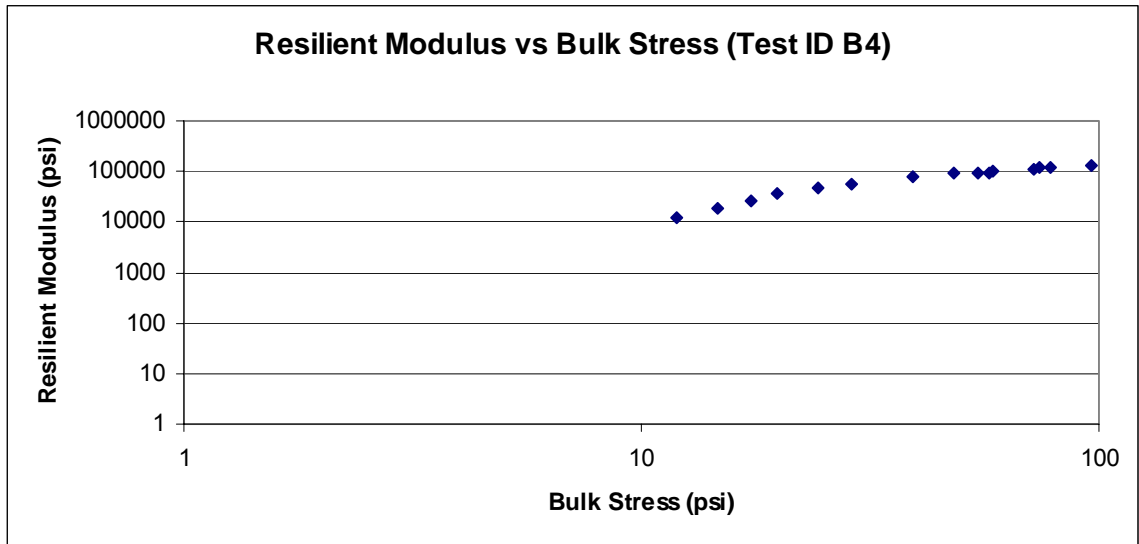
#### Equation of Model:

$$M_r = k_1 P_a \left( \frac{\theta}{P_a} \right)^{k_2} \left( \frac{\tau_{oct}}{P_a} + 1 \right)^{k_3}$$

k <sub>1</sub>	2402.817
k <sub>2</sub>	0.658
k <sub>3</sub>	0.069
R <sup>2</sup>	0.966



## B4



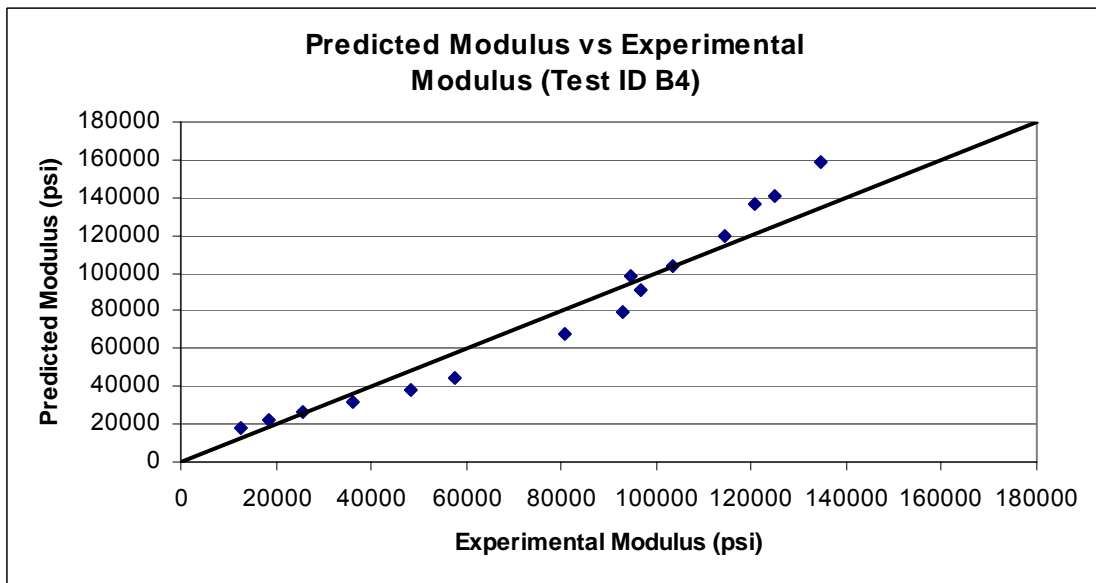
## B4

Sequence Number	Experimental Resilient Modulus	Deviator Stress	Confining Pressure	Bulk Stress	Octahedral Shear Stress	log (M <sub>r</sub> /P <sub>a</sub> )	log (Bulk Stress/P <sub>a</sub> )	log((T <sub>oct</sub> /P <sub>a</sub> )+1)	Regression Predicted Modulus
1	12553	2.938	3	11.938	1.385	2.931	-0.090	0.039	17676
2	18621	5.705	3	14.705	2.690	3.103	0.000	0.073	21919
3	25775	8.415	3	17.415	3.967	3.244	0.074	0.104	26020
4	36059	4.854	5	19.854	2.288	3.390	0.131	0.063	31528
5	48228	9.318	5	24.318	4.393	3.516	0.219	0.114	38241
6	57585	13.846	5	28.846	6.527	3.593	0.293	0.160	44855
7	80887	9.361	10	39.361	4.413	3.741	0.428	0.114	67476
8	93055	18.364	10	48.364	8.657	3.801	0.517	0.201	79472
9	96626	27.331	10	57.331	12.884	3.818	0.591	0.273	90939
10	94539	9.342	15	54.342	4.404	3.808	0.568	0.114	98748
11	103344	13.862	15	58.862	6.534	3.847	0.603	0.160	104059
12	114345	27.391	15	72.391	12.912	3.891	0.692	0.274	119705
13	120609	13.914	20	73.914	6.559	3.914	0.701	0.160	136076
14	124742	18.415	20	78.415	8.681	3.929	0.727	0.202	140510
15	134442	36.381	20	96.381	17.150	3.961	0.817	0.336	158575

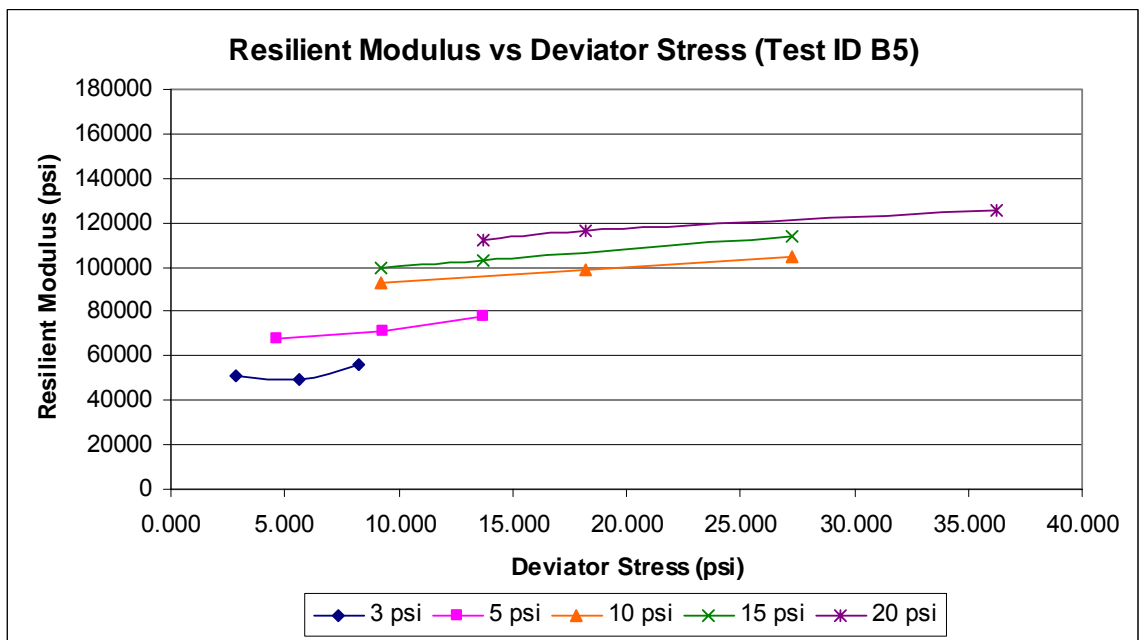
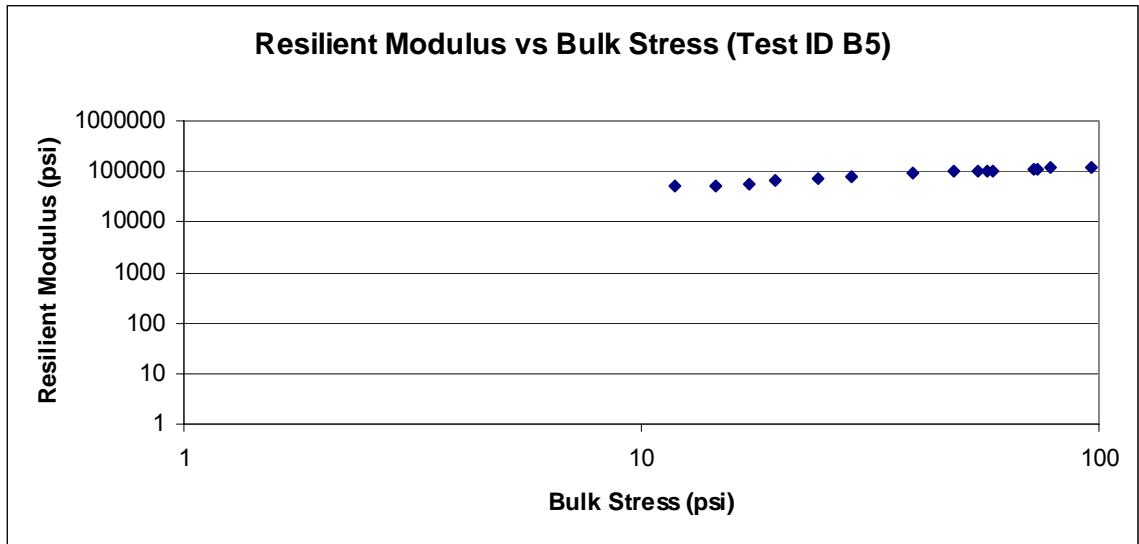
### Equation of Model:

$$M_r = k_1 P_a \left( \frac{\theta}{P_a} \right)^{k_2} \left( \frac{\tau_{oct}}{P_a} + 1 \right)^{k_3}$$

k <sub>1</sub>	1593.053
k <sub>2</sub>	1.180
k <sub>3</sub>	-0.396
R <sup>2</sup>	0.949



## B5





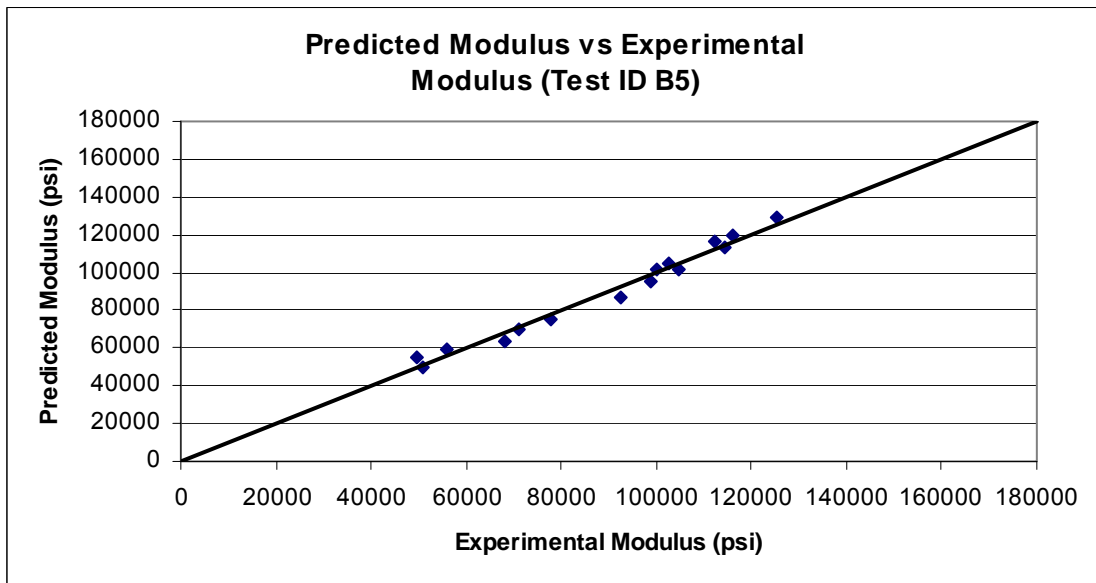
## B5

Sequence Number	Experimental Resilient Modulus	Deviator Stress	Confining Pressure	Bulk Stress	Octahedral Shear Stress	log (M <sub>r</sub> /P <sub>a</sub> )	log (Bulk Stress/P <sub>a</sub> )	log((T <sub>oct</sub> /P <sub>a</sub> )+1)	Regression Predicted Modulus
1	50899	2.834	3	11.834	1.336	3.539	-0.094	0.038	50086
2	49641	5.593	3	14.593	2.636	3.529	-0.003	0.072	55011
3	55965	8.266	3	17.266	3.897	3.581	0.070	0.102	59284
4	68170	4.691	5	19.691	2.211	3.666	0.127	0.061	63473
5	71275	9.319	5	24.319	4.393	3.686	0.219	0.114	69568
6	77727	13.715	5	28.715	6.465	3.723	0.291	0.158	74738
7	92545	9.208	10	39.208	4.341	3.799	0.426	0.112	87180
8	98844	18.197	10	48.197	8.578	3.828	0.516	0.200	94843
9	104810	27.255	10	57.255	12.848	3.853	0.590	0.273	101743
10	99978	9.187	15	54.187	4.331	3.833	0.567	0.112	101571
11	102713	13.674	15	58.674	6.446	3.844	0.601	0.158	104730
12	114229	27.271	15	72.271	12.856	3.890	0.692	0.273	113567
13	112184	13.704	20	73.704	6.460	3.883	0.700	0.158	116631
14	116196	18.209	20	78.209	8.584	3.898	0.726	0.200	119192
15	125296	36.248	20	96.248	17.087	3.931	0.816	0.335	128800

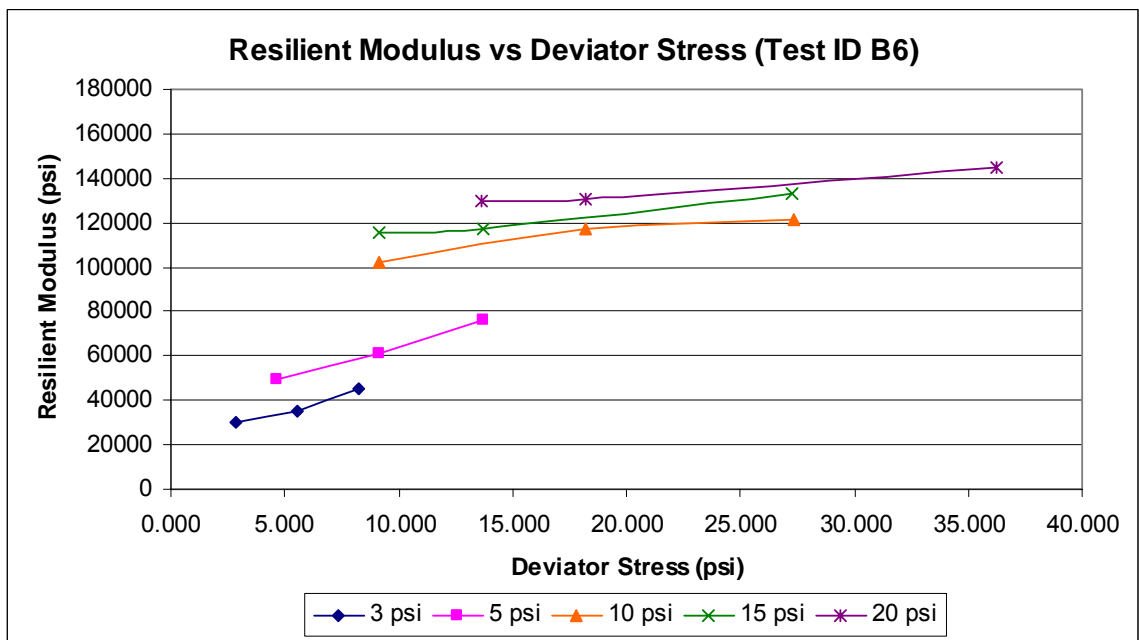
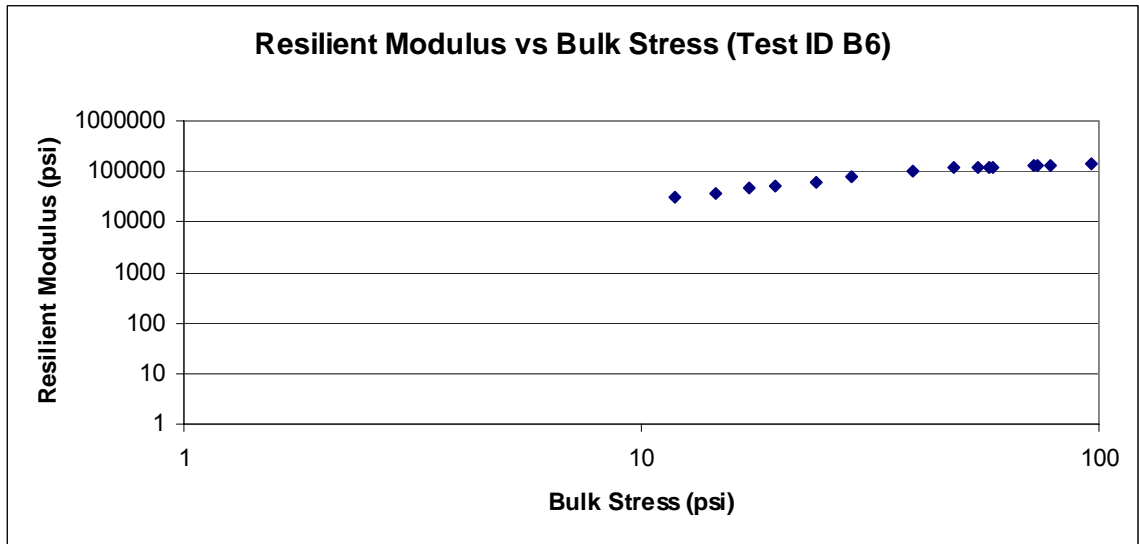
### Equation of Model:

$$M_r = k_1 P_a \left( \frac{\theta}{P_a} \right)^{k_2} \left( \frac{\tau_{oct}}{P_a} + 1 \right)^{k_3}$$

k <sub>1</sub>	3796.166
k <sub>2</sub>	0.472
k <sub>3</sub>	-0.066
R <sup>2</sup>	0.977



## B6



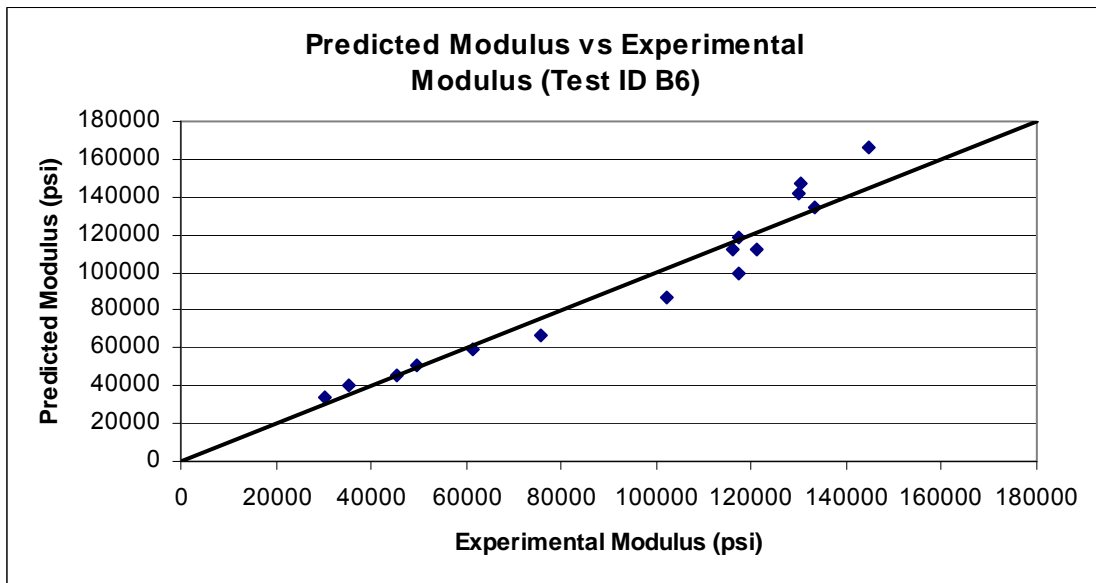
## B6

Sequence Number	Experimental Resilient Modulus	Deviator Stress	Confining Pressure	Bulk Stress	Octahedral Shear Stress	log (M <sub>r</sub> /P <sub>a</sub> )	log (Bulk Stress/P <sub>a</sub> )	log((T <sub>oct</sub> /P <sub>a</sub> )+1)	Regression Predicted Modulus
1	30449	2.850	3	11.850	1.343	3.316	-0.094	0.038	33996
2	35230	5.581	3	14.581	2.631	3.380	-0.004	0.071	39724
3	45457	8.274	3	17.274	3.901	3.490	0.070	0.102	45068
4	49588	4.663	5	19.663	2.198	3.528	0.126	0.061	50702
5	61344	9.168	5	24.168	4.322	3.620	0.216	0.112	58846
6	75790	13.734	5	28.734	6.474	3.712	0.291	0.158	66605
7	102278	9.148	10	39.148	4.312	3.842	0.425	0.112	86724
8	117235	18.205	10	48.205	8.582	3.902	0.516	0.200	99604
9	121125	27.317	10	57.317	12.877	3.916	0.591	0.273	111752
10	115899	9.175	15	54.175	4.325	3.897	0.566	0.112	112595
11	117381	13.723	15	58.723	6.469	3.902	0.601	0.158	118321
12	133422	27.270	15	72.270	12.855	3.958	0.692	0.273	134658
13	129846	13.664	20	73.664	6.441	3.946	0.700	0.158	141998
14	130517	18.175	20	78.175	8.568	3.948	0.726	0.199	146929
15	144514	36.220	20	96.220	17.074	3.993	0.816	0.335	166095

### Equation of Model:

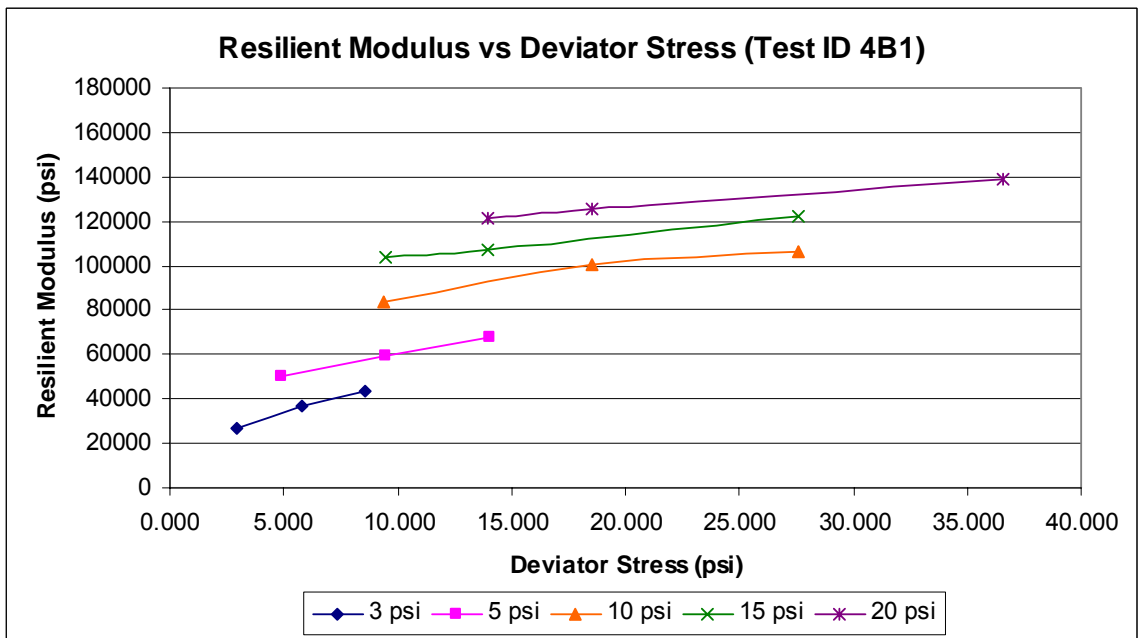
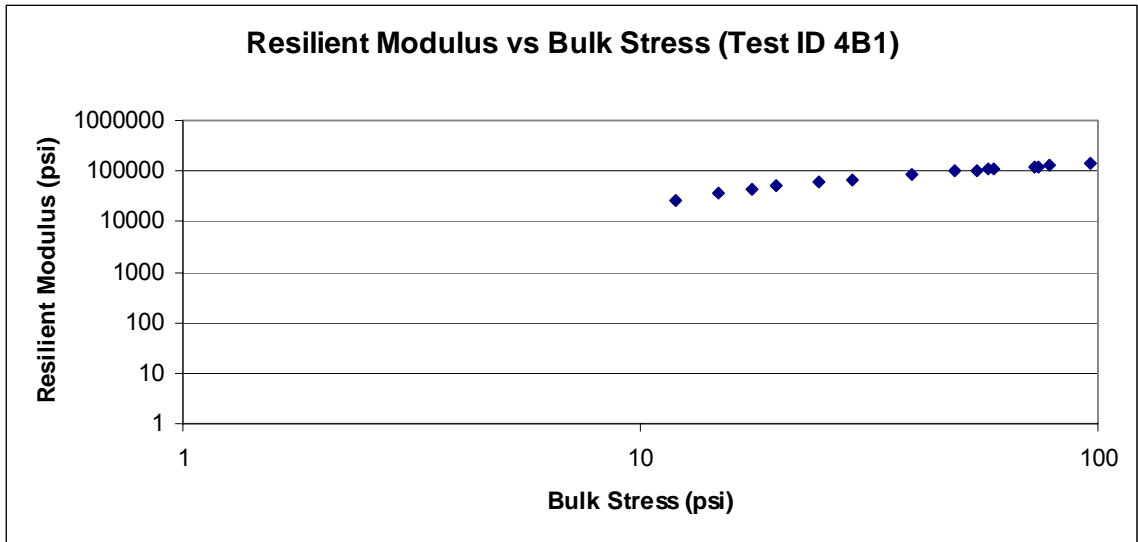
$$M_r = k_1 P_a \left( \frac{\theta}{P_a} \right)^{k_2} \left( \frac{\tau_{oct}}{P_a} + 1 \right)^{k_3}$$

k <sub>1</sub>	2784.585
k <sub>2</sub>	0.804
k <sub>3</sub>	-0.142
R <sup>2</sup>	0.962



Limestone and cement, 28 days

4B1



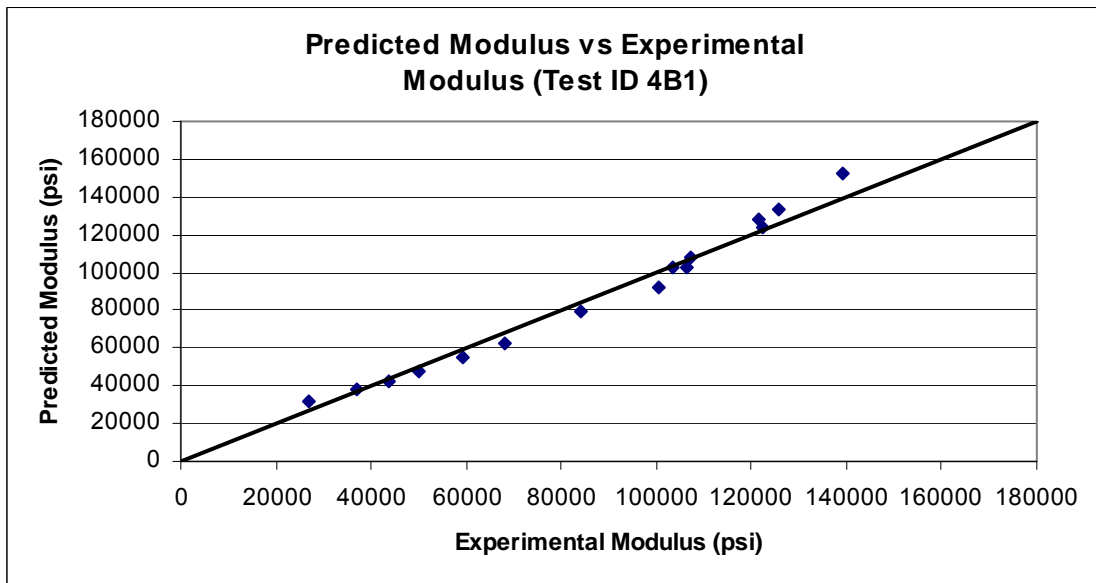
## 4B1

Sequence Number	Experimental Resilient Modulus	Deviator Stress	Confining Pressure	Bulk Stress	Octahedral Shear Stress	log (M <sub>r</sub> /P <sub>a</sub> )	log (Bulk Stress/P <sub>a</sub> )	log((T <sub>oct</sub> /P <sub>a</sub> )+1)	Regression Predicted Modulus
1	26786	2.934	3	11.934	1.383	3.261	-0.091	0.039	32173
2	36928	5.790	3	14.790	2.729	3.400	0.003	0.074	37695
3	43580	8.566	3	17.566	4.038	3.472	0.077	0.105	42768
4	49989	4.871	5	19.871	2.296	3.532	0.131	0.063	47465
5	59180	9.481	5	24.481	4.469	3.605	0.222	0.115	55156
6	68153	14.029	5	29.029	6.613	3.666	0.296	0.161	62310
7	84122	9.385	10	39.385	4.424	3.758	0.428	0.114	79658
8	100704	18.530	10	48.530	8.735	3.836	0.519	0.203	91880
9	106470	27.552	10	57.552	12.988	3.860	0.593	0.275	103230
10	103492	9.464	15	54.464	4.461	3.848	0.569	0.115	102309
11	107431	13.974	15	58.974	6.587	3.864	0.603	0.161	107754
12	122286	27.560	15	72.560	12.992	3.920	0.693	0.275	123467
13	121345	13.971	20	73.971	6.586	3.917	0.702	0.161	128369
14	125726	18.497	20	78.497	8.719	3.932	0.728	0.202	133227
15	139089	36.570	20	96.570	17.239	3.976	0.818	0.337	151985

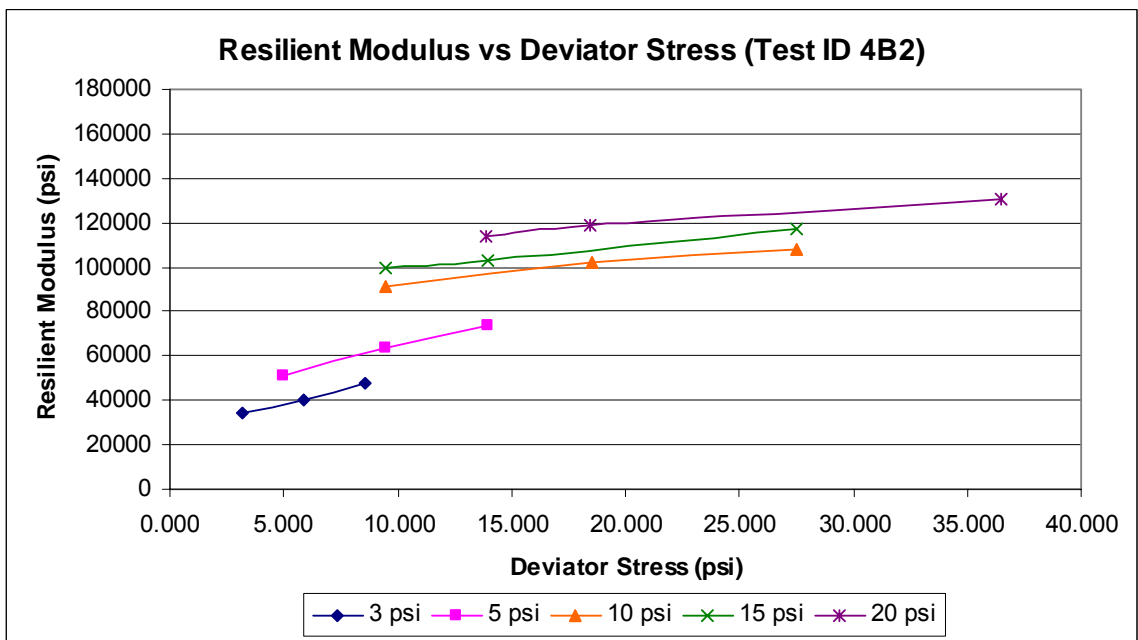
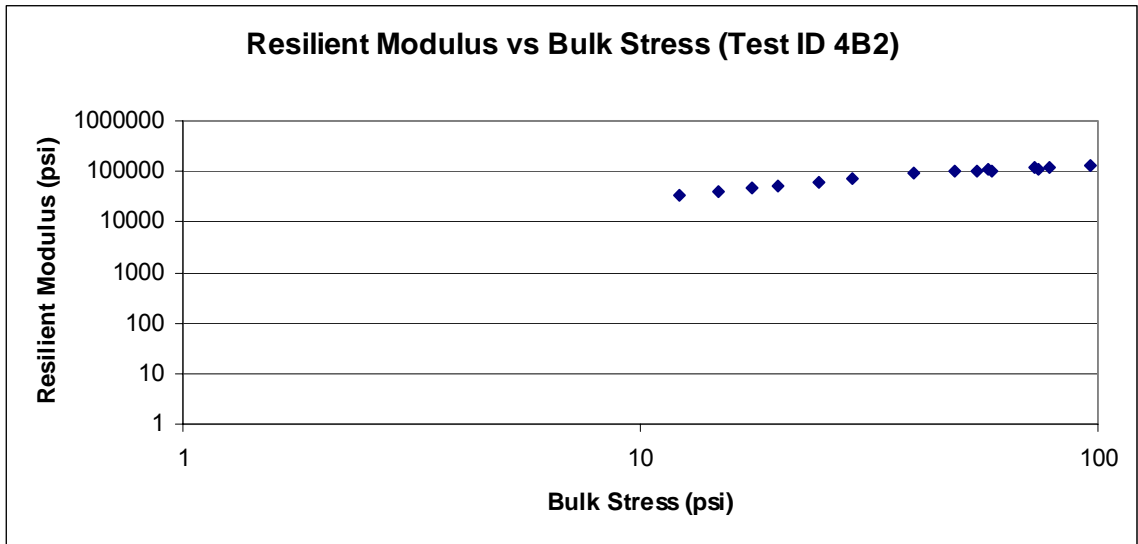
### Equation of Model:

$$M_r = k_1 P_a \left( \frac{\theta}{P_a} \right)^{k_2} \left( \frac{\tau_{oct}}{P_a} + 1 \right)^{k_3}$$

k <sub>1</sub>	2592.266
k <sub>2</sub>	0.773
k <sub>3</sub>	-0.091
R <sup>2</sup>	0.979



## 4B2



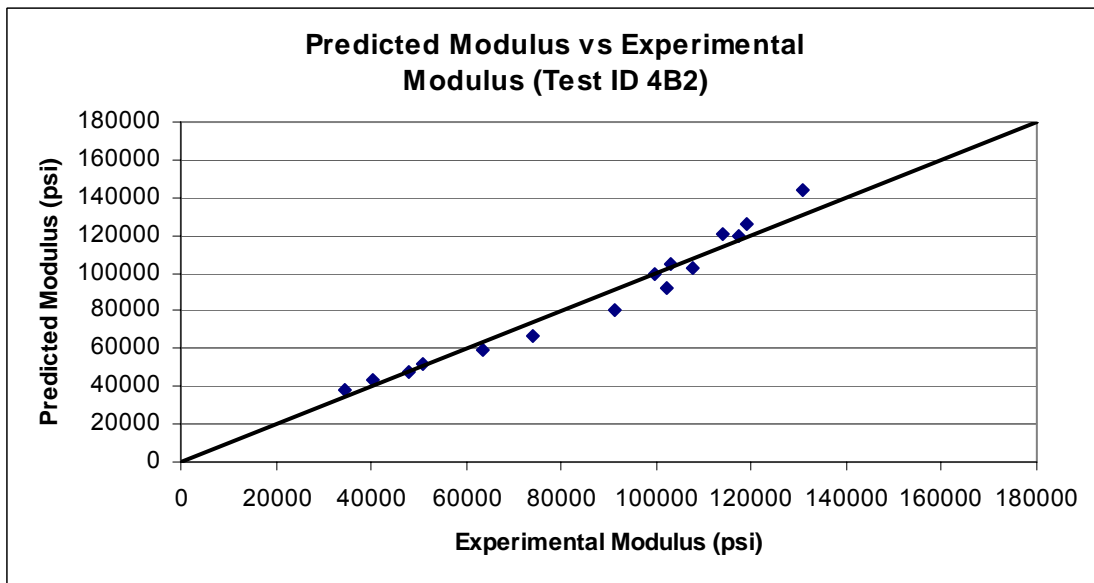
## 4B2

Sequence Number	Experimental Resilient Modulus	Deviator Stress	Confining Pressure	Bulk Stress	Octahedral Shear Stress	log (M <sub>r</sub> /P <sub>a</sub> )	log (Bulk Stress/P <sub>a</sub> )	log((T <sub>oct</sub> /P <sub>a</sub> )+1)	Regression Predicted Modulus
1	34294	3.199	3	12.199	1.508	3.368	-0.081	0.042	38005
2	40413	5.858	3	14.858	2.761	3.439	0.005	0.075	43145
3	47866	8.554	3	17.554	4.032	3.513	0.077	0.105	48034
4	50957	4.996	5	19.996	2.355	3.540	0.134	0.065	52204
5	63369	9.455	5	24.455	4.457	3.635	0.221	0.115	59432
6	73863	13.997	5	28.997	6.598	3.701	0.295	0.161	66328
7	91317	9.481	10	39.481	4.469	3.793	0.429	0.115	80829
8	102232	18.537	10	48.537	8.739	3.842	0.519	0.203	92359
9	107650	27.500	10	57.500	12.964	3.865	0.592	0.275	103039
10	99563	9.431	15	54.431	4.446	3.831	0.569	0.115	99332
11	102900	13.924	15	58.924	6.564	3.845	0.603	0.160	104564
12	117130	27.472	15	72.472	12.951	3.901	0.693	0.274	119542
13	113782	13.910	20	73.910	6.557	3.889	0.701	0.160	120937
14	119019	18.437	20	78.437	8.691	3.908	0.727	0.202	125688
15	130923	36.527	20	96.527	17.219	3.950	0.817	0.337	143771

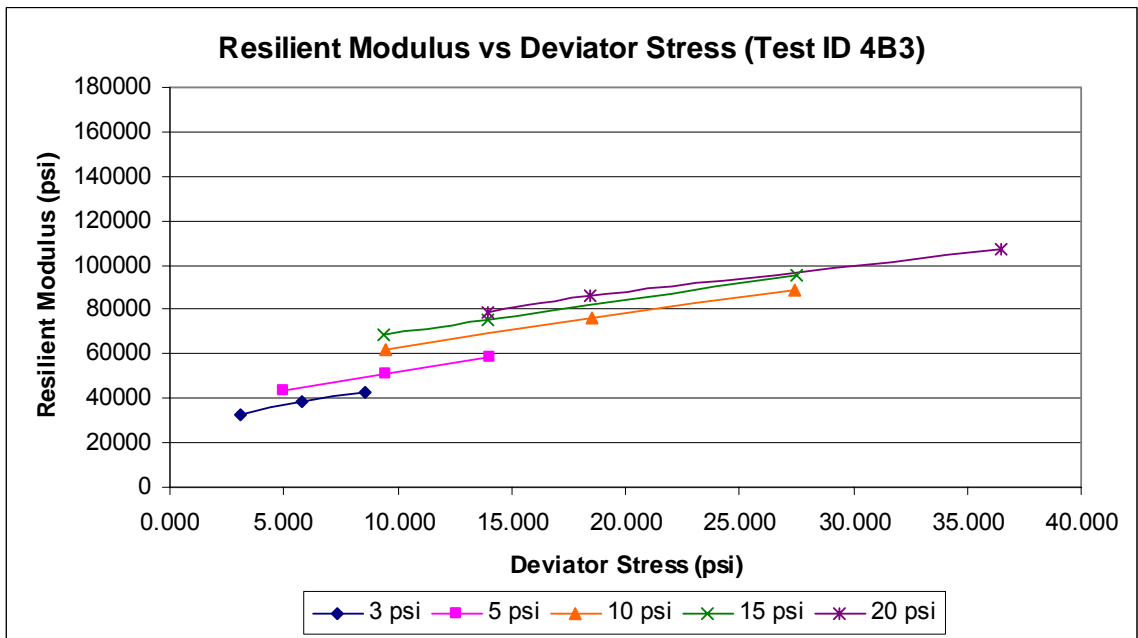
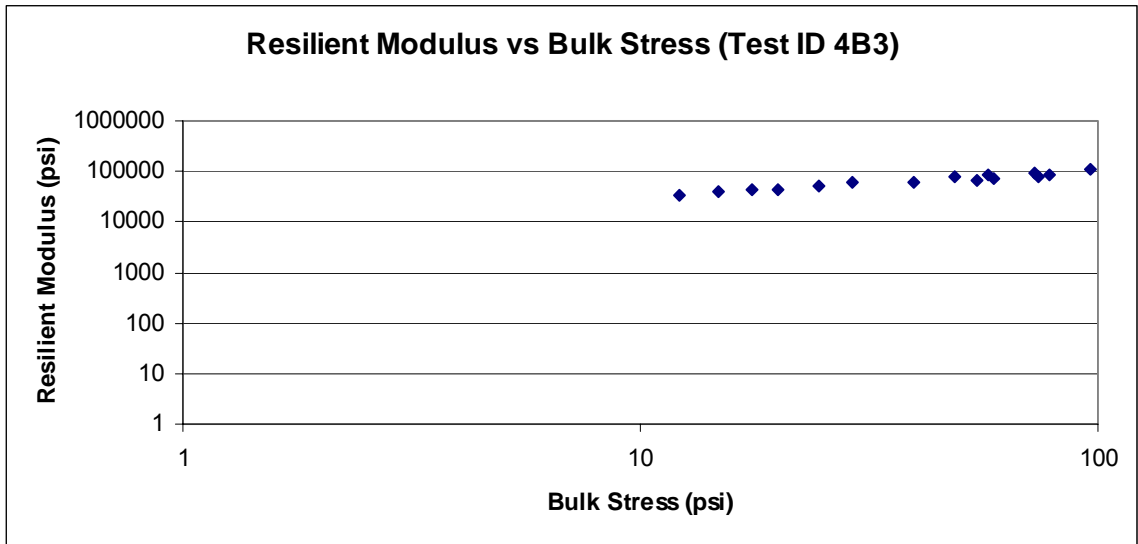
### Equation of Model:

$$M_r = k_1 P_a \left( \frac{\theta}{P_a} \right)^{k_2} \left( \frac{\tau_{oct}}{P_a} + 1 \right)^{k_3}$$

k <sub>1</sub>	2913.109
k <sub>2</sub>	0.642
k <sub>3</sub>	0.004
R <sup>2</sup>	0.972



### 4B3





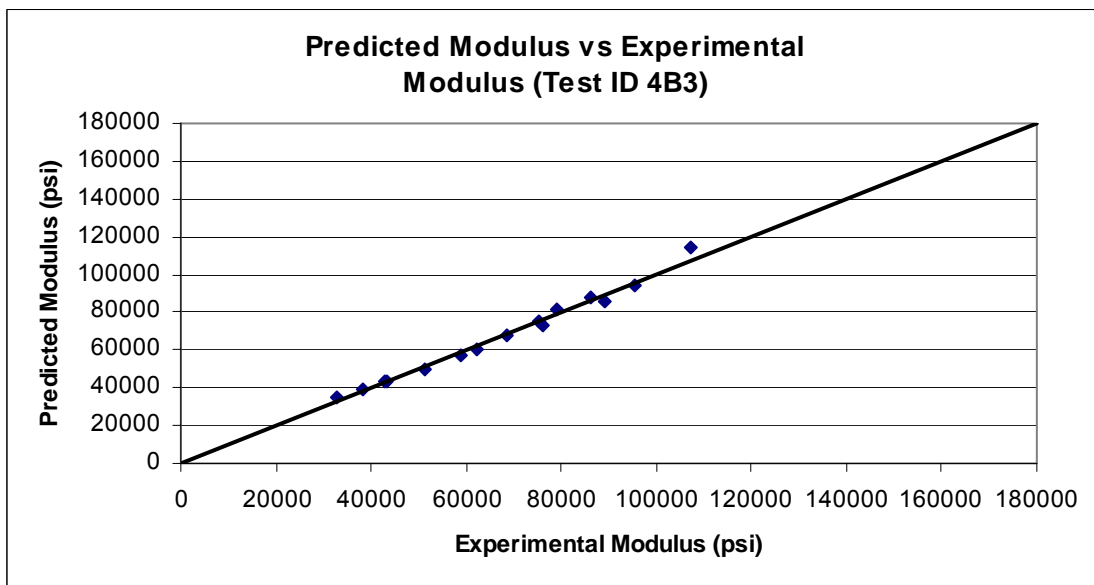
### 4B3

Sequence Number	Experimental Resilient Modulus	Deviator Stress	Confining Pressure	Bulk Stress	Octahedral Shear Stress	log (M <sub>r</sub> /P <sub>a</sub> )	log (Bulk Stress/P <sub>a</sub> )	log((T <sub>oct</sub> /P <sub>a</sub> )+1)	Regression Predicted Modulus
1	32832	3.138	3	12.138	1.479	3.349	-0.083	0.042	34503
2	38283	5.809	3	14.809	2.738	3.416	0.003	0.074	38922
3	42702	8.542	3	17.542	4.027	3.463	0.077	0.105	43314
4	43391	4.940	5	19.940	2.329	3.470	0.132	0.064	43127
5	51304	9.448	5	24.448	4.454	3.543	0.221	0.115	49950
6	58808	14.012	5	29.012	6.605	3.602	0.295	0.161	56755
7	62091	9.464	10	39.464	4.461	3.626	0.429	0.115	60233
8	76128	18.525	10	48.525	8.733	3.714	0.519	0.203	73264
9	89140	27.464	10	57.464	12.947	3.783	0.592	0.274	86029
10	68600	9.409	15	54.409	4.436	3.669	0.568	0.115	68230
11	75297	13.950	15	58.950	6.576	3.709	0.603	0.161	74801
12	95669	27.470	15	72.470	12.949	3.813	0.693	0.274	94193
13	78982	13.947	20	73.947	6.575	3.730	0.702	0.161	81721
14	86394	18.459	20	78.459	8.702	3.769	0.727	0.202	88318
15	107303	36.518	20	96.518	17.215	3.863	0.817	0.337	114356

#### Equation of Model:

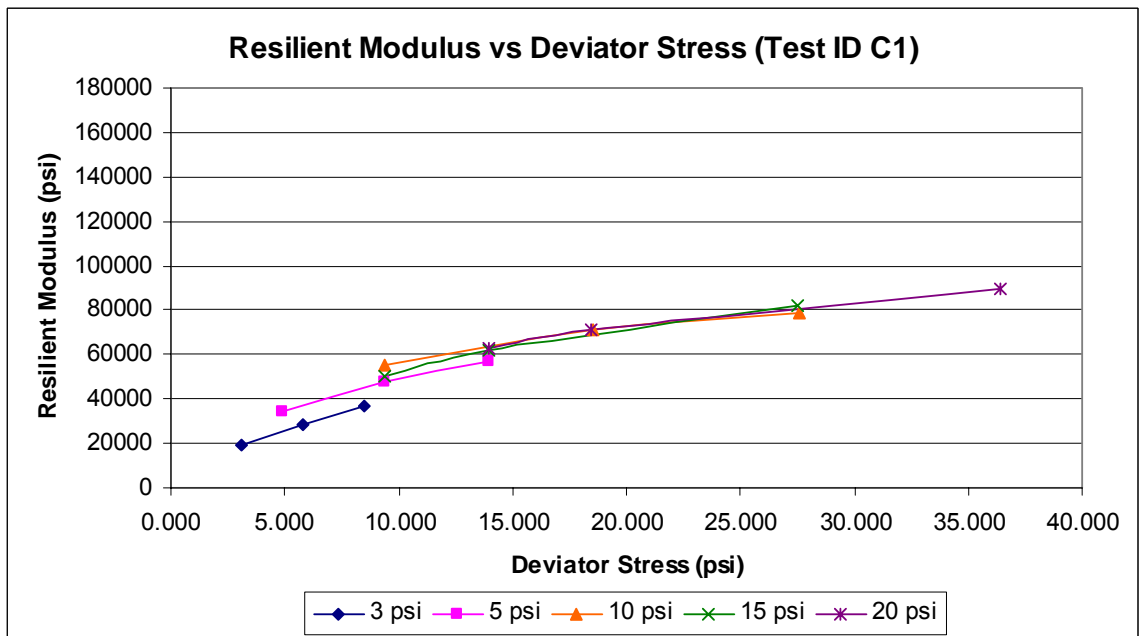
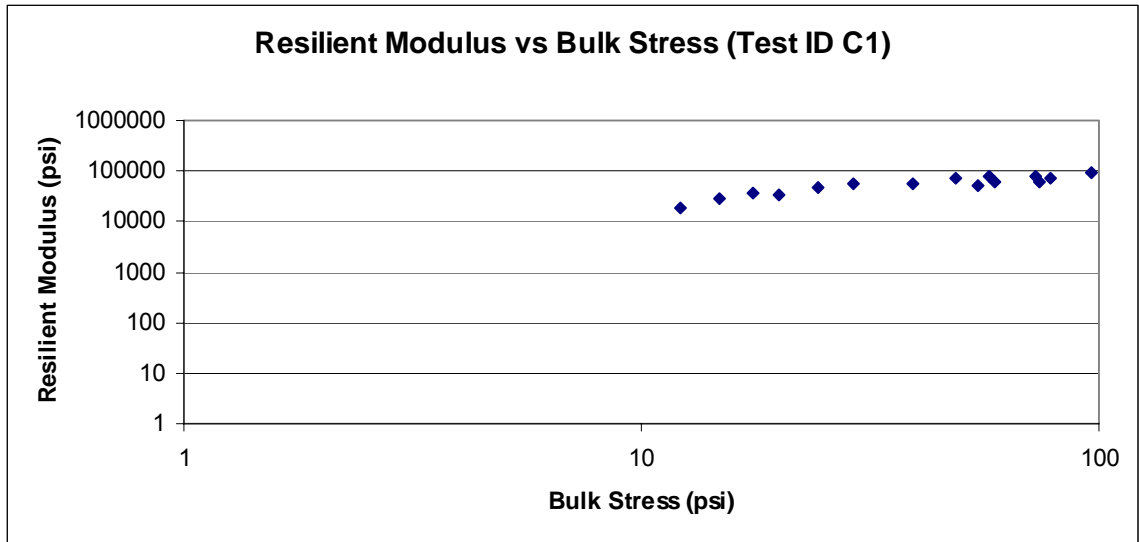
$$M_r = k_1 P_a \left( \frac{\theta}{P_a} \right)^{k_2} \left( \frac{\tau_{oct}}{P_a} + 1 \right)^{k_3}$$

k <sub>1</sub>	2394.377
k <sub>2</sub>	0.391
k <sub>3</sub>	0.572
R <sup>2</sup>	0.992



Limestone, fly ash, and lime, 7 days

C1



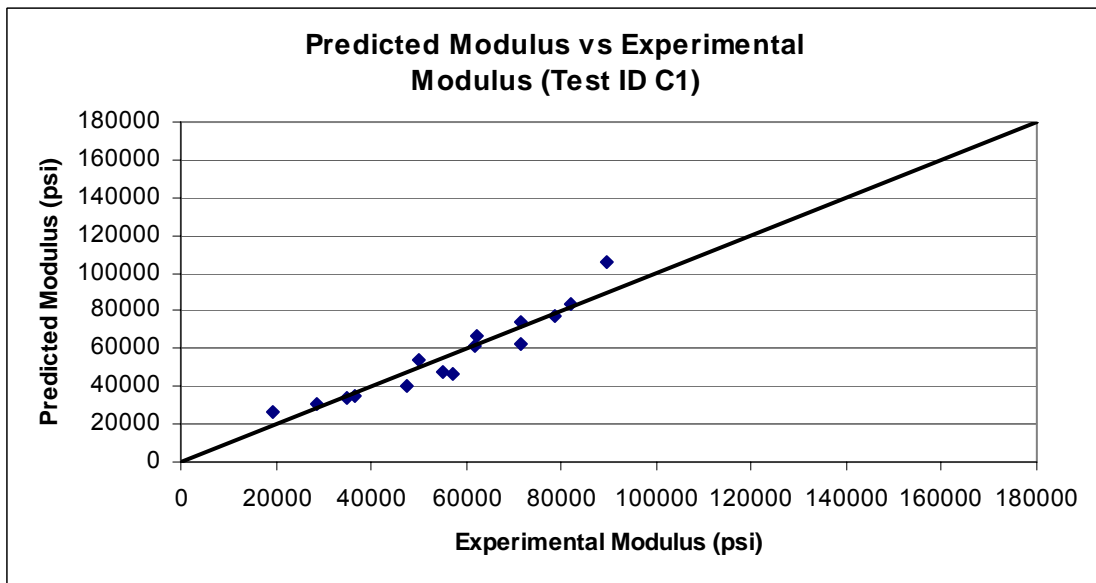
# C1

Sequence Number	Experimental Resilient Modulus	Deviator Stress	Confining Pressure	Bulk Stress	Octahedral Shear Stress	log (M <sub>r</sub> /P <sub>a</sub> )	log (Bulk Stress/P <sub>a</sub> )	log((T <sub>oct</sub> /P <sub>a</sub> )+1)	Regression Predicted Modulus
1	19146	3.131	3	12.131	1.476	3.115	-0.083	0.042	26518
2	28752	5.816	3	14.816	2.742	3.291	0.003	0.074	30580
3	36786	8.486	3	17.486	4.000	3.398	0.075	0.105	34638
4	34742	4.935	5	19.935	2.327	3.374	0.132	0.064	33468
5	47711	9.389	5	24.389	4.426	3.511	0.220	0.114	40057
6	57255	13.992	5	28.992	6.596	3.590	0.295	0.161	47057
7	55123	9.393	10	39.393	4.428	3.574	0.428	0.114	47987
8	71371	18.514	10	48.514	8.728	3.686	0.519	0.202	62201
9	78491	27.558	10	57.558	12.991	3.728	0.593	0.275	77015
10	50144	9.375	15	54.375	4.419	3.533	0.568	0.114	54157
11	61753	13.945	15	58.945	6.574	3.623	0.603	0.161	61412
12	81984	27.546	15	72.546	12.985	3.746	0.693	0.275	84010
13	62408	13.953	20	73.953	6.577	3.628	0.702	0.161	66896
14	71437	18.488	20	78.488	8.715	3.687	0.727	0.202	74517
15	89572	36.430	20	96.430	17.173	3.785	0.817	0.336	106043

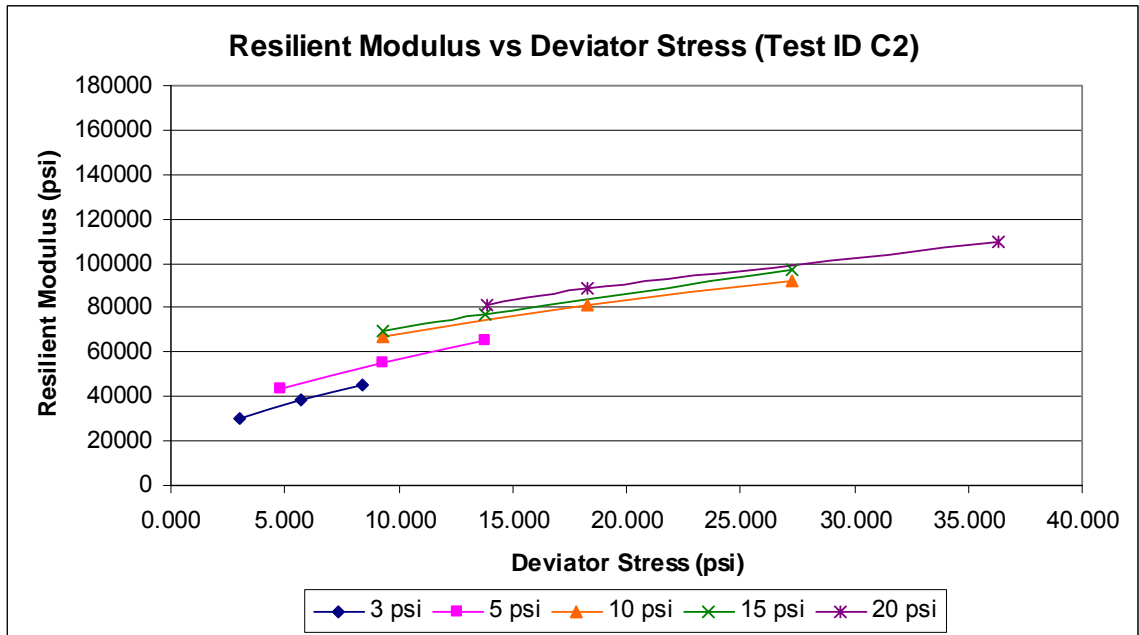
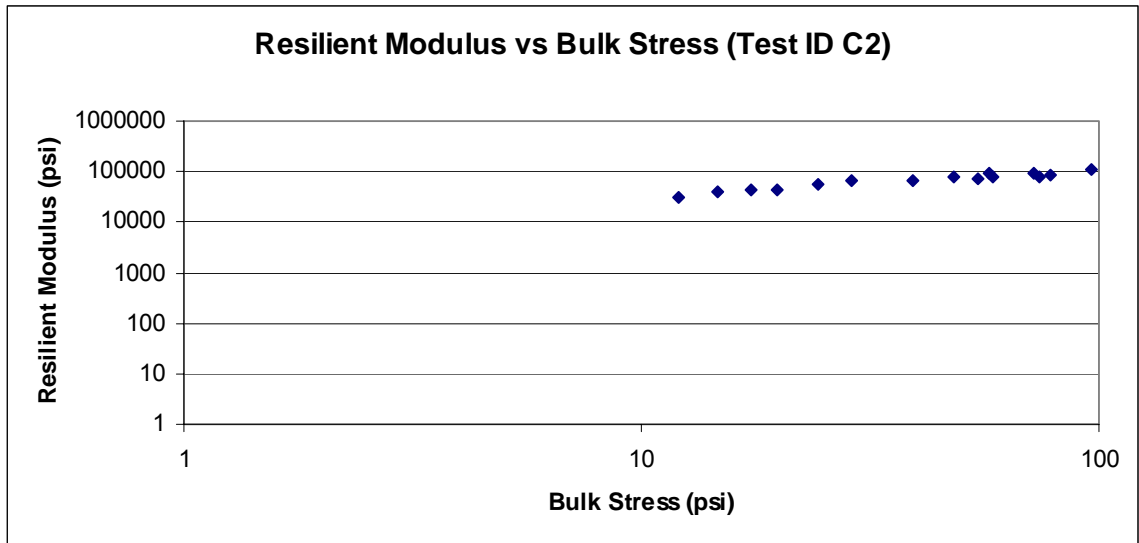
## Equation of Model:

$$M_r = k_1 P_a \left( \frac{\theta}{P_a} \right)^{k_2} \left( \frac{\tau_{oct}}{P_a} + 1 \right)^{k_3}$$

k <sub>1</sub>	1780.476
k <sub>2</sub>	0.377
k <sub>3</sub>	0.893
R <sup>2</sup>	0.898



C2



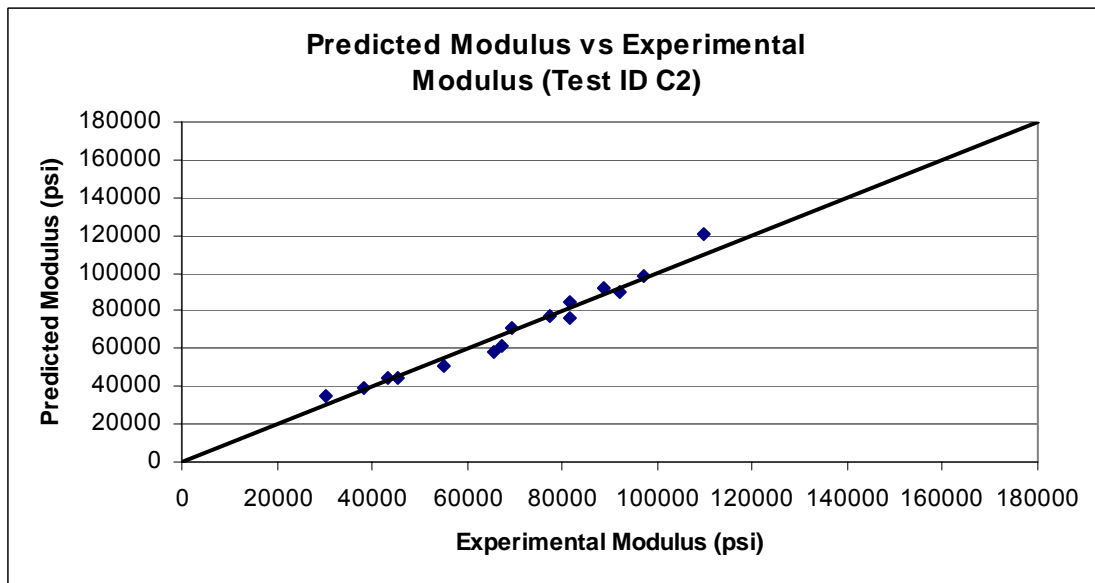
## C2

Sequence Number	Experimental Resilient Modulus	Deviator Stress	Confining Pressure	Bulk Stress	Octahedral Shear Stress	log (M <sub>r</sub> /P <sub>a</sub> )	log (Bulk Stress/P <sub>a</sub> )	log((T <sub>oct</sub> /P <sub>a</sub> )+1)	Regression Predicted Modulus
1	30348	3.013	3	12.013	1.420	3.315	-0.088	0.040	34971
2	38363	5.696	3	14.696	2.685	3.417	0.000	0.073	39647
3	45227	8.376	3	17.376	3.949	3.488	0.073	0.103	44202
4	43230	4.795	5	19.795	2.260	3.468	0.129	0.062	43945
5	55050	9.282	5	24.282	4.375	3.573	0.218	0.113	51158
6	65475	13.820	5	28.820	6.515	3.649	0.292	0.159	58384
7	67150	9.308	10	39.308	4.388	3.660	0.427	0.113	61930
8	81426	18.312	10	48.312	8.632	3.743	0.517	0.201	75876
9	92179	27.299	10	57.299	12.869	3.797	0.591	0.273	89798
10	69423	9.332	15	54.332	4.399	3.674	0.568	0.114	70421
11	77383	13.829	15	58.829	6.519	3.721	0.602	0.159	77452
12	97027	27.236	15	72.236	12.839	3.820	0.691	0.273	98358
13	81454	13.863	20	73.863	6.535	3.744	0.701	0.160	84792
14	88717	18.303	20	78.303	8.628	3.781	0.726	0.201	91850
15	109583	36.356	20	96.356	17.138	3.872	0.817	0.336	120351

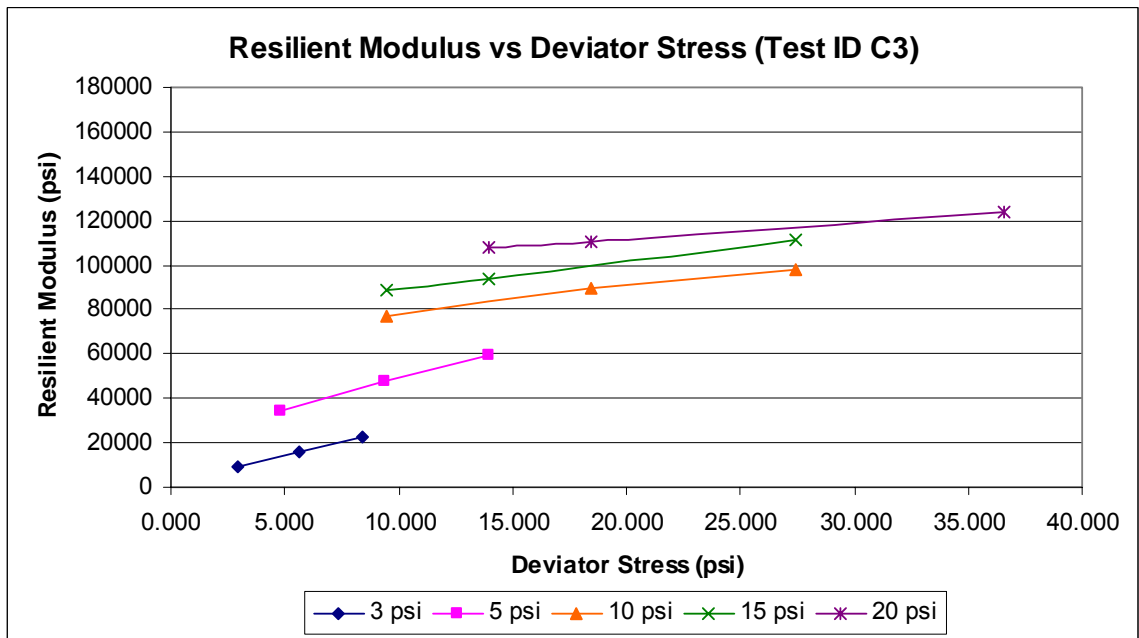
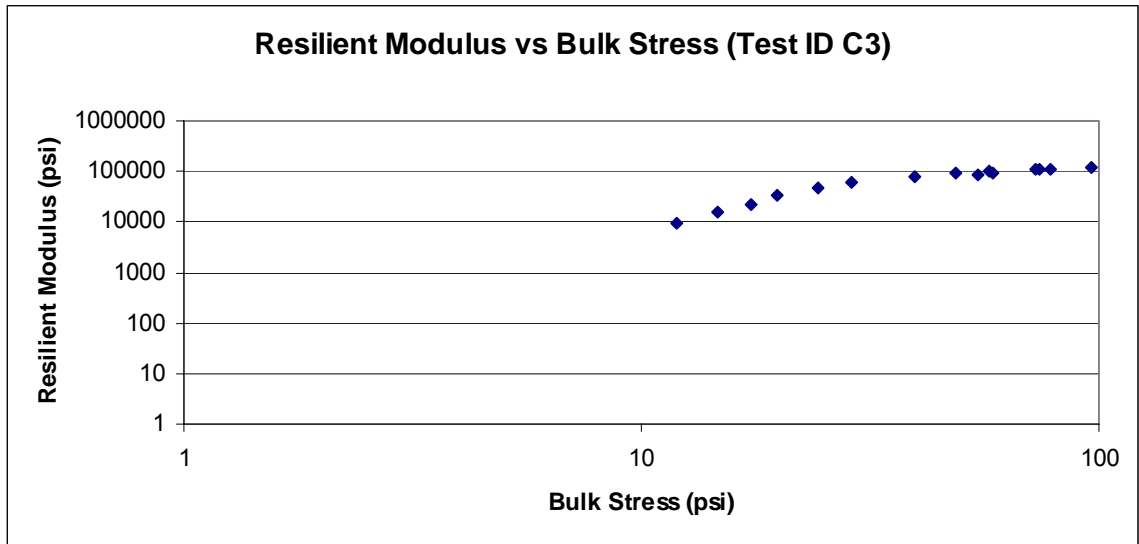
### Equation of Model:

$$M_r = k_1 P_a \left( \frac{\theta}{P_a} \right)^{k_2} \left( \frac{\tau_{oct}}{P_a} + 1 \right)^{k_3}$$

k <sub>1</sub>	2437.056
k <sub>2</sub>	0.396
k <sub>3</sub>	0.605
R <sup>2</sup>	0.967



### C3



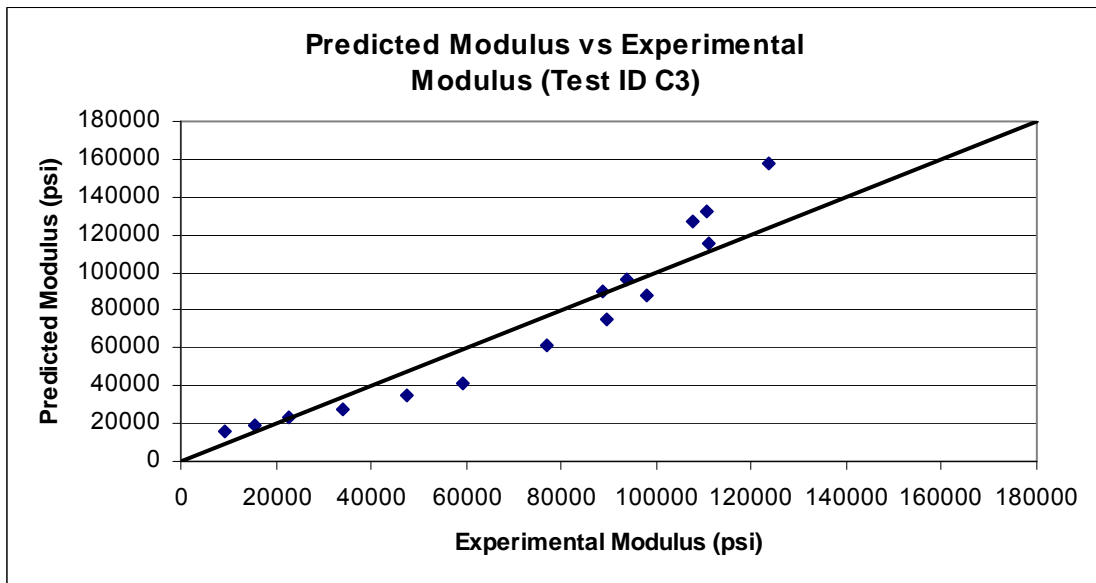
### C3

Sequence Number	Experimental Resilient Modulus	Deviator Stress	Confining Pressure	Bulk Stress	Octahedral Shear Stress	log (M <sub>r</sub> /P <sub>a</sub> )	log (Bulk Stress/P <sub>a</sub> )	log((T <sub>oct</sub> /P <sub>a</sub> )+1)	Regression Predicted Modulus
1	9438	2.899	3	11.899	1.367	2.808	-0.092	0.039	15388
2	15653	5.646	3	14.646	2.662	3.027	-0.002	0.072	19335
3	22867	8.412	3	17.412	3.966	3.192	0.074	0.104	23340
4	34227	4.779	5	19.779	2.253	3.367	0.129	0.062	27819
5	47446	9.410	5	24.410	4.436	3.509	0.220	0.115	34691
6	59105	13.932	5	28.932	6.568	3.604	0.294	0.160	41385
7	77085	9.447	10	39.447	4.453	3.720	0.429	0.115	61441
8	89510	18.451	10	48.451	8.698	3.785	0.518	0.202	74713
9	98164	27.443	10	57.443	12.937	3.825	0.592	0.274	87832
10	88881	9.462	15	54.462	4.460	3.781	0.569	0.115	90220
11	93592	13.925	15	58.925	6.564	3.804	0.603	0.160	96583
12	111063	27.463	15	72.463	12.946	3.878	0.693	0.274	115824
13	107632	13.930	20	73.930	6.567	3.865	0.702	0.160	126549
14	110477	18.456	20	78.456	8.700	3.876	0.727	0.202	132668
15	123563	36.553	20	96.553	17.231	3.925	0.817	0.337	157350

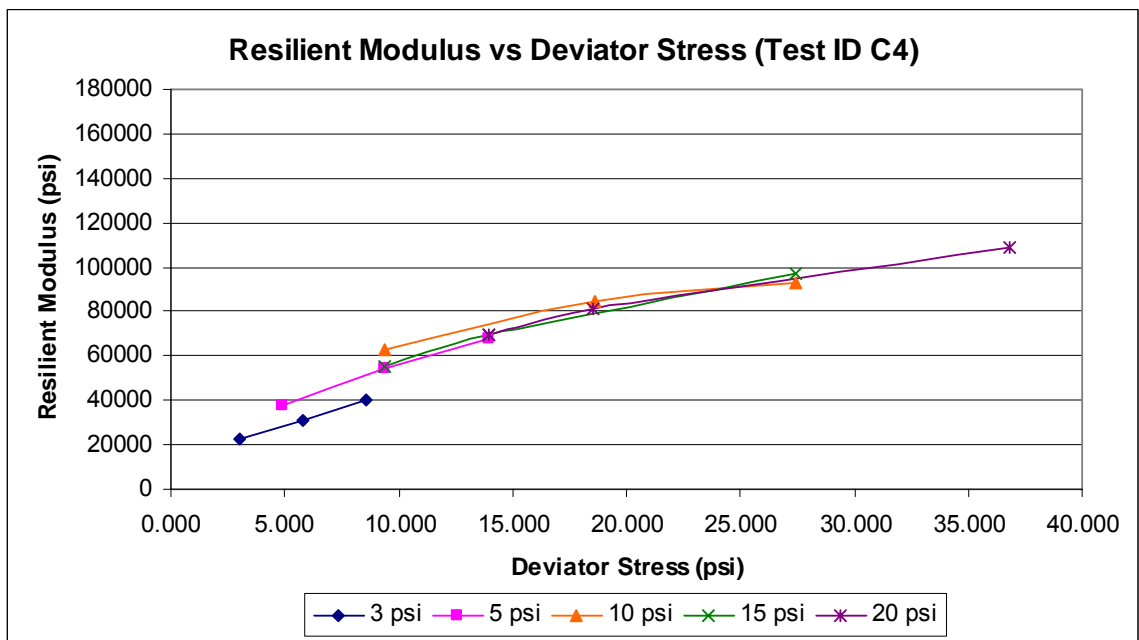
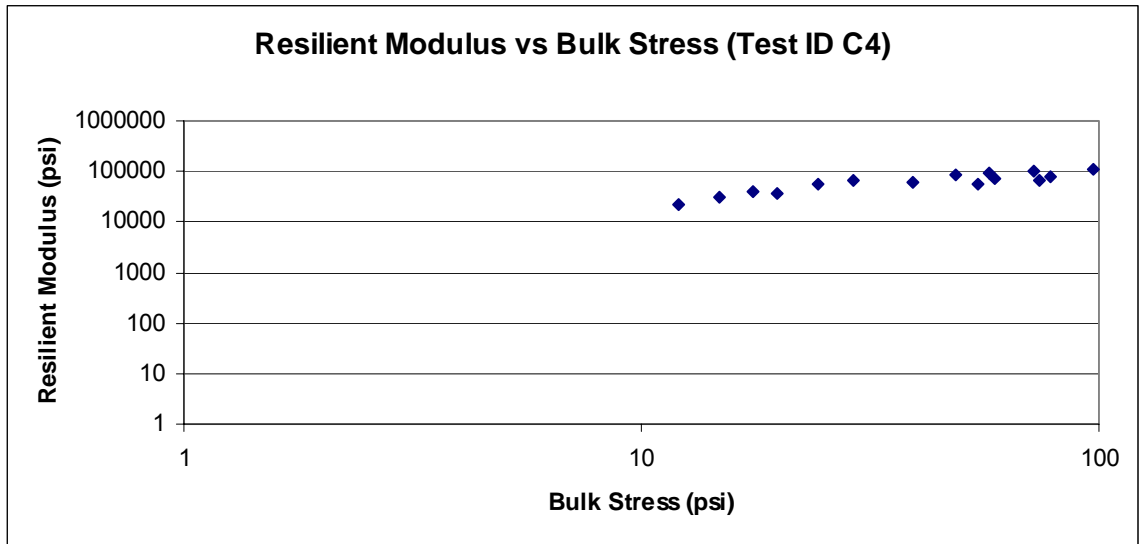
#### Equation of Model:

$$M_r = k_1 P_a \left( \frac{\theta}{P_a} \right)^{k_2} \left( \frac{\tau_{oct}}{P_a} + 1 \right)^{k_3}$$

k <sub>1</sub>	1376.407
k <sub>2</sub>	1.191
k <sub>3</sub>	-0.247
R <sup>2</sup>	0.914



## C4





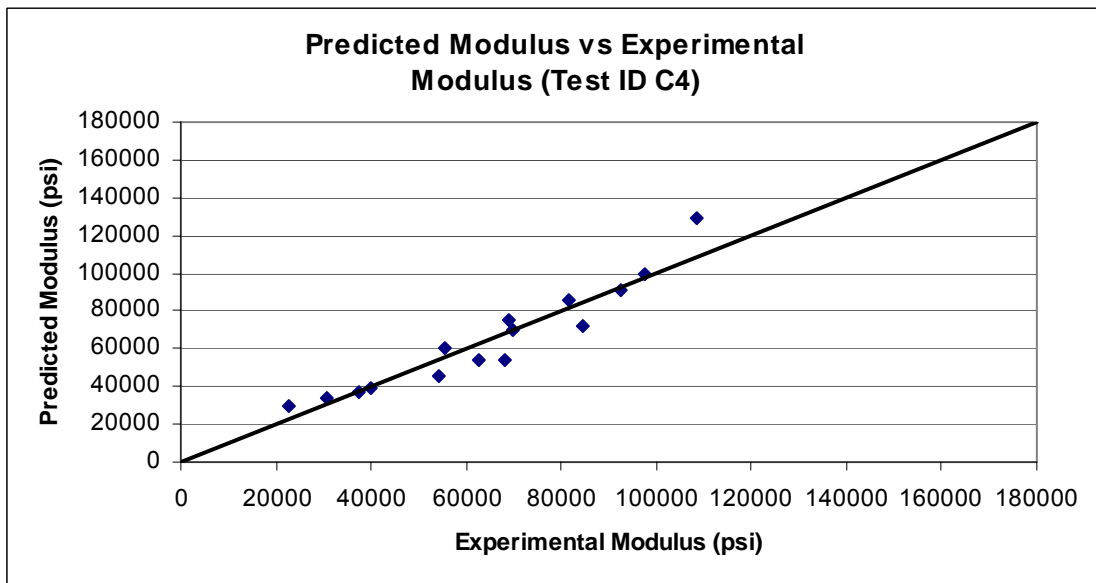
## C4

Sequence Number	Experimental Resilient Modulus	Deviator Stress	Confining Pressure	Bulk Stress	Octahedral Shear Stress	log (M <sub>r</sub> /P <sub>a</sub> )	log (Bulk Stress/P <sub>a</sub> )	log((T <sub>oct</sub> /P <sub>a</sub> )+1)	Regression Predicted Modulus
1	22538	3.013	3	12.013	1.420	3.186	-0.088	0.040	29260
2	30823	5.798	3	14.798	2.733	3.322	0.003	0.074	34302
3	39952	8.535	3	17.535	4.023	3.434	0.077	0.105	39367
4	37457	4.896	5	19.896	2.308	3.406	0.131	0.063	37057
5	54373	9.413	5	24.413	4.437	3.568	0.220	0.115	45302
6	68026	13.965	5	28.965	6.583	3.665	0.295	0.161	54035
7	62489	9.389	10	39.389	4.426	3.628	0.428	0.114	53579
8	84338	18.605	10	48.605	8.770	3.759	0.519	0.203	72149
9	92604	27.397	10	57.397	12.915	3.799	0.592	0.274	91368
10	55554	9.373	15	54.373	4.419	3.577	0.568	0.114	59996
11	69786	13.975	15	58.975	6.588	3.676	0.603	0.161	69426
12	97453	27.398	15	72.398	12.916	3.821	0.692	0.274	99155
13	69147	13.933	20	73.933	6.568	3.672	0.702	0.160	75102
14	81387	18.524	20	78.524	8.732	3.743	0.728	0.202	85276

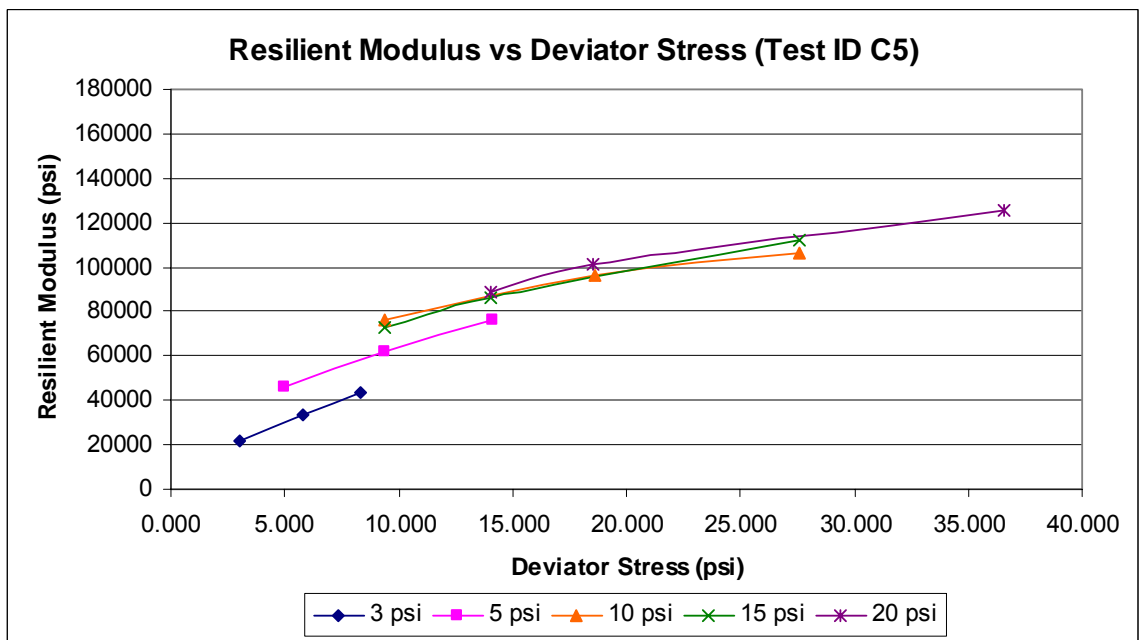
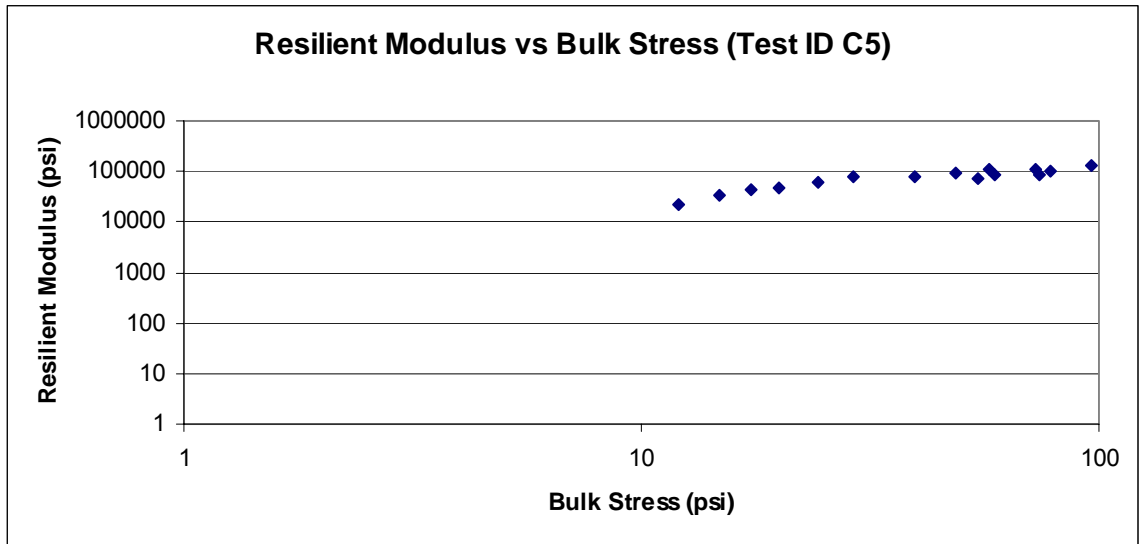
### Equation of Model:

$$M_r = k_1 P_a \left( \frac{\theta}{P_a} \right)^{k_2} \left( \frac{\tau_{oct}}{P_a} + 1 \right)^{k_3}$$

k <sub>1</sub>	1932.406
k <sub>2</sub>	0.352
k <sub>3</sub>	1.092
R <sup>2</sup>	0.909



C5



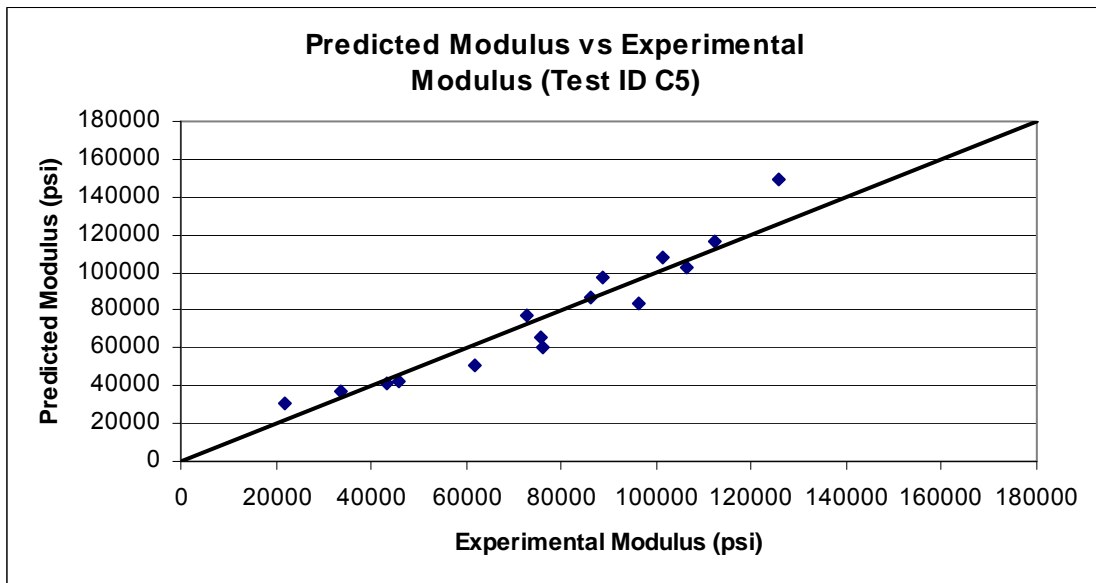
# C5

Sequence Number	Experimental Resilient Modulus	Deviator Stress	Confining Pressure	Bulk Stress	Octahedral Shear Stress	log (M <sub>r</sub> /P <sub>a</sub> )	log (Bulk Stress/P <sub>a</sub> )	log((T <sub>oct</sub> /P <sub>a</sub> )+1)	Regression Predicted Modulus
1	21847	3.040	3	12.040	1.433	3.172	-0.087	0.040	31172
2	33496	5.804	3	14.804	2.736	3.358	0.003	0.074	36655
3	43332	8.348	3	17.348	3.935	3.469	0.072	0.103	41711
4	45856	4.982	5	19.982	2.349	3.494	0.133	0.064	42196
5	61779	9.369	5	24.369	4.417	3.624	0.220	0.114	50697
6	75924	14.117	5	29.117	6.655	3.713	0.297	0.162	60103
7	75787	9.408	10	39.408	4.435	3.712	0.428	0.115	65183
8	96186	18.616	10	48.616	8.776	3.816	0.519	0.203	83899
9	106194	27.631	10	57.631	13.025	3.859	0.593	0.276	102988
10	72606	9.425	15	54.425	4.443	3.694	0.568	0.115	77161
11	86355	14.029	15	59.029	6.613	3.769	0.604	0.161	86774
12	112272	27.627	15	72.627	13.024	3.883	0.694	0.276	116186
13	88942	14.023	20	74.023	6.611	3.782	0.702	0.161	97638
14	101236	18.551	20	78.551	8.745	3.838	0.728	0.203	107656
15	125584	36.611	20	96.611	17.259	3.932	0.818	0.337	148915

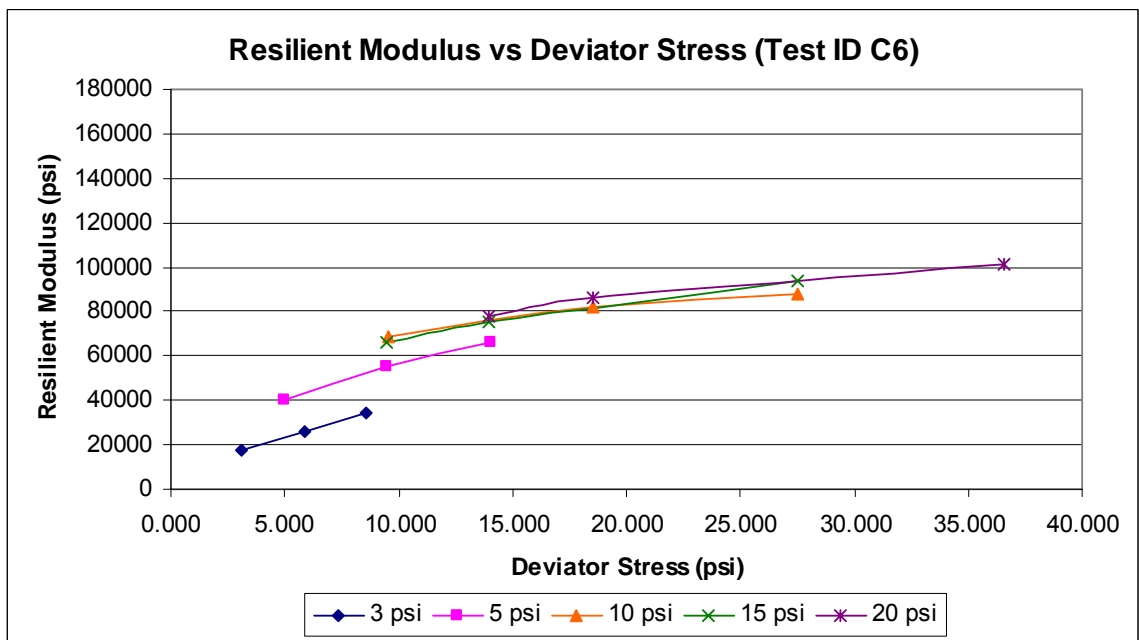
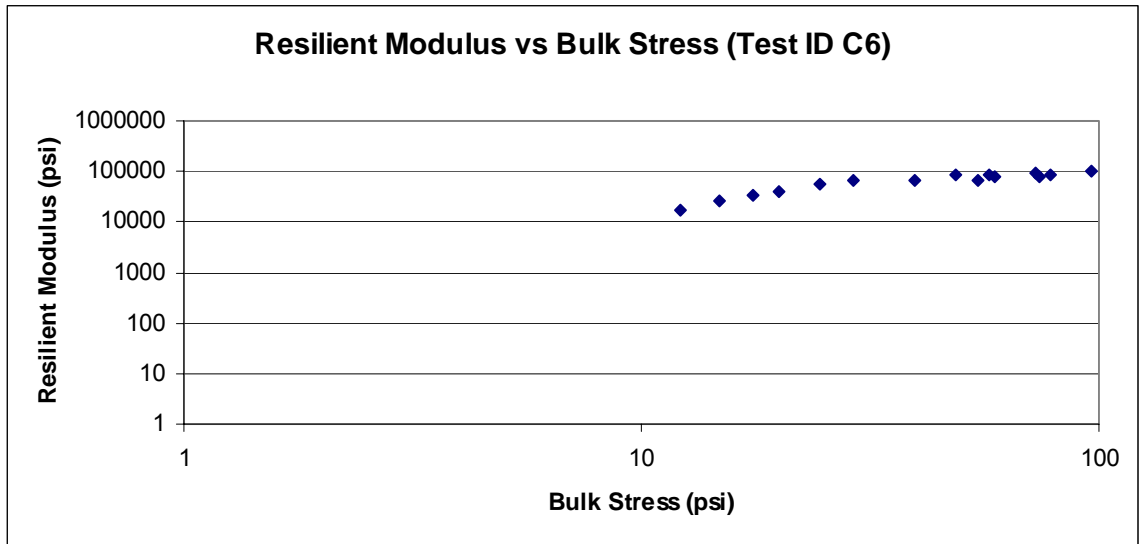
## Equation of Model:

$$M_r = k_1 P_a \left( \frac{\theta}{P_a} \right)^{k_2} \left( \frac{\tau_{oct}}{P_a} + 1 \right)^{k_3}$$

k <sub>1</sub>	2205.087
k <sub>2</sub>	0.522
k <sub>3</sub>	0.699
R <sup>2</sup>	0.905



## C6



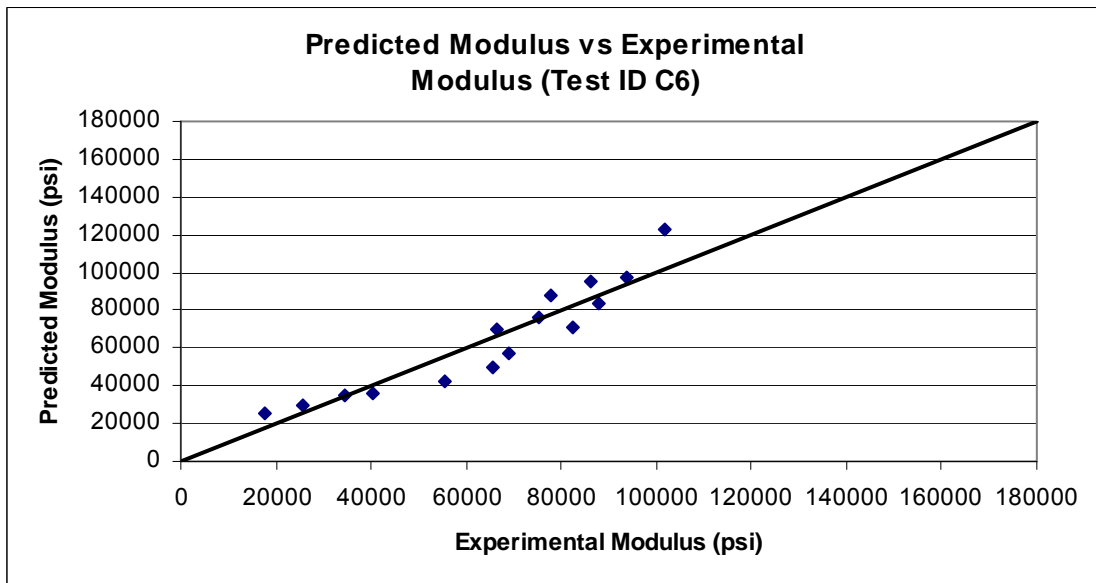
## C6

Sequence Number	Experimental Resilient Modulus	Deviator Stress	Confining Pressure	Bulk Stress	Octahedral Shear Stress	log (M <sub>r</sub> /P <sub>a</sub> )	log (Bulk Stress/P <sub>a</sub> )	log((T <sub>oct</sub> /P <sub>a</sub> )+1)	Regression Predicted Modulus
1	17709	3.138	3	12.138	1.479	3.081	-0.083	0.042	25753
2	25697	5.880	3	14.880	2.772	3.243	0.005	0.075	30150
3	34290	8.589	3	17.589	4.049	3.368	0.078	0.106	34421
4	40268	4.973	5	19.973	2.344	3.438	0.133	0.064	35788
5	55333	9.497	5	24.497	4.477	3.576	0.222	0.115	42628
6	65799	14.037	5	29.037	6.617	3.651	0.296	0.161	49468
7	68982	9.514	10	39.514	4.485	3.671	0.429	0.116	57271
8	82341	18.527	10	48.527	8.734	3.748	0.519	0.203	70637
9	87984	27.521	10	57.521	12.973	3.777	0.593	0.275	84055
10	66296	9.479	15	54.479	4.469	3.654	0.569	0.115	69803
11	75411	13.995	15	58.995	6.597	3.710	0.603	0.161	76593
12	93936	27.538	15	72.538	12.982	3.806	0.693	0.275	97007
13	77737	13.993	20	73.993	6.597	3.723	0.702	0.161	88086
14	86181	18.497	20	78.497	8.719	3.768	0.728	0.202	95029
15	101653	36.560	20	96.560	17.235	3.840	0.817	0.337	122807

### Equation of Model:

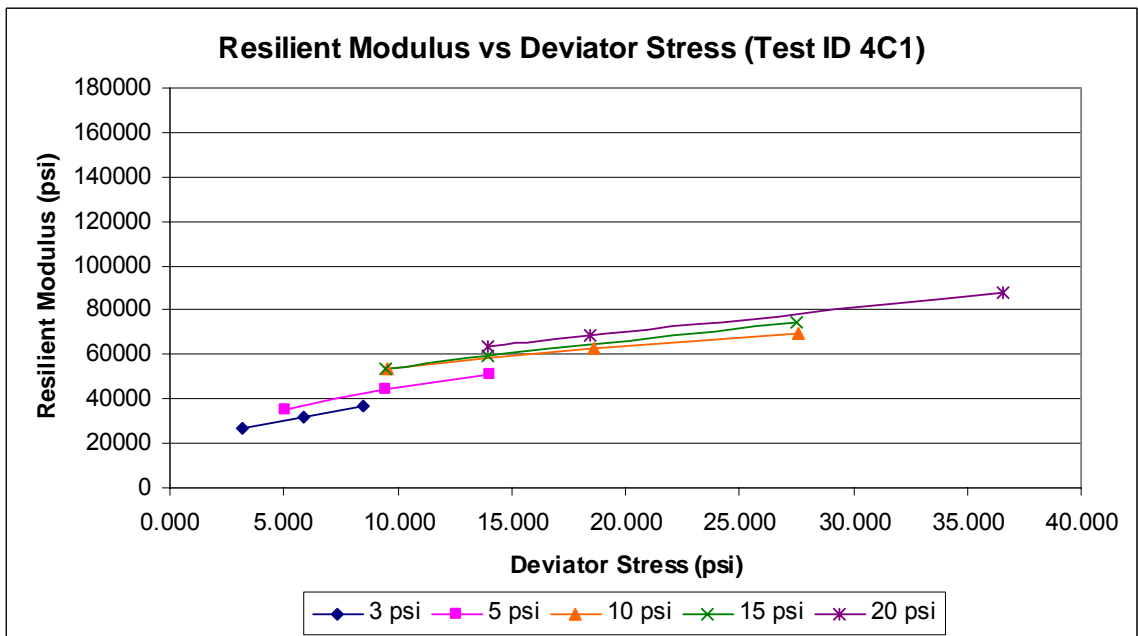
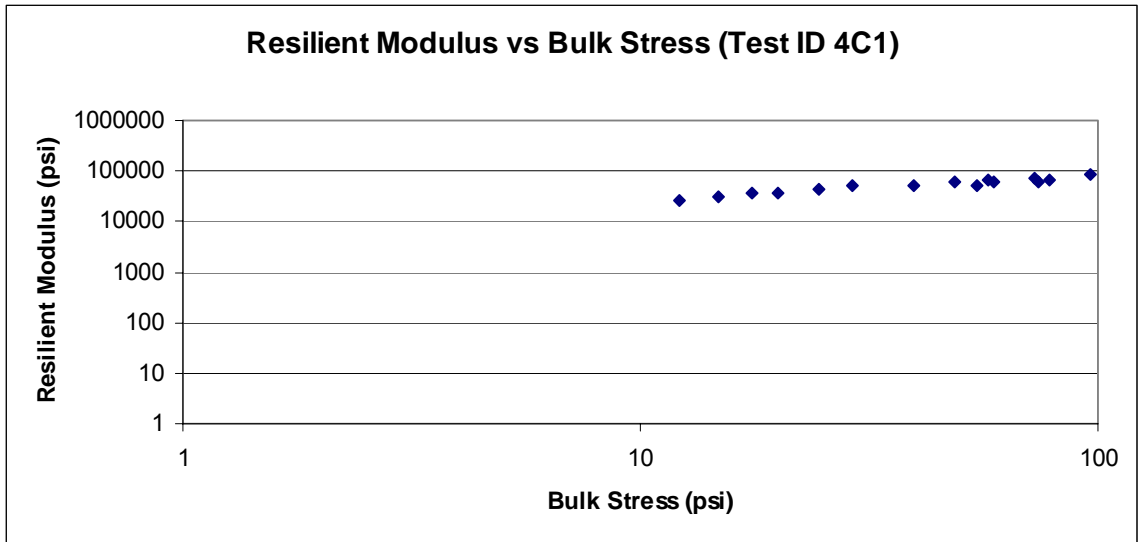
$$M_r = k_1 P_a \left( \frac{\theta}{P_a} \right)^{k_2} \left( \frac{\tau_{oct}}{P_a} + 1 \right)^{k_3}$$

k <sub>1</sub>	1894.927
k <sub>2</sub>	0.617
k <sub>3</sub>	0.415
R <sup>2</sup>	0.877



Limestone, fly ash, and lime, 28 days

4C1



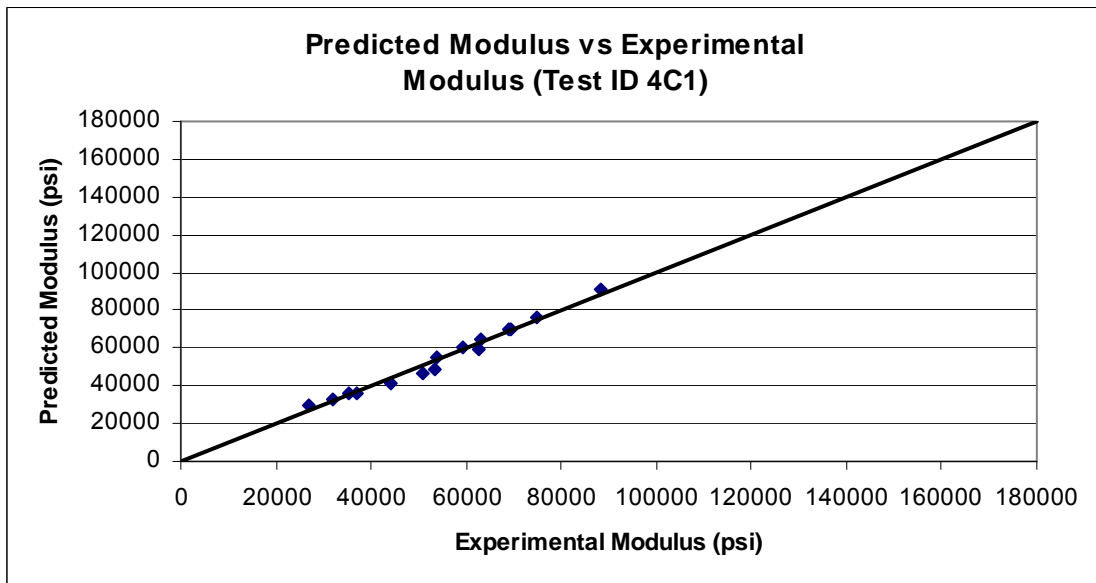
# 4C1

Sequence Number	Experimental Resilient Modulus	Deviator Stress	Confining Pressure	Bulk Stress	Octahedral Shear Stress	log (M <sub>r</sub> /P <sub>a</sub> )	log (Bulk Stress/P <sub>a</sub> )	log((T <sub>oct</sub> /P <sub>a</sub> )+1)	Regression Predicted Modulus
1	26775	3.191	3	12.191	1.504	3.260	-0.081	0.042	29383
2	32064	5.863	3	14.863	2.764	3.339	0.005	0.075	32961
3	37077	8.523	3	17.523	4.018	3.402	0.076	0.105	36421
4	35529	5.042	5	20.042	2.377	3.383	0.135	0.065	36075
5	43985	9.475	5	24.475	4.467	3.476	0.221	0.115	41511
6	50751	14.025	5	29.025	6.611	3.538	0.295	0.161	47009
7	53240	9.547	10	39.547	4.501	3.559	0.430	0.116	49105
8	62758	18.615	10	48.615	8.775	3.630	0.519	0.203	59688
9	69217	27.603	10	57.603	13.012	3.673	0.593	0.275	70103
10	53708	9.472	15	54.472	4.465	3.563	0.569	0.115	54829
11	59380	13.973	15	58.973	6.587	3.606	0.603	0.161	60117
12	74769	27.542	15	72.542	12.984	3.706	0.693	0.275	75911
13	63230	13.939	20	73.939	6.571	3.634	0.702	0.160	65008
14	68904	18.471	20	78.471	8.707	3.671	0.727	0.202	70381
15	88110	36.533	20	96.533	17.222	3.778	0.817	0.337	91503

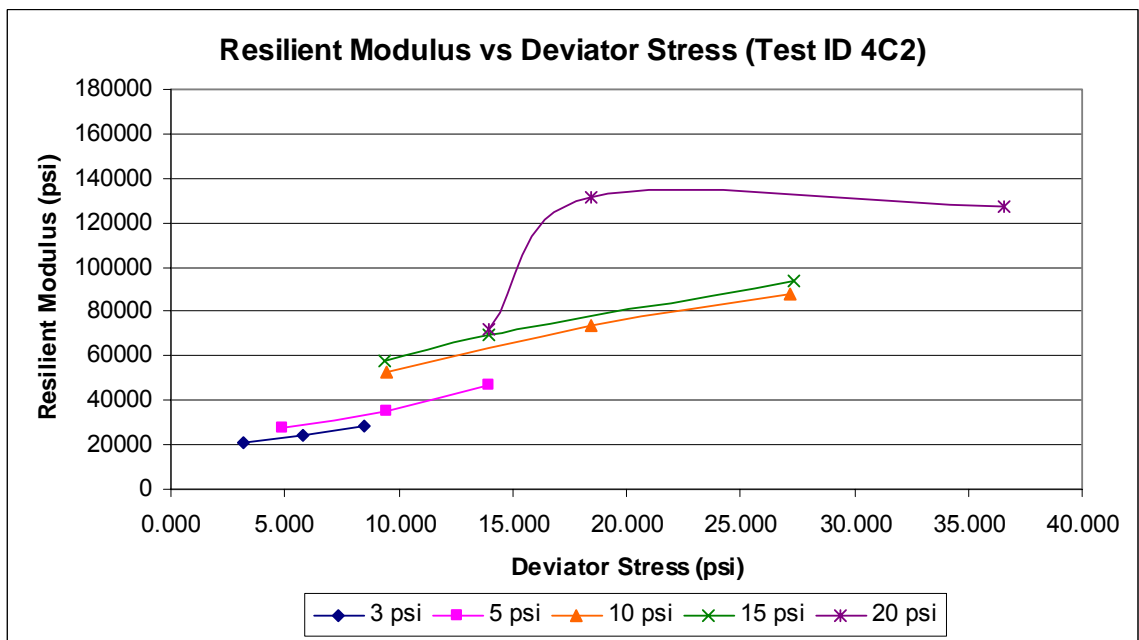
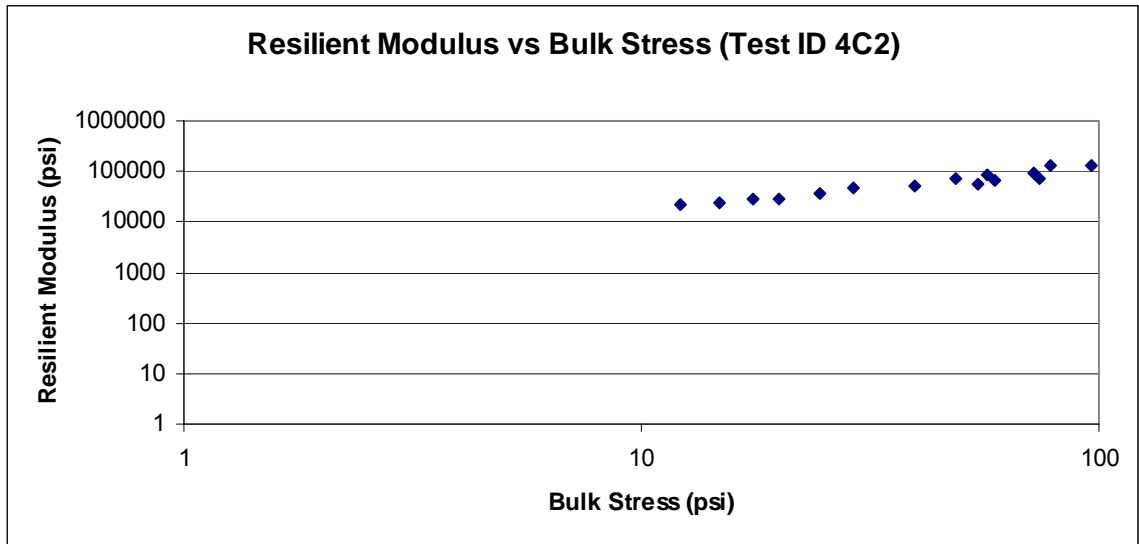
## Equation of Model:

$$M_r = k_1 P_a \left( \frac{\theta}{P_a} \right)^{k_2} \left( \frac{\tau_{oct}}{P_a} + 1 \right)^{k_3}$$

k <sub>1</sub>	2009.565
k <sub>2</sub>	0.348
k <sub>3</sub>	0.614
R <sup>2</sup>	0.980



## 4C2





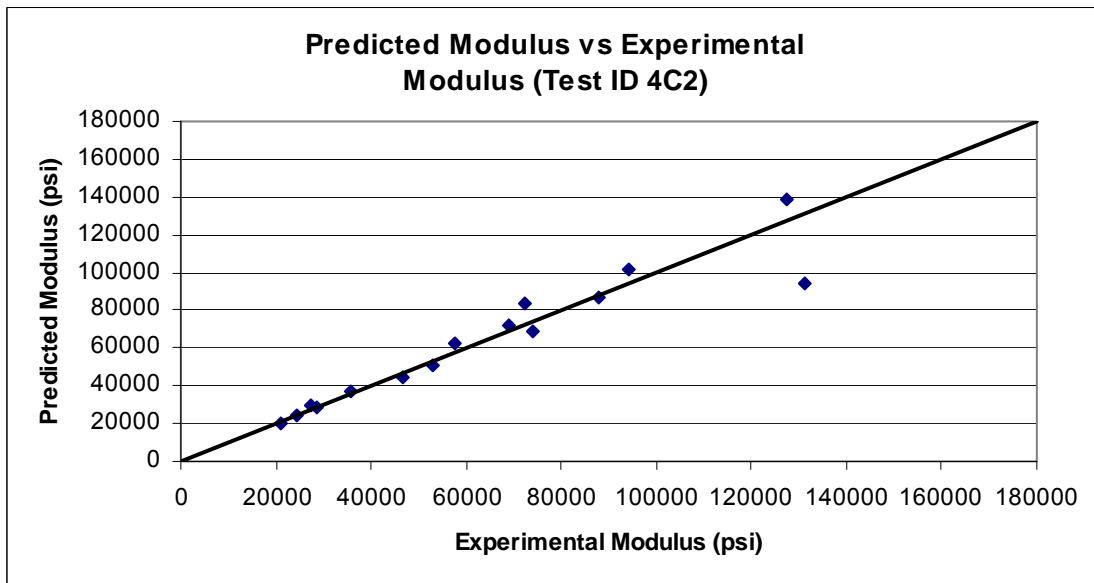
## 4C2

Sequence Number	Experimental Resilient Modulus	Deviator Stress	Confining Pressure	Bulk Stress	Octahedral Shear Stress	log (M <sub>r</sub> /P <sub>a</sub> )	log (Bulk Stress/P <sub>a</sub> )	log((T <sub>oct</sub> /P <sub>a</sub> )+1)	Regression Predicted Modulus
1	21144	3.176	3	12.176	1.497	3.158	-0.082	0.042	20258
2	24575	5.811	3	14.811	2.739	3.223	0.003	0.074	24496
3	28583	8.506	3	17.506	4.010	3.289	0.076	0.105	28975
4	27278	4.937	5	19.937	2.327	3.268	0.132	0.064	29266
5	35542	9.456	5	24.456	4.457	3.383	0.221	0.115	36876
6	46754	13.980	5	28.980	6.590	3.503	0.295	0.161	44963
7	53108	9.449	10	39.449	4.454	3.558	0.429	0.115	50647
8	74085	18.468	10	48.468	8.706	3.702	0.518	0.202	68310
9	88090	27.203	10	57.203	12.824	3.778	0.590	0.272	86955
10	57566	9.414	15	54.414	4.438	3.593	0.568	0.115	62658
11	69102	13.952	15	58.952	6.577	3.672	0.603	0.161	72007
12	94058	27.369	15	72.369	12.902	3.806	0.692	0.274	101883
13	72210	13.935	20	73.935	6.569	3.691	0.702	0.160	83664
14	131207	18.449	20	78.449	8.697	3.951	0.727	0.202	94012
15	127458	36.583	20	96.583	17.246	3.938	0.818	0.337	138919

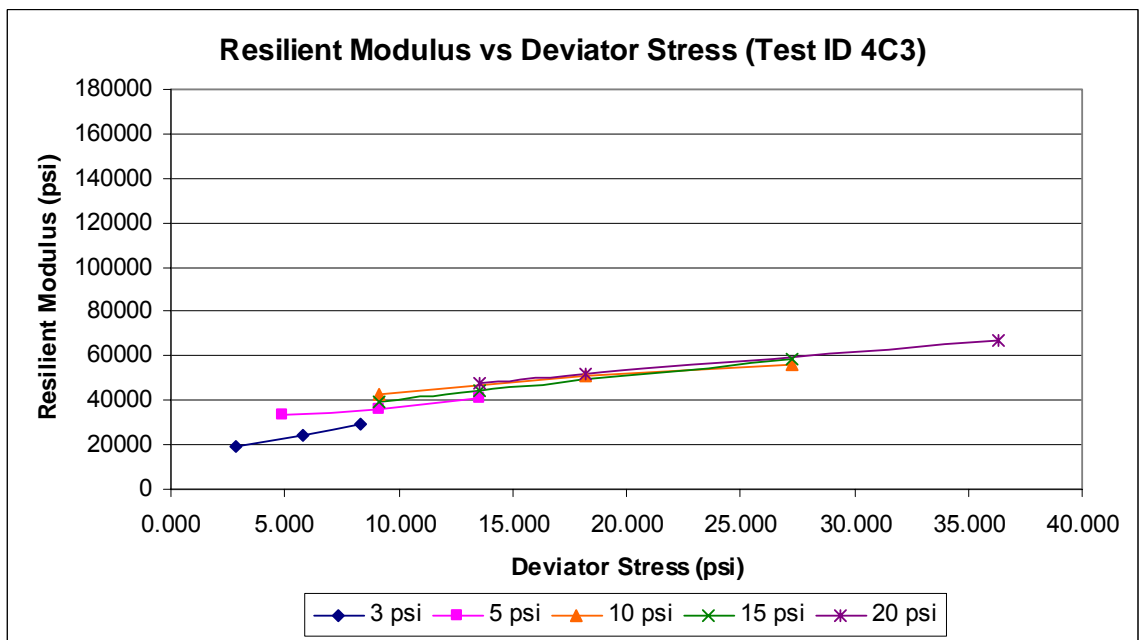
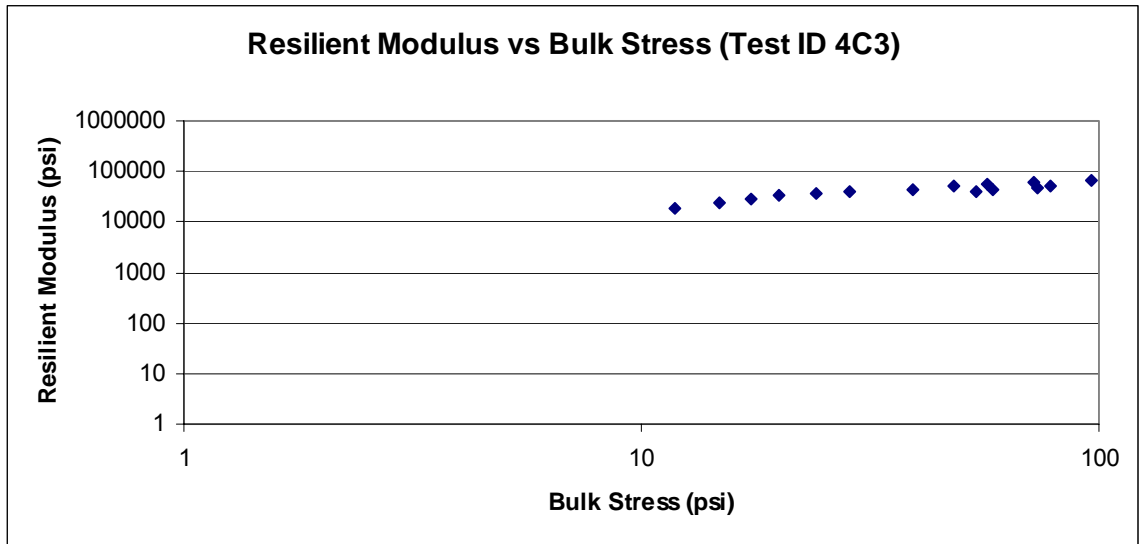
### Equation of Model:

$$M_r = k_1 P_a \left( \frac{\theta}{P_a} \right)^{k_2} \left( \frac{\tau_{oct}}{P_a} + 1 \right)^{k_3}$$

k <sub>1</sub>	1443.606
k <sub>2</sub>	0.664
k <sub>3</sub>	0.810
R <sup>2</sup>	0.964



### 4C3



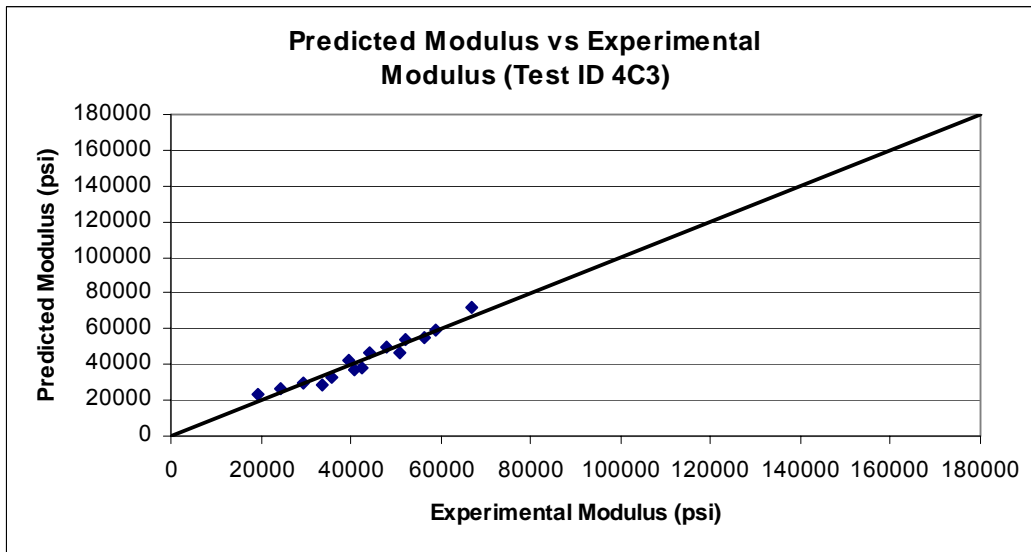
### 4C3

Sequence Number	Experimental Resilient Modulus	Deviator Stress	Confining Pressure	Bulk Stress	Octahedral Shear Stress	log (M <sub>r</sub> /P <sub>a</sub> )	log (Bulk Stress/P <sub>a</sub> )	log((T <sub>oct</sub> /P <sub>a</sub> )+1)	Regression Predicted Modulus
1	19377	2.876	3	11.876	1.356	3.120	-0.093	0.038	23524
2	24417	5.776	3	14.776	2.723	3.220	0.002	0.074	26610
3	29415	8.321	3	17.321	3.922	3.301	0.071	0.103	29248
4	33579	4.917	5	19.917	2.318	3.359	0.132	0.064	28710
5	35861	9.155	5	24.155	4.316	3.387	0.216	0.112	32873
6	40622	13.573	5	28.573	6.398	3.441	0.289	0.157	37171
7	42344	9.140	10	39.140	4.309	3.459	0.425	0.112	38139
8	50708	18.243	10	48.243	8.600	3.538	0.516	0.200	46755
9	56489	27.268	10	57.268	12.854	3.585	0.591	0.273	55284
10	39601	9.157	15	54.157	4.317	3.430	0.566	0.112	42168
11	44325	13.533	15	58.533	6.380	3.479	0.600	0.157	46342
12	58976	27.275	15	72.275	12.858	3.603	0.692	0.273	59403
13	47869	13.583	20	73.583	6.403	3.513	0.699	0.157	49767
14	52115	18.225	20	78.225	8.591	3.550	0.726	0.200	54255
15	66683	36.358	20	96.358	17.139	3.657	0.817	0.336	71650

#### Equation of Model:

$$M_r = k_1 P_a \left( \frac{\theta}{P_a} \right)^{k_2} \left( \frac{\tau_{oct}}{P_a} + 1 \right)^{k_3}$$

k <sub>1</sub>	1609.028
k <sub>2</sub>	0.308
k <sub>3</sub>	0.684
R <sup>2</sup>	0.927



## **C. APPENDIX C**

### **Materials**

Unconfined Compression/ CBR tests:

- Universal Testing System. Instron SATEC Series Model 5590 HVL Series. Static Hydraulic Universal Testing System.

Resilient Modulus Tests:

- Controller- MTS Material Testing Sysem 458.20 Microconsole (Figure C-2)
- Data Acquisition System- National Instruments NI SCXI-1000, Panel BNC2095, Software – Labview7.1, 2004. (Figure C-3)
- Load Frame – SBEL Structural Behavior Engineering Laboratories (Figure C-4)
- Load Cell- Interface Model 1210ATY-2K , 2000 lb.
- LVDTs (2)- Schaevitz Sensors GCA-121-250  $\frac{3}{4}$  inch range
- Hydraulic System – MTS Flextest SE and pump
- Large Sample Triaxial Cells(2) (Figure C-5)
- Air panel – manufactured by Brainard Killman, capable of 100 psi
- Vacuum pump – Gast, Model DOA-V185A-AA, capable of -25 psi

**Table 7-4 Material Composition of Type I Portland Cement (Tinsley, 2007)**

[Buzzi Unicem USA, INC., Signal Mountain Plant]

Composition	Percent (mass)
Silicon Dioxide	20.3
Aluminum Dioxide	4.9
Ferric Oxide	3.6
Calcium Oxide	63.3
Magnesium Oxide	3.1
Sulfur Trioxide	2.9
Loss in Ignition	1.4
Insoluble Residue	0.21
<b>Total</b>	<b>100.0</b>

**Table 7-5 Chemical Properties of Class F Fly Ash (Tinsley, 2007)**

Element		Typical Range of Concentration
1	Silica ( $\text{SiO}_2$ )	41 - 58%
	Amorphous	42 - 53.5
	Crysalline	3.0 - 7.0
2	Alumina ( $\text{Al}_2\text{O}_3$ )	18.1 - 28.6%
3	Iron oxide ( $\text{Fe}_2\text{O}_3$ )	9.9 - 26%
4	Calcium oxide ( $\text{CaO}$ )	0.8 - 4.5%
5	Magnesium oxide ( $\text{MgO}$ )	0.7 - 1.4%
6	Sodium oxide ( $\text{Na}_2\text{O}$ )	0.2 - 0.6%
7	Potassium oxide ( $\text{K}_2\text{O}$ )	1.5 - 3.3%
8	Titanium dioxide ( $\text{TiO}_2$ )	1.0 - 1.9%
9	Sulfur trioxide ( $\text{SO}_3$ )	0.1 - 2.2%
	Phosphorus pentoxide	
10	( $\text{P}_2\text{O}_5$ )	nil - 1.5%
11	Loss on ignition	1.9 - 8.0%
12	pH	4.1 - 9.5

**Figure 7-1 MTS Micro console**



**Figure 7-2 Data Acquisition System**



**Figure 7-3 Load Frame with Load Cell and Large Triaxial Cell**

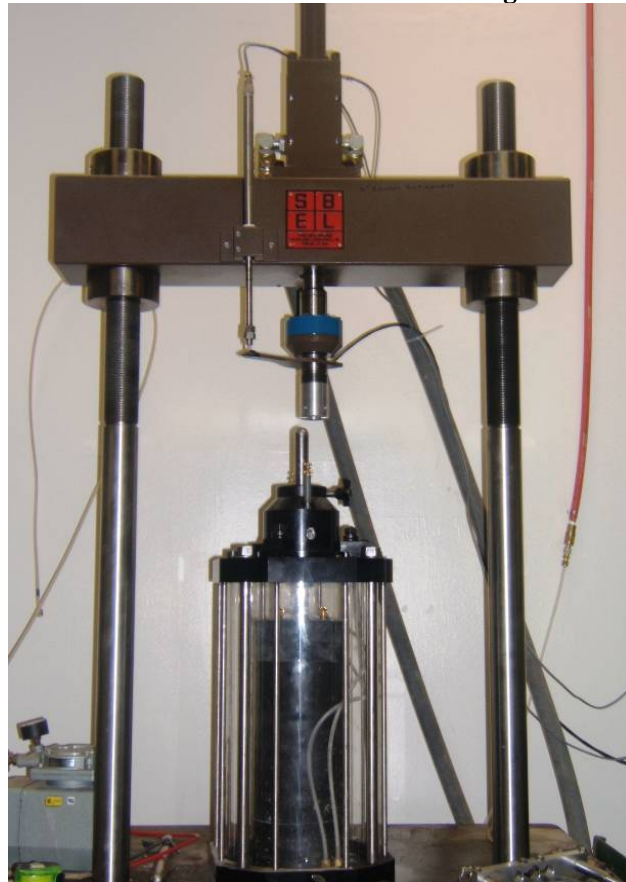
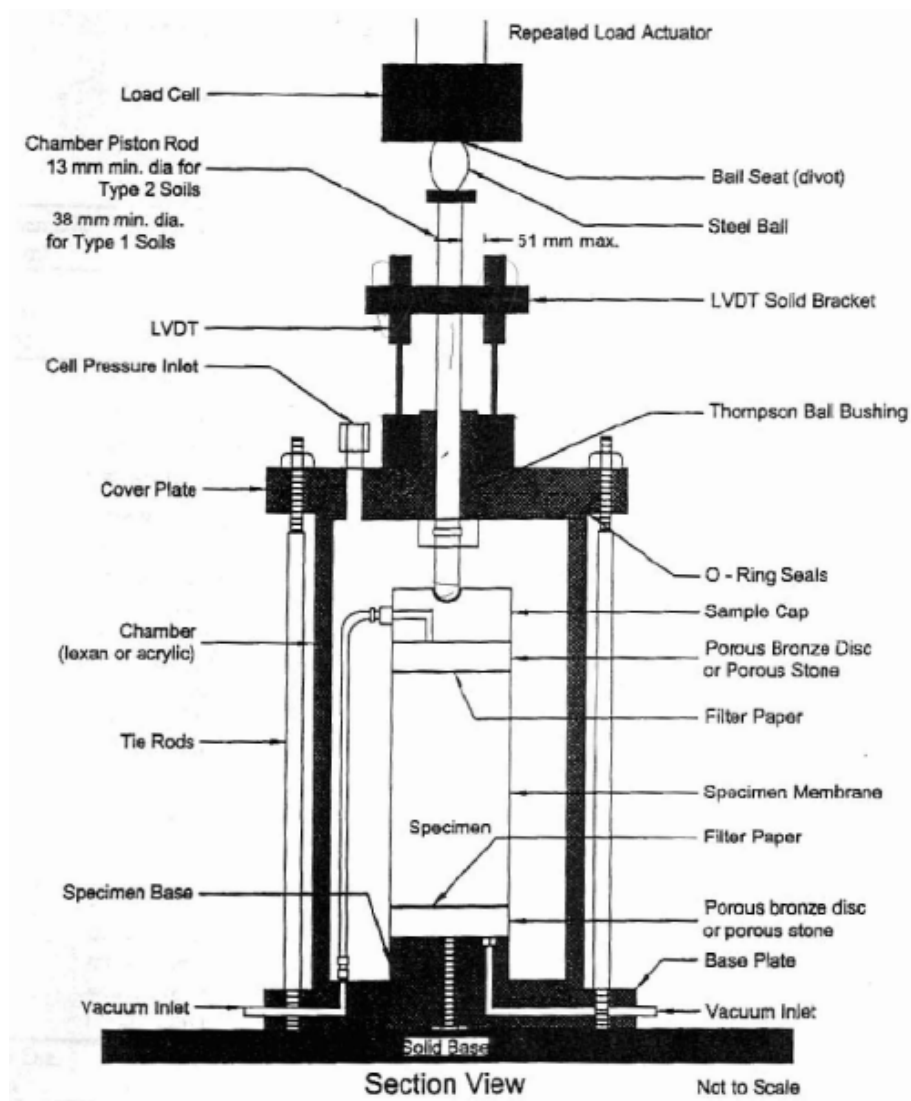




**Figure 7-4 Large Triaxial Cell with Sample with Sample Inside**



Figure 7-5 Schematic setup of Resilient Modulus Test





## **VITA**

Wesley MacDonald was born in Nashville, Tennessee, on May 6, 1983 to parents Shannon Lee Allen (Duke) and Michael John MacDonald. He lived in Hermitage, Nashville, Joelton, Madison, Oak Ridge, and Thompson's Station, Tennessee, before graduating from Fred J. Page High School in 2001. He attended Georgia Institute of Technology for one year before transferring to the University of Tennessee and receiving his Bachelor of Science Degree in Civil Engineering from the University of Tennessee in May 2006.